Energy Research and Development Division
FINAL PROJECT REPORT

EFFECTS OF METEOROLOGICAL CONDITIONS ON OZONE SENSITIVITY IN THE SAN JOAQUIN VALLEY

Prepared for: California Energy Commission
Prepared by: Lawrence Berkeley National Laboratory

DECEMBER 2011
CEC-500-2014-032

PREPARED BY:

Primary Author(s):
Nancy Brown
Ling Jin
Aurore Loisy

Lawrence Berkeley National Laboratory
Berkeley, CA 96270

Contract Number: UC MR-026 POM26-L96

Prepared for:

California Energy Commission

Marla Mueller
Contract Manager

Linda Spiegel
Office Manager
Energy Generation Research Office

Laurie ten Hope
Deputy Director
ENERGY RESEARCH AND DEVELOPMENT DIVISION

Robert P. Oglesby
Executive Director

DISCLAIMER

This report was prepared as the result of work sponsored by the California Energy Commission. It does not necessarily represent the views of the Energy Commission, its employees or the State of California. The Energy Commission, the State of California, its employees, contractors and subcontractors make no warranty, express or implied, and assume no legal liability for the information in this report; nor does any party represent that the uses of this information will not infringe upon privately owned rights. This report has not been approved or disapproved by the California Energy Commission nor has the California Energy Commission passed upon the accuracy or adequacy of the information in this report.

PREFACE

The California Energy Commission Energy Research and Development Division supports public interest energy research and development that will help improve the quality of life in California by bringing environmentally safe, affordable, and reliable energy services and products to the marketplace.

The Energy Research and Development Division conducts public interest research, development, and demonstration (RD&D) projects to benefit California.

The Energy Research and Development Division strives to conduct the most promising public interest energy research by partnering with RD&D entities, including individuals, businesses, utilities, and public or private research institutions.

Energy Research and Development Division funding efforts are focused on the following RD&D program areas:

- Buildings End-Use Energy Efficiency
- Energy Innovations Small Grants
- Energy-Related Environmental Research
- Energy Systems Integration
- Environmentally Preferred Advanced Generation
- Industrial/Agricultural/Water End-Use Energy Efficiency
- Renewable Energy Technologies
- Transportation

Effects of Meteorological Conditions on Ozone Sensitivity in the San Joaquin Valley is the final report for the Impact of Meteorology on Ozone Control Strategies project (contract number UC MR-026 POM26-L96) conducted by Lawrence Berkeley National Laboratory. The information from this project contributes to Energy Research and Development Division's Energy-Related Environmental Research Program.

For more information about the Energy Research and Development Division, please visit the Energy Commission's website at www.energy.ca.gov/research/ or contact the Energy Commission at 916-327-1551.

ABSTRACT

The San Joaquin Valley air basin of California is designated as an extreme nonattainment area for ozone due to its unique trough-like topography and diverse emissions from both local and upwind sources. Summer is a time of high electricity generation loads in the valley due to high air condition demands. Summer is also the season when ozone is high. Ozone production can be reduced by controlling either volatile organic compounds or nitrogen oxides. Designing control strategies to reduce ozone concentrations is especially challenging because ozone control regimes of nitrogen oxides- and volatile organic compounds-limitation change in both time and space as meteorology changes. This report described an ozone sensitivity analysis performed with the CMAQ modeling system. Ozone sensitivity analysis to nitrogen oxides and volatile organic compounds in the San Joaquin Valley was conducted for four high-ozone episodes exemplifying different meteorological conditions during the summer of 2000. Ozone sensitivities to nitrogen oxides and volatile organic compounds were used to define appropriate control strategies. Meteorological conditions were found to be a decisive factor in identifying ozone limiting reagents. Contributions of upwind air basins such as the San Francisco Bay Area to ozone sensitivity in the San Joaquin Valley were also investigated. The variability associated with contribution from upwind sources identified for the four episodes considered was found to be strongly influenced by meteorological conditions. The most efficient control strategies in terms of the species (nitrogen oxides or volatile organic compounds) and location (upwind or local) were established for different meteorological regimes.

Keywords: Sensitivity analysis, tropospheric ozone, NOx, VOCs, limiting reagent, control option, San Joaquin Valley, meteorological conditions, interbasin influence

Please use the following citation for this report:

Brown, Nancy; Ling Jin; Aurore Loisy. (Lawrence Berkeley National Laboratory). 2011. ***Effects of Meteorological Conditions on Ozone Sensitivity in the San Joaquin Valley.*** California Energy Commission. Publication number: CEC-500-2014-032.

TABLE OF CONTENTS

PREFACE ..... **i**

ABSTRACT ..... **ii**

TABLE OF CONTENTS ..... **iii**

LIST OF FIGURES ..... **v**

LIST OF TABLES ..... **vi**

EXECUTIVE SUMMARY **1**

Introduction 1

Project Purpose 1

Project Results 1

Project Benefits 4

CHAPTER 1: Research, Scope, and Objectives **5**

1.1 Motivation and Context 5

1.2 Research, Objectives, and Approach Summary 7

CHAPTER 2: Theoretical Background **8**

2.1 Ozone Generation and Limiting Regime 8

2.1.1 Primary Photolytic Cycle 8

2.1.2 Termination Reactions and Limiting Reagent 10

2.1.3 Overview 10

2.1.4 Modeling Components 11

2.1.5 Meteorological Modeling 11

2.1.6 Chemical Transport Modeling 11

CHAPTER 3: Data and Methods **13**

3.1 Modeling Domain 13

3.2 Episode Selection 14

3.3 CMAQ Inputs 17

3.3.1 Emissions 17

3.3.2 Meteorological Fields 18

3.4 Brute Force Sensitivity Analysis 19
3.5 Alternative Emission Cases 19
CHAPTER 4: Characteristics of Four Ozone Episodes 20
4.1 Analysis Methods 20
4.2 Surface Temperature 20
4.2.1 Summer Average 20
4.2.2 Episode Anomalies 21
4.3 Flow Patterns 22
4.3.1 Synoptic Features 22
4.3.2 Summer Averages 23
4.3.3 Episode Anomalies 26
4.4 8-h Ozone 29
4.4.1 Summer average 29
4.4.2 Episode Anomalies 30
CHAPTER 5: First Order Sensitivity Analysis 32
5.1 Ozone Peak Time Statistical Analysis 32
5.2 Ozone Sensitivities and Control Options 34
5.2.1 Wind Patterns Effects 36
5.2.2 Temperature Effects 37
5.2.3 Alternative Emission Cases 38
5.3 Local Versus Interbasin Contributions 41
5.3.1 Ozone Sensitivity to NOx and AVOC Emissions from the SJV, the SFB and the SV 41
5.3.2 Predominant Contribution Patterns within the SJV 42
5.3.3 Contribution of the SJV, the SFB and the SV to SJV Ozone Sensitivity 44
CHAPTER 6: Conclusions 51
GLOSSARY 53
REFERENCES 55
APPENDIX A: Ozone Regulation in the United States A-1

APPENDIX B: Science Process Modules in Models-3 CMAQ B-1

APPENDIX C: Wind Fields and Anomalies..... C-1

APPENDIX D: Influences of Meteorology and Emissions D-1

APPENDIX E: Ozone Sensitivities to SJV, SFB and SV Air Basins Emissions..... E-1

LIST OF FIGURES

Figure 1: Photolytic Cycle (A) and Ozone Production Chain (B)..... 9
Figure 2: CCOS Domain Shown in the Outer Red Rectangle, a Grid of 185 x 185 with Each Cell Having a Resolution of 4 km x 4 km 13
Figure 3: Cluster Memberships..... 16
Figure 4: Anthropogenic (NOx and AVOCs) and Biogenic (BVOCs) Average Emissions for Summer 2000 17
Figure 5: Emissions of NOx, AVOC, Isoprene and Terpene in Tons/Day, Averaged by Episode18
Figure 6: Summer Average Surface Temperature over [11 AM, 6 PM] 20
Figure 7: Surface Temperature Anomaly for Each Episode..... 21
Figure 8: Summer Average Sea Surface Pressure and Summer Average Wind 23
Figure 9: SJV Study Region and Major Flows (Red Arrows) Generated under Synoptic Influences 24
Figure 10a and Figure 10b: Summer Average Wind Fields in the SJV at 4:00 p.m. (a) and 8:00 a.m. (b) (PDT) 25
Figure 11: Sea Surface Pressure Anomaly Averaged over [11 AM, 6 PM] for Each Episode..... 26
Figure 12: Surface Wind Anomaly Averaged over [11 AM, 6 PM] for Each Episode..... 27
Figure 13: Summer Average 8-h Ozone Concentrations over [11 AM, 6 PM] (PDT)..... 29
Figure 14: 8-hr Average Ozone Concentrations Anomalies over [11 AM, 6 PM] (PDT) for Each Episode 30
Figure 15: Frequencies (Shown as Probability Density) of the Peak Time of 8-h Ozone Average Maximum (for 8h Ozone Average Levels > 75 ppb) for Each Episode 33
Figure 16: Definition of Ozone Control Options in Terms of Ozone Sensitivity Coefficients, i.e., Ozone Concentration Sensitivity with Respect to NOx and/or VOCs Concentrations 34
Figure 17: Ozone Sensitivities to NOx and AVOC and Ozone Control Regimes for Each Episode 35
Figure 18 Control Options as Determined from the Sensitivity Analysis under Three Alternative Emission Cases: mAVOC, mNOx, mAVOCmNOx Where the m Indicates That the Emissions Are Reduced by 20% of the Nominal Value..... 39
Figure 19: Contribution Maps Associated with Each Episode That Indicates the Relative Importance of Local vs. Upwind Contributions to Ozone Sensitivity to AVOC..... 43
Figure 20: Eastern (Red) and Western (Green) Transects in the SJV 45
Figure 21: Contributions of the SJV, SFB and SV NOx Emissions to Ozone Sensitivity to NOx Emissions along Locations on the Western Transect for Each Specified Episode 46
Figure 22: Contributions of the SJV, SFB and SV NOx Emissions to Ozone Sensitivity to AVOC Emissions along Locations on the Western Transect for Each Specified Episode 47

Figure 23: Contributions of the SJV, SFB and SV NOx Emissions to Ozone Sensitivity to NOx Emissions along Locations on the Eastern Transect for Each Specified Episode 48
Figure 24: Contributions of the SJV, SFB and SV NOx Emissions to Ozone Sensitivity to AVOC Emissions along Locations on the Eastern Transect for Each Specified Episode 49

LIST OF TABLES

Table 1: Characteristics of SJV Moderate to High Ozone Clusters 14
Table 2: Changes in Ozone Exceedances in the SJV (% of Number of Grids with Ozone > 75 ppb) under Alternative Emission Cases..... 40

EXECUTIVE SUMMARY

Introduction

Ozone is designated as a criteria pollutant and regulated by the U.S. Environmental Protection Agency (EPA) due to its adverse health effects. Reducing ozone pollution is challenging because it is not directly emitted but formed via photochemical reactions involving nitrogen oxides (NO_x) and volatile organic compounds (VOCs). Linking emissions of VOCs and NO_x to the concentration of ozone (O_3) at a particular location and time is not straightforward. Ambient levels of ozone depend on its precursor emissions (NO_x and VOCs) and on meteorological conditions. For example, wind circulation alters pollutant transport and accumulation, boundary layer height limits the degree of pollutant dilution and solar radiation and temperature change chemical reaction rates and biogenic emissions. Ozone concentrations are not only sensitive to meteorological changes but ozone responses to emission reductions of its precursor species also varies with meteorology. Understanding these relationships is key to designing effective ozone control strategies for regions with diverse meteorological conditions and is a topic that has not been studied very much.

California's San Joaquin Valley (SJV) has experienced some of the poorest air quality in the country and is designated as an "extreme" nonattainment area for the federal eight-hour (8-h) ozone standard. EPA (Federal Register 2008) has strengthened the ozone standard to 75 parts per billion (ppb) from the previous value of 84 ppb for 8-h ozone, which makes it even more challenging to bring the SJV into compliance with federal and state standards. Diverse emission sources from both local and occasionally upwind regions such as the San Francisco Bay area (SFB), Sacramento Valley (SV) and some coastal air basins further complicate source and receptor relationships and make the issue of ozone control in the SJV a regional problem.

Project Purpose

The objective of this study was to understand the extent to which different meteorological regimes alter the characteristics of the ozone limitation chemistry and to resolve the relative importance of local versus upwind emission contributions to ozone production in different parts of the SJV. In earlier studies a first order sensitivity analysis of a five-day ozone episode (Jin et al. 2008) was conducted to delineate the spatial variations in the ozone control options (NOx versus VOC) in the SJV and to identify local versus upwind source contributions to SJV ozone pollution. Modeling studies were expanded to provide a more complete understanding by identifying statistically determined meteorological regimes that give rise to different spatial distributions of high ozone levels. Whether the ozone control options and inter-basin contributions derived previously from studying the single ozone episode can be applied to ozone formed in other meteorological regimes had not been previously investigated.

Project Results

Four meteorologically episodes were identified for investigating SJV ozone pollution and transport. Selection of the episodes was based on previous modeling and observational studies.

The June episode occurred under a pressure trough associated with relatively well-ventilated conditions. Higher temperatures were observed in the SV and the northern part of the domain.

The resulting thermally induced pressure gradient (from south to north) weakened northerly winds and strengthened southerly flow in the SV and created a stronger westerly flow through the SFB. The pollutant concentrations increased in the northern part of the SJV and in the SV basin as a result.

The August episode occurred under a "western U.S. high" anticyclone system located inland, which thermally drove a strong north-westerly flow at the surface that enhanced the down-valley and upslope ventilation flows in the SJV. Pollutant levels increased in the southeastern part of the valley as a result. The SV and SFB were relatively clean in this episode.

The September episode occurred under the influence of an "eastern Pacific high" system that heated up the ocean and coastal areas. The resulting thermal effects produced a surface pressure gradient from land to sea that led to very stagnant conditions. Pollutant levels tended to increase on the western side of the SJV and in the SFB coastal regions due to these weakened onshore flows (from west to east).

The above three episodes with their ozone concentrations levels in the three air basins (SJV, SFB, and SV) had temperature and flow conditions that were also found to be representative of those observed frequently in previous years.

The July-August episode featured a persistent "western U.S. high" system with light winds and much higher temperatures over the land than other episodes. The flow pattern resembled the summer averages with slightly enhanced southward flow in the SV. Elevated ozone levels were observed in many of the SJV, SFB and SV metropolitan areas.

First-order ozone sensitivities to domain-wide anthropogenic NOx emissions and to anthropogenic VOC (AVOC) emissions were used to determine ozone control options (VOC-control, NOx-control, and transition). Researchers' observations included:

- Ozone sensitivities to AVOC were positive throughout the domain, which indicated that reducing AVOC would lead to reduced ozone levels. Ozone sensitivities to NOx changed signs. The negative sensitivities indicated that reducing NOx led to an increase in ozone concentrations (NOx-disbenefit). In general, the urban areas of the San Francisco Bay area, Sacramento and the urban areas in the SJV such as Fresno and Bakersfield all exhibited a NOx disbenefit for the various meteorological conditions associated with the different episodes. The spatial extent of the NOx-disbenefit changed from episode to episode, especially for the northern part of the SJV.
- The extent of the NOx-disbenefit varied for the different meteorological conditions associated with the four episodes at the high ozone (>75 ppb) locations. Researchers had previously found that NOx-control was overall more beneficial for reducing 8-h ozone when they focused on a single ozone episode (July-August). The current results considered four episodes and indicated that AVOC control became important, especially for the most stagnant (September) episode.
- Wind speed, mixing height and ventilation rates affected the rate at which pollutants were diluted. NOx concentrations were reduced and ozone chemistry shifted towards NOx-

limitation under more ventilated conditions, while concentrated NOx titrates ozone over larger areas led to an increase in VOC-limited locations under very stagnant conditions,.

- The dependence of ozone control options on meteorology found here were not affected under alternative reduced AVOC emission cases but was shifted towards more NOx-control under alternative reduced NOx emission cases.

Researchers evaluated the source-receptor relationships among the SJV, the SFB and the SV air basins as a function of meteorological conditions and quantified the local versus upwind contributions to ozone sensitivity in the SJV. Their findings included:

- A stagnant flow regime as exemplified by the September episode had little interbasin transport. There was turbulent mixing in the morning as evidenced by the presence of the Fresno Eddy but stagnation prevented dispersion of pollutants during the day and enhanced their recirculation in the morning following the morning commute period. This regime was characterized by a NOx-disbenefit in the SJV that was locally based.
- The June episode showed the strong influence of pollutants transported from the SFB into the northern SJV. The NOx disbenefit occurring near Modesto was mainly due to NOx emitted in the SFB that was transported through the Coastal Range gaps and accumulated in the northern part of the valley as a result of the weak ventilation flow. A reduction of SFB NOx emissions increased the ozone in the northern parts of the SJV in this episode. Southwesterly marine wind also carried SFB NOx emissions to the southern SV and affected the Sacramento urban center. This episode was less sensitive to local emissions than the September episode.
- In the August episode stronger marine ventilation led to greater sensitivities to SFB NOx along the western side of the northern SJV. In this episode the northern part of the SJV was also influenced by air masses containing SV emissions. It was the only episode that allowed a significant upwind contribution of emissions by the SV.
- The July-August episode was similar to the August episode except that the SV influences on the SJV were reduced due to reduced southward flow.

Overall the ozone sensitivity patterns and source contributions suggested that the SJV should be divided into four subregions: the northern parts of the SJV, the southern parts of the SJV, and the western and eastern sides of the middle SJV. The northern part of the valley was mainly influenced by SFB emissions. Reducing AVOC emissions in the SFB would be very beneficial for this part of the SJV. It would also decrease ozone levels downwind of urban centers in the eastern SJV. The efficiency of AVOC control increased with the strength of the marine flow from the SFB.

Remote areas on the western side of the middle SJV showed a strong trend toward NOx-limitation, and both local and upwind sources were important to control in order to reduce ozone concentration in this location.

The limiting reagent was highly dependent on meteorological conditions and location along the eastern side of the middle SJV, but the most important sources were local even for different wind flow patterns. Reduction of local VOC emissions would be the most efficient control option under stagnant flow conditions, while local NOx reductions would be a better option for other meteorological conditions.

Both ozone control options and source contributions varied with meteorology in the southern part of the SJV. Ozone formation in this area was generally dominated by both local and upwind sources and was mostly limited by NOx except in the urban areas. Local contributions become more important and ozone chemistry shifted toward more VOC limitation under very stagnant conditions such as those that occurred in September.

Project Benefits

The results obtained in this study provided a more complete understanding of ozone control options for the SJV and from an air quality perspective could be used to identify the best regions for adding distributed generation and for siting future power plants in the SJV.

CHAPTER 1:
Research, Scope, and Objectives

1.1 Motivation and Context

Ozone is an important component of the stratosphere that protects the biosphere from the harmful effects of ultraviolet radiation from the sun. In the troposphere ozone is formed from the interactions of oxides of nitrogen (NOx), volatile organic compounds (VOCs), and sunlight. It is a strong oxidizer, and as such, it is a threat to human and ecological health. It is a criterion pollutant regulated by the Clean Air Act.

People with lung and/or cardiac disease, children, older adults, and people who are active can be affected when ozone levels are particularly high. Breathing ozone can trigger a variety of health problems including chest pain, coughing, throat irritation, and congestion. It can worsen bronchitis, emphysema, and asthma. Ground-level ozone also can reduce lung function and inflame the linings of the lungs. Repeated exposure may permanently scar lung tissue (American Lung Association, 2010). Ground-level ozone can also have detrimental effects on plants and ecosystems and affect agricultural productivity (United States Environmental Protection Agency, 2010).

Because ozone is considered harmful to public health and the environment, it is designated as a criteria pollutant by the Federal Clean Air Act (1990). The Clean Air Act established two types of National Ambient Air Quality Standards (NAAQS) for criteria pollutants. Primary standards set limits to protect public health, with an adequate margin of safety, including the health of "sensitive" populations such as children, the elderly, and individuals suffering from respiratory disease. Secondary standards set limits to protect public welfare from any known or anticipated adverse effects of a pollutant, including protection against decreased visibility, damage to animals, crops, vegetation, and buildings. Both standards, usually referred as to 2007 standards, are currently set at 75 ppb with an averaging time of 8 hours for ozone[1] (see Appendix A). To a significant degree, the United States and especially California are not in compliance with these standards (see US nonattainment areas shown in Appendix A.4) (United States Environmental Protection Agency, 2010).

Reducing ozone is challenging because it is a secondary pollutant, formed in the atmosphere by chemical reactions involving volatile organic compounds (VOCs) in the presence of nitrogen oxides (NOx) and sunlight. Although it is tempting to infer that the severity of ozone pollution could be reduced in a given area by lowering emissions of VOCs and/or NOx, this is not the case due to the complicated and non-linear nature of its formation chemistry. The rate of ozone production can be limited by either VOCs or NOx. However linking emissions of VOCs and

[1] Note: The Environmental Protection Agency (EPA) has proposed to strengthen the primary standard to a level within the range of 0.060-0.070 parts-per-million (ppm). EPA is also proposing to establish a distinct cumulative, seasonal 'secondary' standard, designed to protect sensitive vegetation and ecosystems. EPA is proposing to set the level of the secondary standard within the range of 7-15 ppm-hours (see Appendix A).

NOx to the concentration of ozone (O3) at a particular location and time is not straightforward. Particularly controversial for at least three decades has been the issue of control of VOCs versus NOx. (Nazaroff & Alvarez-Cohen, 2001) (Finlayson-Pitts & Pitts, 1997). At high NOx/VOC ratios, decreasing NOx can actually lead to an increase in O3 (so called "NOx-disbenefit"); in this VOC-limited regime, control of organic compounds is most effective. On the other hand, at high VOC/NOx ratios, the chemistry becomes NOx-limited. In this regime, ozone concentrations decline with reductions in NOx emissions but show little response to VOCs. The transitional regime occurs when the reduction of either precursor is only slightly helpful; however, in this regime, ozone reductions are not as great as the conditions with only one limiting precursor. NOx-limited regimes are usually found in remote areas, such as forested rural areas with abundant biogenic VOC emissions, while urban centers are major sources of NOx and are more conducive to VOC limitation. The issues are even more complicated, because the chemical mix of pollutants tends to change from a VOC-limited regime to a NOx-limited regime as an air mass moves downwind from an urban center.

Reducing ozone concentrations is especially challenging for Central California, which suffers from serious air-quality problems due to its unique trough-like topography (see Appendix A.2) and diverse emissions sources. The San Joaquin Valley (SJV) air basin of California (see Appendix A.1) has air pollution levels that are among the worst in the country and is designated as an extreme nonattainment area for ozone (see Appendix A.4). Between 2005 and 2007 ambient ozone levels in the San Joaquin exceeded the health-based 8-hour NAAQS from 112 to 139 days a year (Hall et al. 2008). Not only is the standard frequently exceeded, but also between 2005 and 2007 the maximum 8-hour concentration was significantly above the standard. While ozone levels in much of California have fallen steadily over a period of years, progress in the San Joaquin Valley has been slower than in other major air basins (Hall et al. 2008).

The situation is complicated because ozone control regimes of NOx-, and VOC-limitation, and transitional behavior change in both time and space as a result of meteorology changes. California's coastal areas tend to have high-pressure systems over them, especially in summer. These high-pressure systems are associated with light winds and temperature inversions, both of which limit the vertical dispersion of pollutants. Emissions are converted into ozone, generating high ozone concentrations at the ground level. Because tropospheric ozone forms as a result of reactions involving other pollutants, the highest concentrations tend to occur in the afternoon. The photochemical reactions that create ozone generally require a few hours after the emissions of substantial VOC emissions, and are most effective when sunlight is intense and air temperatures are warm. Hence, ozone concentrations in California are usually higher in the summer (Feather River Air Quality Management District, 2010).

Moreover, the direction and strength of the wind affect ozone concentrations by transporting pollutants from air basins with high emissions to other ones. The prevailing daytime winds in summer are on-shore, bringing relatively clean marine air to the immediate coastal areas, but carrying emissions of ozone precursors further inland. As a result the San Joaquin Valley contains pollutants emitted or formed from upwind source regions, as well as its diverse local

emissions. This further confounds source-receptor relationships, which are crucial for identifying potential control strategies.

Photochemical air quality models integrate scientific understanding of how pollutants evolve in the atmosphere at regional or larger scales and have played an important role in developing air quality managements plans (Russel & Dennis, 2000). Current practices for developing control strategies rely on simulating a few ozone episodes with "worst case" weather conditions. Due to diverse meteorology in the SJV and other regions in Central California, it is not known whether control strategies developed from the worst-case situations are effective under other conditions.

1.2 Research, Objectives, and Approach Summary

The purpose of our study is to investigate the effects of meteorological conditions on ozone control strategies in the San Joaquin Valley (SJV). This study compliments a previous one (Jin et al. 2010) which sought a comprehensive evaluation of the Community Multiscale Air Quality (CMAQ) air quality model performance and development of analysis methods to characterize ozone variability through application of the CMAQ model to Central California for the entire summer 2000 (Jin et al. 2008, 2011; Tonse et al. 2008). Using cluster analysis, distinctive meteorological regimes that are associated with different ozone spatial patterns in the SJV have been determined. These results serve as a foundation for the current study that investigates variability in ozone responses to emissions controls and interbasin pollutant transport for a range of representative meteorological conditions.

Four high-ozone episodes during summer 2000 representative of meteorological conditions of central California are selected based on previous cluster analysis (Jin et al. 2011) of modeling data and observational analysis (Fujita et al. 1999).

We conducted simulations of ozone concentrations during the four episodes using the CMAQ modeling system and determined the source contribution to ozone concentration in the SJV by analyzing the results from a brute force sensitivity analysis of ozone formation and transport. Sensitivity analysis method has already been applied to investigate ozone response to emissions during high-ozone episodes (Sillman et al.1990) (Dabdub et al. 1999 ; Jin et al. 2008). Air quality modeling efforts for summer 2000 focused on the July-August episode, which has the highest ozone and temperature levels. Flow patterns in this episode are not representative of those found in other high-ozone episodes (Jin et al. 2011). This study represents the first attempt to investigate how ozone limiting reagent and source-receptor relationships vary in the San Joaquin Valley under different temperature and flow regimes associated with high ozone levels.

CHAPTER 2:
Theoretical Background

2.1 Ozone Generation and Limiting Regime

Ozone is formed by chemical reactions involving nitrogen oxides (NOx) and volatile organic compounds (VOCs) in the presence of sunlight. The severity of ozone pollution in a given region can be reduced by lowering the emissions of its precursors, i.e., NOx and/or VOCs. Linking emissions of NOx and VOCs to the concentration of O_3 at a particular location and time is not straightforward because the rate of ozone formation is a complex and variable function of the concentrations of its precursors as well as meteorological conditions (Committee on Ozone-Forming Potential of Reformulated Gasoline, National Research Council, 1999).

2.1.1 Primary Photolytic Cycle

The primary photolytic cycle is a set of three reactions.

$$NO_2 + h\nu \rightarrow NO + O^*$$ ***Reaction 1.1***

$$O^* + O_2 + M \rightarrow O_3 + M$$ ***Reaction 1.2***

$$NO + O_3 \rightarrow NO_2 + O_2$$ ***Reaction 1.3***

In reaction 1.1, nitrogen dioxide NO_2 absorbs a photon of light (hν) and dissociates into nitric oxide NO and a free oxygen radical. The radical combines with an oxygen molecule to form an ozone molecule via reaction 1.2. In reaction 1.3, ozone oxidizes nitric oxide to nitrogen dioxide that is converted back to oxygen, completing the cycle. This cycle cannot account for net accumulation of ozone since each ozone molecule produced by this path is followed by the consumption of another ozone molecule (Nazaroff & Alvarez-Cohen, 2001).

The primary photolytic cycle is perturbed when sunlight causes certain organic gases (VOCs) to dissociate, producing peroxy radicals (HO_2 and RO_2). Peroxy radicals convert NO to NO_2 in competition with Reaction 1.3. Consequently, the rate at which ozone is produced by NO_2 increases while the rate at which it is consumed decreases, leading to ozone accumulation in the atmosphere.

The ozone production chain begins with the oxidation of VOCs (represented by RH) by the hydroxyl radical (OH).

$$RH + OH \rightarrow R\cdot + H_2O$$ ***Reaction 1.4***

This is followed by reaction of hydrocarbon radical (R) with oxygen in the air to generate the peroxy radical (RO_2).

$$R + O_2 + M \rightarrow RO_2^* + M$$ ***Reaction 1.5***

Although some NO_2 is emitted directly into the atmosphere by combustion processes, most is formed by the oxidation of NO (the major nitrogenous byproduct of combustion) after dilution in the atmosphere approximately 90 percent of NOx emissions are actually NO emissions. The

oxidation takes place through the fast radical transfer reaction with NO (Committee on Ozone-Forming Potential of Reformulated Gasoline, National Research Council, 1999).

$$NO + RO_2^* \rightarrow NO_2 + RO^*$$ ***Reaction 1.6***

Two other reactions follow, leading to the production of greater amounts of NO_2 and to the regeneration of OH.

$$RO^* + O_2 \rightarrow HO_2 + R'H$$ ***Reaction 1.7***

$$HO_2 + NO \rightarrow OH + NO_2$$ ***Reaction 1.8***

The photolysis of NO_2 by the ultraviolet portion of solar radiation (hν) produces the oxygen atoms that combine with oxygen to form ozone (O_3) in the troposphere (Nazaroff & Alvarez-Cohen, 2001).

$$NO_2 + h\nu \rightarrow NO + O^*$$ ***Reaction 1.9***

$$O^* + O_2 + M \rightarrow O_3 + M$$ ***Reaction 1.10***

In this sequence where VOCs are consumed, both OH and NOx act as catalysts, since they are regenerated.

Figure 1 shows the difference between the primary photolytic cycle (in absence of VOCs) and the ozone production chain (in presence of VOCs).

Figure 1: Photolytic Cycle (A) and Ozone Production Chain (B).

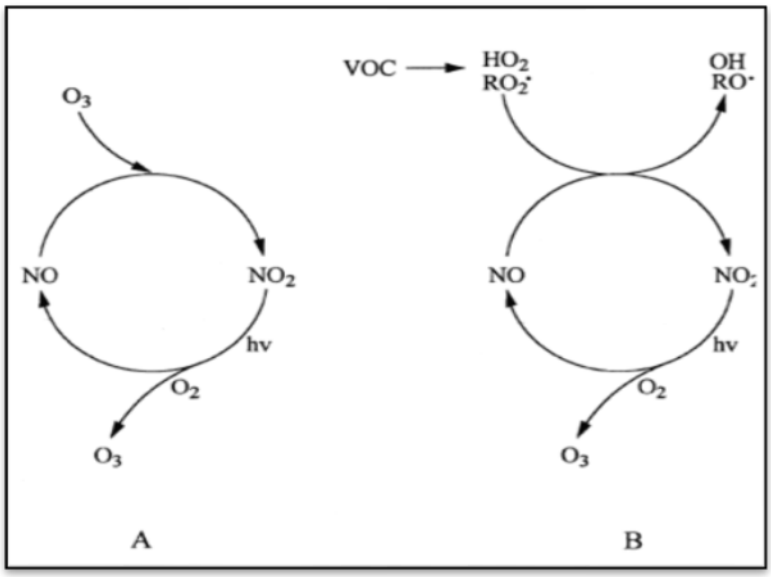

Modified from Atkinson, 2000

2.1.2 Termination Reactions and Limiting Reagent

Termination of the above ozone-generating cycle occurs when either OH or NOx are removed.

When the rate of OH production is greater than the rate of production of NOx, NOx is in short supply and Reaction 1.8 is in competition with Reaction 1.6 leading to the termination of ozone generation (Finlayson-Pitts & Pitts, 1997).

$$HO_2 + HO_2 \rightarrow H_2O_2 + O_2$$ ***Reaction 2.1***

NOx is the limiting reagent and the regime is called NOx-limited. Reducing NOx emissions is consequently the best option to control ozone concentrations.

When the rate of OH production is less than the rate of production of NOx, termination of the ozone-forming chain proceeds via Reaction 2.2.

$$OH + NO_2 \rightarrow HNO_3$$ ***Reaction 2.2***

NOx is relatively abundant and diverts OH from the oxidation of VOCs (Reaction 1.4), which effectively reduces the formation of O_3. Moreover, high NO concentrations increase ozone titration via Reaction 1.3, which reduces ozone concentration, and decreasing NOx can actually lead to an increase in O_3 at high NOx/VOC ratios. Under this VOC-limited regime, control of organic compounds is most effective (Finlayson-Pitts & Pitts, 1997).

Finally between these two extremes lies a transitional region in which ozone is about equally sensitive to NOx and VOCs. However, compared to NOx- and VOC-limited regimes, ozone is relatively insensitive to both.

The limiting reagent is not uniquely defined by location or emissions. It varies dynamically with transport, dispersion and dilution. The effectiveness of control is critically dependent upon the meteorological as well as the chemical conditions that prevail during any given episode, as we will demonstrate subsequently.

2.1.3 Overview

The Community Multiscale Air Quality (CMAQ) modeling system is an active open-source development project of the U.S. EPA Atmospheric Science Modeling Division that consists of a suite of programs for conducting air quality model simulations. CMAQ is supported and distributed by the Community Modeling and Analysis System (CMAS) Center.

CMAQ is a three-dimensional Eulerian atmospheric chemical transport modeling system. CMAQ is designed for modeling several air quality applications, including tropospheric ozone, fine particles, acid deposition and visibility degradation. CMAQ is also designed to have multi-scale capabilities. The grid resolutions and domain sizes for CMAQ range spatially and temporally over several orders of magnitude. By making CMAQ a modeling system that addresses multiple pollutants and different spatial scales, CMAQ has a "one atmosphere" perspective.

CMAQ is designed to handle scale-dependent meteorological formulations and has a large amount of flexibility. CMAQ's governing equations are expressed in a generalized coordinate

system. CMAQ's design ensures consistency between CMAQ and the meteorological modeling system. The generalized coordinate system determines the necessary grid and coordinate transformations, and it can accommodate various vertical coordinates and map projections. The CMAQ modeling system simulates various chemical and physical processes that are thought to be important for understanding atmospheric trace gas transformations and distributions (Community Modeling and Analysis System (CMAS) Center, 2010).

2.1.4 Modeling Components

The CMAQ modeling system consists of three primary modeling components: (1) a meteorological modeling system for the description of atmospheric states and motions, (2) emission models for anthropogenic and natural emissions, and (3) a chemical transport modeling system for solving the reaction-diffusion equation for simulating species transport and transformations. The CMAQ chemical transport model (CCTM) includes the following process modules: horizontal advection, vertical advection, mass conservation adjustments for advection processes, horizontal diffusion, vertical diffusion, gas-phase chemical reactions and solvers, photolytic rate computation, aqueous-phase reactions and cloud mixing, aerosol dynamics, size distributions and chemistry, plume chemistry effects, and gas and aerosol deposition velocity estimation. The three independent processors are related to each other via several interface processors (Buyn & Schere, 2006). Further details about the relationships between the CMAQ processors are shown in Appendix B.

2.1.5 Meteorological Modeling

Meteorology encompasses many atmosphere processes that strongly influence the evolution of emissions, chemical species and aerosols. These processes include horizontal and vertical transport, turbulent mixing, convection and lightning-induced generation of nitrogen oxides, and dry and wet deposition to the surface. The rates at which secondary species and aerosols form and certain chemical reactions take place are also affected directly by the relative humidity, solar energy, temperature and the presence of clouds (Seaman, 1999).

The meteorology model used in this CMAQ application is the Fifth-Generation Pennsylvania State University/National Center for Atmospheric Research (NCAR) Mesoscale Model (MM5).

In most numerical weather prediction models, temperature, pressure, and moisture variables represent the thermodynamics of the system, and their dynamic equations are often expressed in their advective form. For multiscale air quality applications where strict mass conservation is required, prognostic equations for the thermodynamic variables are expressed in conservative forms similar to the continuity equations (Buyn & Schere, 2006). The output variables that are generated by an MM5 simulation must be converted into fields that are required by the chemistry and emission models. The conversion is accomplished in the Meteorology Chemistry Interface Processor (MCIP). MCIP computes variables that are useful to the subsequent models in Models-3.

2.1.6 Chemical Transport Modeling

Chemical transport modeling is governed by the conservation equation for the trace species in a generalized coordinate system, which is suitable for multiscale atmospheric applications (Byun

& Young, 1999). This equation is composed of several terms, explicitly related to the science processes in CMAQ, and are simply summarized as:

$$\frac{\partial C_i}{\partial t} + adv + diff = chem + emis + cloud + pig + aero$$

with:

C_i: concentration of the specie i

$\frac{\partial C_i}{\partial t}$: time rate of change of C_i (implemented with fractional time step)

adv: advection;

$diff$: diffusion

$chem$: production or loss from chemical reactions

$emis$: emissions

$cloud$: cloud mixing and aqueous production or loss

pig: plume-in-grid process (for major point sources specific treatment)

$aero$: aerosol process

Usually, the output time step is set to be 1 hour (Buyn & Schere, 2006). In principal, the transport processes consist of advection and diffusion that cause the movement and dispersion of pollutants in space and time. A more comprehensive description of transport modeling schemes is available in Byun et al. 1999. Numerical schemes used in chemistry, plume-in-grid, aerosol and cloud mixing modules are described in Byun et al. 1999.

CHAPTER 3:
Data and Methods

3.1 Modeling Domain

The Central California Ozone Study (CCOS) domain is shown in Figure 2. It extends from approximately 34 to 41°N and 116 to 124 °W and is gridded into 185 by 185 cells, with a horizontal resolution of 4 km. Vertically, the domain is divided into 27 layers from the surface to about 17 km. The Central Valley is surrounded by the Sierra Nevada and coastal mountains ranges. The San Francisco Bay Area (SFB) and Sacramento Valley (SV) are the major upwind emission sources affecting air quality in the San Joaquin Valley (SJV). The SJV is further divided into northern, central, and southern parts as shown in the map. Relief maps are presented in Appendix A.2.

Figure 2: CCOS Domain Shown in the Outer Red Rectangle, a Grid of 185 x 185 with Each Cell Having a Resolution of 4 km x 4 km

Major air basins labeled on the map are: San Joaquin Valley (SJV), Sacramento Valley (SV), San Francisco Bay Area (SFB), Mountain Counties (MC), North Central and South Central Coasts (NCC and SCC). SJV is divided into the Northern, Central and Southern SJV.

3.2 Episode Selection

Four meteorologically representative episodes are identified for investigating SJV ozone pollution and transport. Selection of the episodes is based on previous modeling and observational studies.

Jin et al. (2011) applied cluster analysis to model simulation results for California's San Joaquin Valley (SJV) for the purpose of identifying meteorologically representative pollution regimes. Six regimes are clustered according to the spatial distribution of SJV 8 h ozone maxima and four regimes (clusters 3 to 6) are associated with moderate to high ozone concentrations. Pollution regimes in the SFB and SV were also identified for investigating the inter-basin relationship between the SJV and its major upwind air basins. The cluster membership of each day in summer 2000 for SJV, SFB, and SV are shown in Figure 4. The cluster membership is color coded according to average ozone levels at measurement locations. The characteristics of the four SJV clusters are summarized in Table 1 below in conjunction with the associated meteorology and upwind air basin ozone pollution regimes. Meteorological effects (temperature and winds) are shown to explain the observed ozone spatial distributions in the SJV, and their relationship to those in the upwind San Francisco Bay Area air basin (SFB) under certain prevailing wind flow patterns. In general, average ozone levels in the SJV increase with temperature; while their spatial distributions depend on flow regimes, especially the strength of sea breezes and upslope flows. More ventilated flow regimes, associated with stronger sea breeze and upslope flows, cause eastward transport of pollutants, increasing ozone in the southeastern SJV and decreasing it in the northwest SJV. The opposite occurs during the most stagnant conditions associated with the weakest sea breeze and upslope flows. The two most prominent relationships between the SFB and SJV were found to be associated with the most ventilated and the most stagnant conditions, respectively, indicating a strong inter-basin transport (or the lack thereof) event.

Table 1: Characteristics of SJV Moderate to High Ozone Clusters

SJV Cluster 3	Ozone Patterns	SJV	Moderate ozone, higher than average ozone in the northern part.
		SFB	Generally low ozone levels (cluster 2)
		SV	Moderate to high ozone levels (clusters 2,4,5).
	Meteorological conditions	Temperature	Moderate temperature, higher than average temperature seen in the northern part of the SJV and the domain (mainly SV)
		Flow Patterns	Moderate sea breeze and upslope flow during the day.

SJV Cluster 4	Ozone Patterns	SJV	Moderate ozone, higher than average ozone seen in the western side of the valley.
		SFB	Generally high ozone levels (clusters 3 and 4)
		SV	Moderate to low ozone levels (clusters 1,2).
	Meteorological Conditions	Temperature	Moderate temperature, higher than average temperature seen along the coasts.
		Flow patterns	Weakest sea breeze and upslope flow during the day. Weakest outflow in the southern SJV.
SJV Cluster 5	Ozone Patterns	SJV	Moderate ozone, higher than average ozone seen mainly in the southeastern downwind areas (of Fresno and Bakersfield).
		SFB	Generally low ozone levels (cluster 2)
		SV	Moderate ozone levels (clusters 2,4).
	Meteorological Conditions	Temperature	Moderate temperature, higher than average temperature seen in the southeastern part of the SJV and in the Sierras and Mojave desert.
		Flow patterns	Strongest sea breeze and upslope flow during the day.
SJV Cluster 6	Ozone Patterns	SJV	High ozone throughout the whole SJV
		SFB	Mostly high ozone (cluster 3)
		SV	Moderate ozone levels (clusters 2,4).
	Meteorological Conditions	Temperature	Highest temperature throughout the valley
		Flow Patterns	Moderate sea breeze and upslope flow during the day.

Figure 3: Cluster Memberships

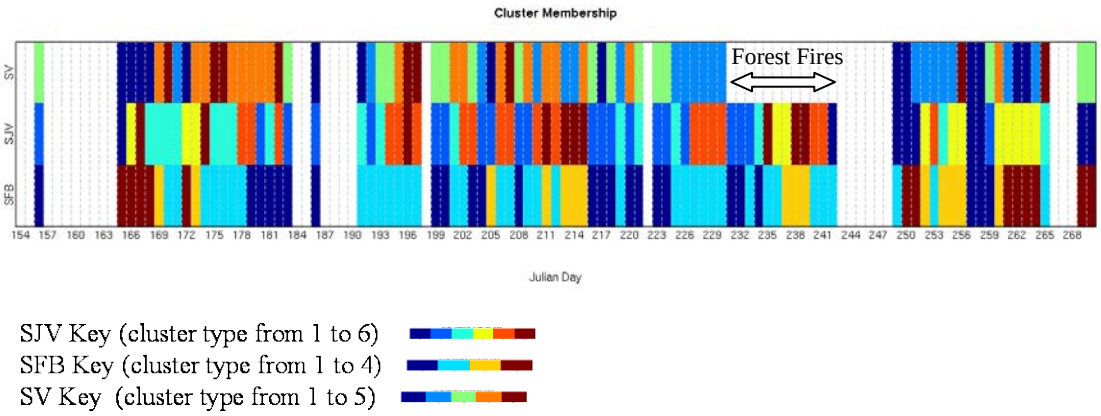

Investigators, who were part of the Central California Ozone Study (CCOS), conducted cluster analysis of past ozone data (126 sites, from 1996 to 1998) based on the spatial patterns of several very high ozone days selected by the local air quality districts (Fujita et al. 1999). Three clusters were identified based on these historical observational data: (1) the SFB has its highest basin-wide ozone, while the SJV ozone is also very high, which is characterized by the weakest sea breeze; (2) the SJV has its highest basin-wide ozone, while SFB and SV are relatively cleaner, which is characterized by a stronger sea breeze, moving pollutants from SFB and SV to SJV; (3) SV has its highest basin-wide ozone values, which, similar with the second cluster, has stronger sea breezes but higher temperature in the Sacramento Valley; SJV ozone in this cluster is also high. These three historical ozone clusters are characterized by SJV ozone patterns 4, 5, 3, and their associated meteorological conditions, as well as the relationship to upwind ozone levels as described in Table 1.

Figure 4 indicates that these historical ozone clusters appear in summer 2000 episodes: days 261 to 264 (Sep 17th to 20th) are characterized by SJV cluster 4, high ozone in the SFB and moderate to low ozone in the SV; days 227 to 230 (Aug 14th to Aug 17th) are characterized by SJV cluster 5, low ozone in the SFB and moderately low ozone in the SV; days 175 to 177 (Jun 23rd to 25th) are characterized by SJV cluster 3, low ozone in the SFB and high ozone in the SV. The worst-case scenario in summer 2000 days 211-215 (July 29th to Aug 2nd) is largely aligned with high SJV ozone (cluster 6) levels, high SFB ozone, and moderate SV ozone.

Based upon the aforementioned modeling and observational analysis results, four high-ozone episodes during summer 2000 are selected that differ from each other in their meteorological conditions. The first one is from June 21st to June 25th (EP1: days 173-177), the second one from July 29th to August 2rd (EP2: days 211-215), the third one from the 13th to the 17th August (EP3: days 226-230) and the last one from the 16th to the 20th September (EP4: days 260-264). Three of the episodes (EPs 1, 3, and 4) were found to have distinctive flow regimes and are associated with representative historical ozone spatial behavior in the Central California. The July-August episode (EP2) had especially higher temperature than others and is associated with the highest overall ozone levels. These episodes are representative of most of the summertime temperature and flow conditions.

For convenience, the model simulations and analysis of the four episodes are expanded to five days:

- "June episode": from June 21st to June 25th (days 173-177)
- "July-August episode": from July 29th to August 3rd (days 211-215)
- "August episode": from the 13th to the 17th August (days 226-230)
- "September episode": from the 16th to the 20th September (days 260-264)

The first two days of each episode are used in CMAQ as a spin-up. Initial concentrations of all chemical species used in the model are unknown. We input arbitrary, but reasonable, initial concentrations and sensitivity to them disappear in two days. Meteorological variables and chemical simulation results are presented for the last three days.

3.3 CMAQ Inputs

CMAQ parameterization and inputs data (meteorology, emissions, initial and boundary conditions) have been thoroughly discussed and evaluated in Jin et al. 2010 and 2011. We focus here on relevant inputs for our study.

3.3.1 Emissions

Emission inventory files were provided by the California Air Resources Board (CARB). The highest anthropogenic emissions are located near urban centers and highway systems. Biogenic VOC emissions occur in vegetated regions, especially in the foothills of the Sierra Nevada and the Coastal Range Mountains (see Figure 4).

Figure 4: Anthropogenic (NOx and AVOCs) and Biogenic (BVOCs) Average Emissions for Summer 2000

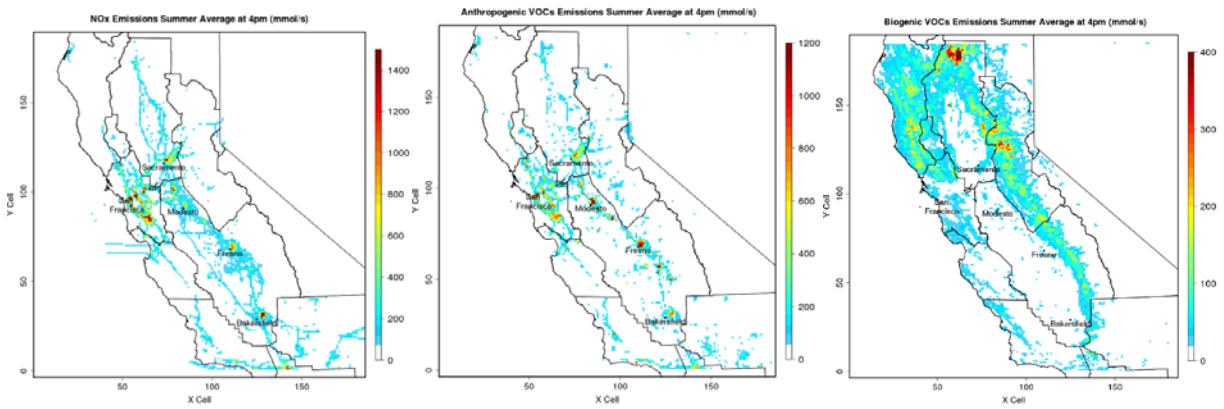

Concentrations at 4:00 p.m. are averaged over 8-hours centered at 4:00 PM.

Anthropogenic emissions usually differ on weekends from weekday values. We use controlled anthropogenic emissions, i.e., we input typical Monday anthropogenic emissions every day of each episode, to eliminate the effect of changes in anthropogenic emissions on our results. Hourly biogenic emissions were estimated for each individual day by applying date-specific temperatures and sunlight intensity to adjusted leaf-cover estimates. It is well established that

emissions of biogenic hydrocarbons increase with temperature (Sharkey et al. 1999; Hanson & Sharkey, 2001; Lamanna & Goldstein, 1999). Comparison of August and July-August episodes, which mainly differ by their temperature levels (see Figure 7), shows that isoprene and terpene, respectively increase by 23 percent and 7 percent with higher temperatures. Total biogenic emissions in July-August episode are 17 percent higher than in the August episode. Biogenic emissions variability within the three other episodes is less than 4 percent.

Figure 5: Emissions of NOx, AVOC, Isoprene and Terpene in Tons/Day, Averaged by Episode

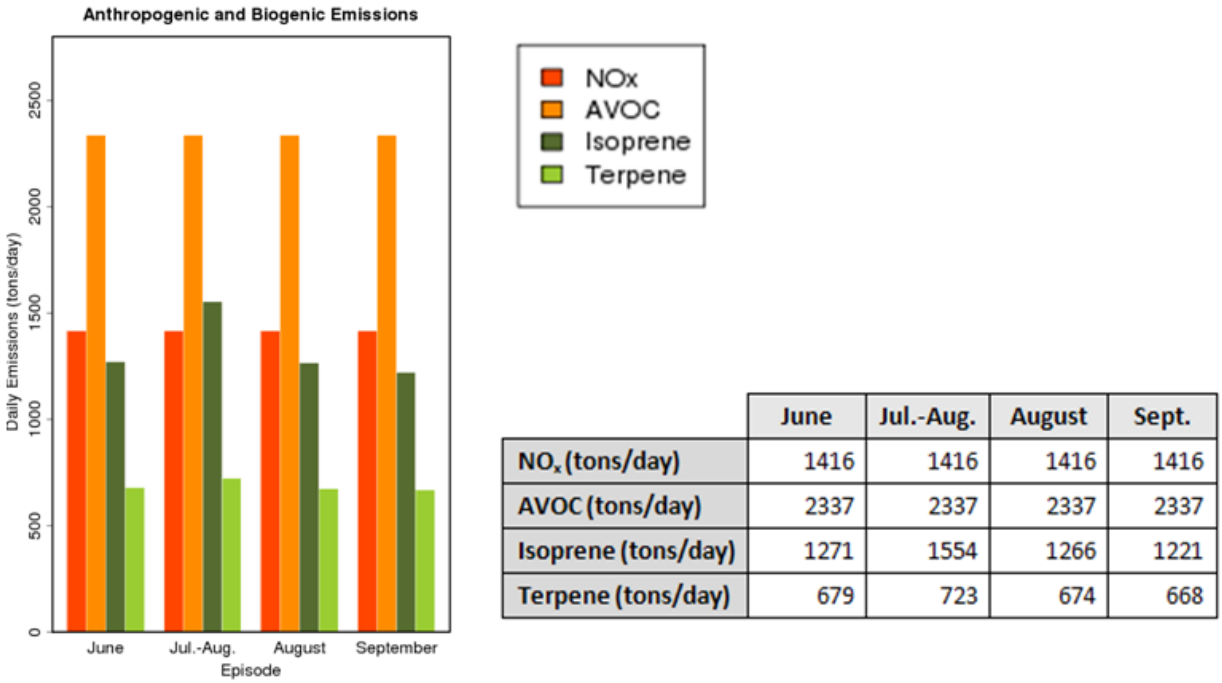

	June	Jul.-Aug.	August	Sept.
NO_x (tons/day)	1416	1416	1416	1416
AVOC (tons/day)	2337	2337	2337	2337
Isoprene (tons/day)	1271	1554	1266	1221
Terpene (tons/day)	679	723	674	668

3.3.2 Meteorological Fields

Meteorological fields with 4 km resolution were used as input for air quality modeling in this study. The Meteorology to Chemistry Interface Processor (MCIP version 3.3) was used to construct CMAQ model-ready input files from the PSU/NCAR mesoscale model (known as MM5) output, and it allows for consolidation of vertical layers. We used 27 layers for CMAQ from the original 50 MM5 layers without changing the first 200 m (9 layers) to preserve high resolution near the ground. To avoid the potential influences of boundary grid cells, the origin of the meteorological domain was shifted inside by 2 grid cells, and a subset of the full 190×190 MM5 4 km domain was used for driving air quality simulations.

3.4 Brute Force Sensitivity Analysis

The first-order semi-normalized sensitivity coefficient ($S_i^{(1)}$) is defined as below:

$$S_i^{(1)} = P_i \frac{\partial C}{\partial p_i} = \frac{\partial C}{\partial \varepsilon_i}$$

where, P_i is an input parameter, whose perturbation p_i is considered in a relative sense by defining a scaling variable ε_i, with its nominal value (unperturbed) being 1; C is the species concentration; and the sensitivity coefficient has concentration units. $S_i^{(1)} = \alpha$ (ppb) implies that a $\pm$10 percent change in the parameter would cause ($\pm 0.10\alpha$) ppb change in the ozone concentration while all other parameters are held constant.

In this report, a brute force sensitivity analysis is performed: NOx and AVOC are successively perturbed by +10 percent of their nominal values. Ozone sensitivities to its precursors are:

$$S_{E_{NO_x}}^{(1)} = \frac{\partial [O_3]}{0.10}$$

$$S_{E_{AVOC}}^{(1)} = \frac{\partial [O_3]}{0.10}$$

Control option maps are determined (see Section 5.2 and 5.2.3) by perturbing domain-wide emissions. Air basin contributions are assessed by perturbing each air basin emissions separately as discussed in Section 5.3.

3.5 Alternative Emission Cases

We are also interested in determining how sensitivities might change with different emissions. This is important because it very possible that the emissions we obtained from CARB might have uncertainties as large as $\pm$20 percent. First order sensitivity coefficients are also calculated for alternative emission cases to investigate how ozone responses to precursor emissions may vary under different emission scenarios. The new alternative base cases (nominal values) are:

Case 'mAVOC': AVOC emissions described in C.1 are reduced by 20 percent.
Case 'mNOx': NOx emissions described in C.1 are reduced by 20 percent.
Case 'mAVOCmNOx': both AVOC and NOx emissions described in C.1 are reduced by 20 percent.

CHAPTER 4:
Characteristics of Four Ozone Episodes

4.1 Analysis Methods

Variables considered in this analysis are temperature, sea surface pressure, wind, and ozone concentration. All variables are hourly values in their original form. The analysis is presented for daily values averaged over an 8-h average between 11 AM to 7 PM, when maximum 8-h average ozone concentrations tend to occur (see section V.A). As most of the hours in this 8-h interval are in the afternoon, for the convenience of notation, it will be referred to as "afternoon" in the subsequent text.

The summer average of an afternoon quantity (temperature, sea surface pressure, wind, and ozone concentration) is calculated by averaging over the entire summer 2000 between 1 June to 30 September. Anomalies are defined as the subtraction of the summer mean value from the current value of a variable. Episodic anomalies are calculated by averaging the meteorological variable of interest anomalies for the last three days of each episode. For example, the episodic temperature anomaly for the June episode is: $\Delta T = \frac{1}{3}\sum_{day=175}^{day=177} T - \frac{1}{122}\sum_{day=153}^{day=274} T$, where T is the daily maximum temperature and ΔT is the anomaly.

4.2 Surface Temperature

4.2.1 Summer Average

Figure 6: Summer Average Surface Temperature over [11 AM, 6 PM]

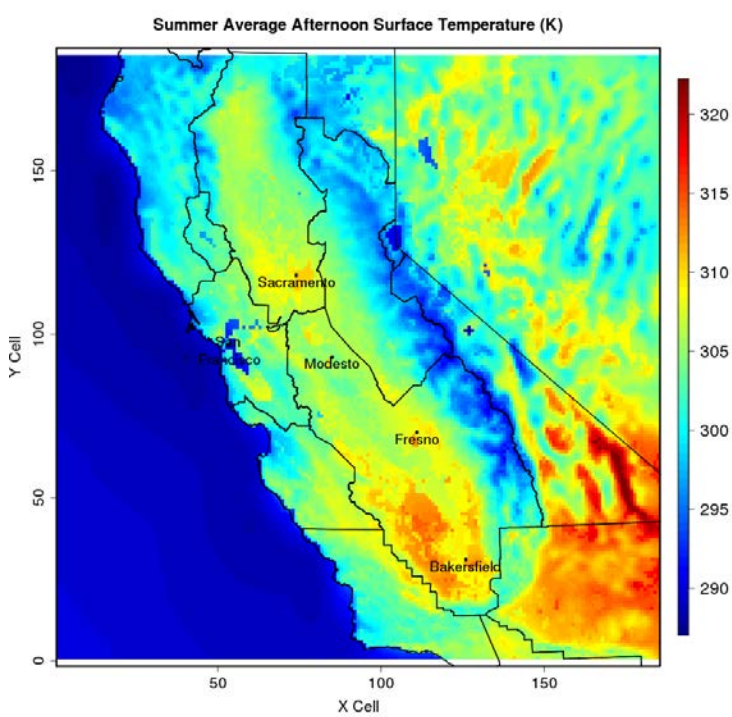

Summer average afternoon temperature is shown in Figure 6. The highest temperature levels are observed in the Mojave Desert and in the southern Great Basin Valley (see air basins map in Appendix A.1). These air basins do not significantly affect air quality in the upwind SJV. High temperature levels occur in the valleys, especially in the southern SJV (about 315 K). Temperature decreases with altitude (< 300 K in the Sierra Nevada) and relatively low temperature levels (300-305 K) are observed along the coastal ranges and in the bays due to influence of cooler marine layers. Although the Mojave Desert and the Great Basin Valley show the highest maximum temperatures, these air basins do not have major emissions sources, and are not of great interest for this study.

4.2.2 Episode Anomalies

Figure 7: Surface Temperature Anomaly for Each Episode

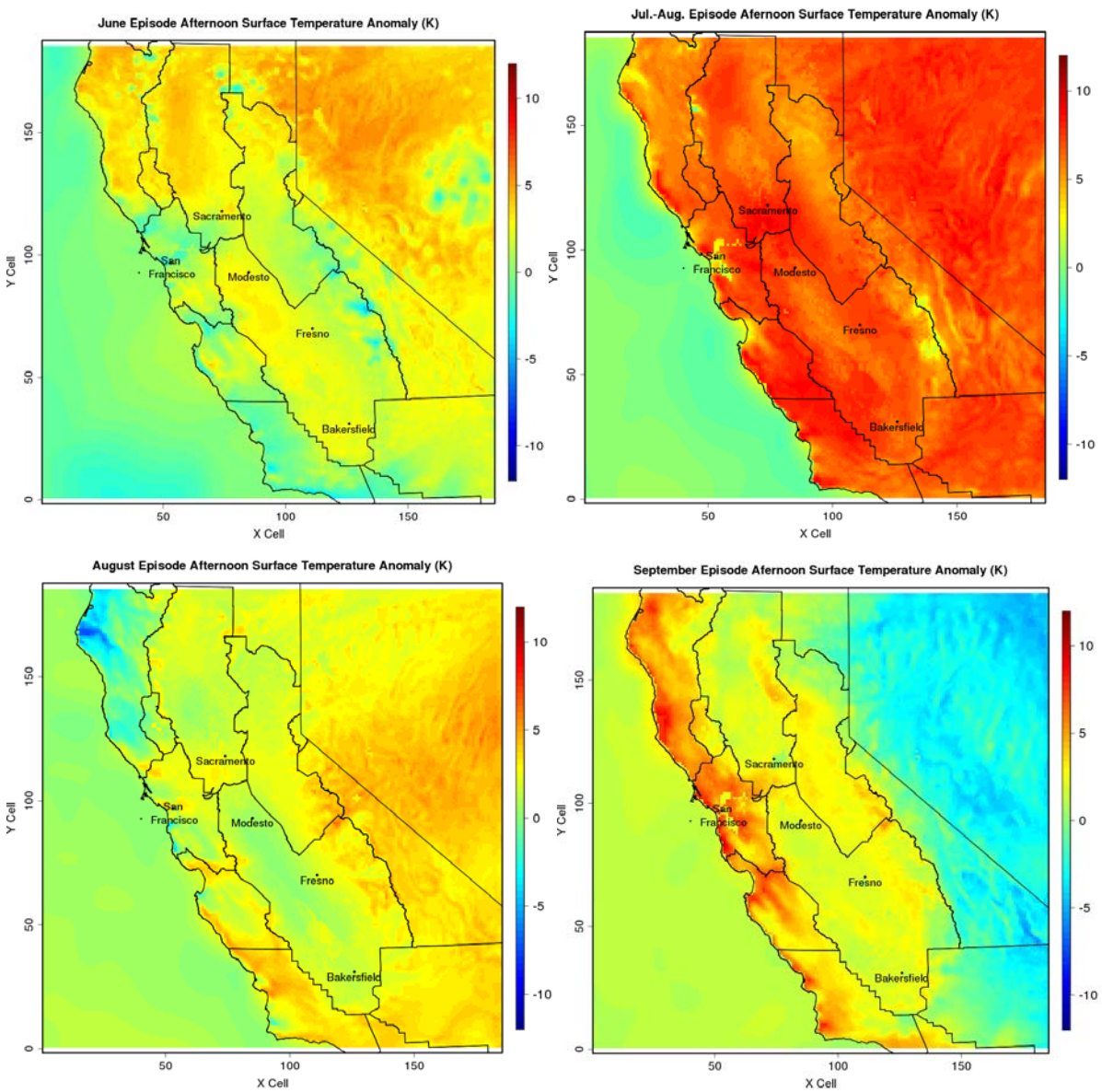

Episodic temperature anomalies are shown in Figure 7. The July-August episode is a remarkably hot period of the summer 2000: we observe a positive anomaly within the range of 8 to 10 K over the entire modeling domain indicating that the temperature level is much higher than the mean values. The temperature spatial pattern is quite similar to the summer average pattern. This episode is referred to as the “hot” episode.

Compared to the hot episode, temperature fields are much more similar in the Central Valley during the three other episodes. They all show regional scale temperature gradients, but the September episode has larger gradients that are in the opposite direction from the other two episodes. August and June episodes are typical of the summer (low magnitude anomalies, mostly within the range of [-2 K; 5 K]) with an eastward temperature gradient, whereas the September episode anomalies show higher temperatures (+8 to +10 K) along the coast and lower widespread temperatures (-3 to -4 K) in the inland. Since sea breeze is driven by the temperature gradient between the land and the sea, we expect to see a strong decrease or even an inversion of the sea breeze in the September episode.

Anomalies occurring during June and August are relatively moderate, but their patterns are different. The valleys (SV and SJV air basins) are slightly hotter in June, when the actinic flux is largest. In August the largest positive anomalies are located along the coast and the mountains in August.

Despite the variability of the temperature fields among the four episodes the episode temperature anomalies tends to be positive.

4.3 Flow Patterns

Air flow at the surface level results from the combination of synoptic and mesoscale phenomena. Synoptic motions occur in the upper atmosphere and affect the vertical structure of the boundary layer and the large-scale horizontal pressure gradients. Mesoscale flows are generated by thermal gradients and orographic forcings. They are of finer temporal and spatial scales than synoptic features (Beaver & Palazoglu, 2009).

4.3.1 Synoptic Features

In order to understand how the high-pressure systems evolve during the four episodes, we need data at a larger scale, i.e., the United States or the continental scale. We use a meteorological variable, the geopotential height, which is a vertical coordinate referenced to Earth's mean sea level — an adjustment to geometric height (elevation above mean sea level) using the variation of gravity with latitude and elevation. Geopotential height can be considered a "gravity-adjusted” height. One usually speaks of the geopotential height of a certain pressure level, which would correspond to the geopotential height necessary to reach the given pressure. Data used for this analysis are provided by NCEP/NOAA (http://www.ncep.noaa.gov/).

During the June episode, a high pressure system is located over the Pacific Ocean and it moved to California coast while another high pressure system developed in Mexico. Our modeling

domain is located in a moderately high pressure zone between these anticyclones, which simultaneously influence the California flows.

In contrast, the only high pressure system growing during the second and the third episode is onshore in the western United States. While Central California is in a moderate pressure zone during August, the highest pressures occur very close to our modeling domain in the July-August episode. Note that such anticyclonic patterns are often related to hot weather, which is consistent with the high temperature levels we observe during the July-August episode.

The high pressure systems for the September episode are different from the other episodes: it is a transition period when the anticyclone tends to move from inland to the Pacific Ocean where the high pressure system grows and expands.

Even if the location of the anticyclones differs from one episode to another, all four episodes can be more generally classified as anticyclonic. Anticyclonic systems exhibit relatively low surface wind speeds, subsidence (downward air movement) and tend to be more stagnant than cyclonic systems.

4.3.2 Summer Averages

Figure 8: Summer Average Sea Surface Pressure and Summer Average Wind

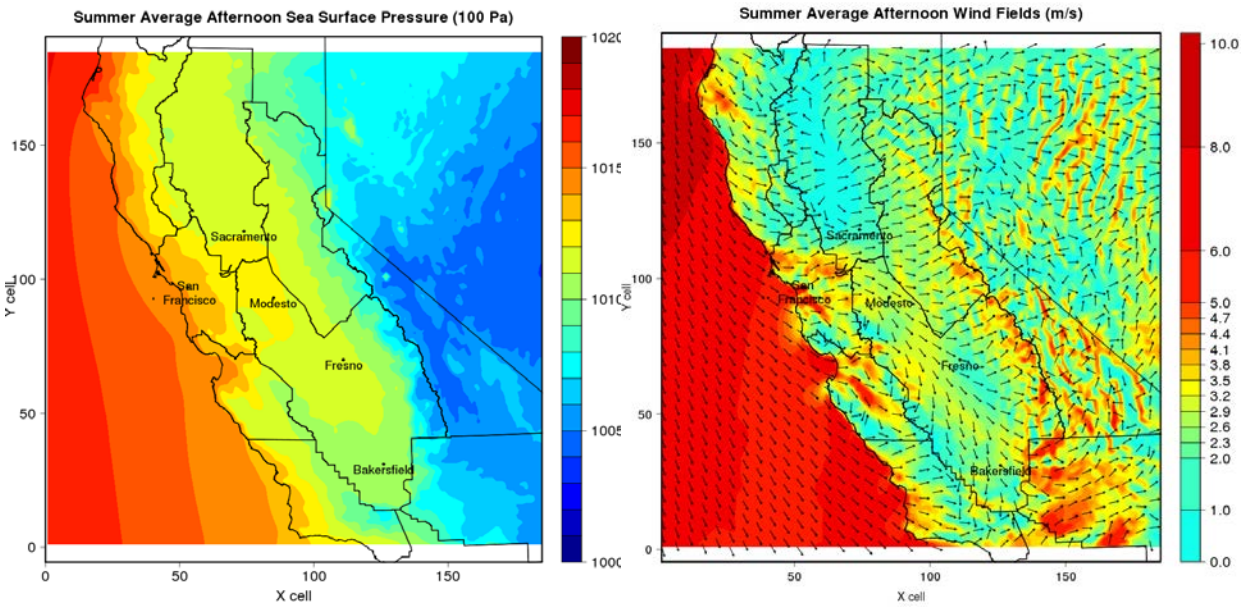

Afternoon sea surface pressure and wind fields averaged over the entire summer are presented in Figure 8 to reveal the dominant flow pattern. On typical summer days, westerly winds are funneled into the valley through gaps in the coastal range by the North Pacific High surface pressure system off the coastline, along with pollutants transported from the San Francisco Bay area (Kenyon, 1999). The sea surface pressure gradient from the land to the Pacific Ocean that we observe is also due to the temperature gradient between ocean and land. When air above the land gets warmer, it rises because of its lower density, generating a low pressure at the surface. Above the sea, cooler (denser) air is associated with higher pressures at the surface. This

imbalance between sea and land generates surface air motion from high to low pressures creating a sea breeze, a phenomenon commonly observed along coasts. Sea breeze enhances surface winds between the Pacific Ocean and Central Valley. The flow, entering the SJV through gaps in the coastal range, is confined between the SJV rims. Much of the flow is directed toward the South, providing the bulk of northwesterly flow through the SJV, and exits through the southern gap in the Sierra Nevada into the Mojave Desert, where the highest wind speeds are found (Beaver & Palazoglu, 2009).

At a smaller scale, flows are generated by thermal and orographic forcing of the low-level winds along the perimeter of SJV. During the daylight hours, mountain surfaces are heated by sunlight. Temperature contrast between the valley and mountains leads to lower pressure over the Sierras and relatively higher pressure in the valley which generates upslope flows, while at night, flows reverse creating a downslope flow that recirculates local pollutants. This downslope flow interacts with the marine flow channeling through the valley and generates a cyclonic eddy to the east of Fresno and also near Sacramento during the overnight hours, known as the "Fresno eddy" and the "Sacramento eddy" (Fujita et al. 1995).

Figure 9: SJV Study Region and Major Flows (Red Arrows) Generated under Synoptic Influences

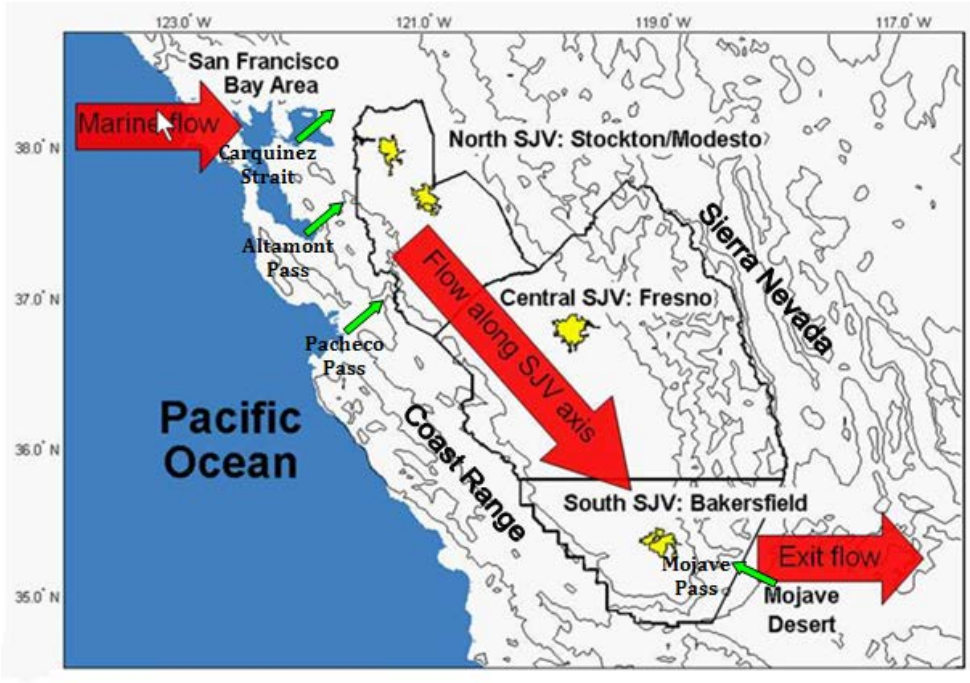

Contours are at 500, 1000, 2000, 3000 and 4000 m. Major urban areas are shown in yellow. Black lines indicate boundaries for northern, central and southern SJV. Green arrows show approximate locations of mountain passes.

Since we are concerned with the San Joaquin Valley, it is important to understand more thoroughly mesoscale phenomena occurring in this air basin. The SJV is divided into three subregions: northern, central and northern (see Figure 9) and each region contains major urban area(s) and their pollution. The urban areas are: Modesto for the northern SJV, Fresno for the central SJV, and Bakersfield for the southern SJV. Each subregion has a specific local flow feature that significantly influences its flows patterns (Beaver & Palazoglu, 2009). As explained

above, mesoscale surface pressure high pressure systems generate westerly marine flows that are channeled through the Coastal Range passes and are driven through the valley between the mountains, to finally exit through Mojave Pass. The flows are symbolized by red arrows in Figure 9.

Figure 10a and Figure 10b: Summer Average Wind Fields in the SJV at 4:00 p.m. (a) and 8:00 a.m. (b) (PDT)

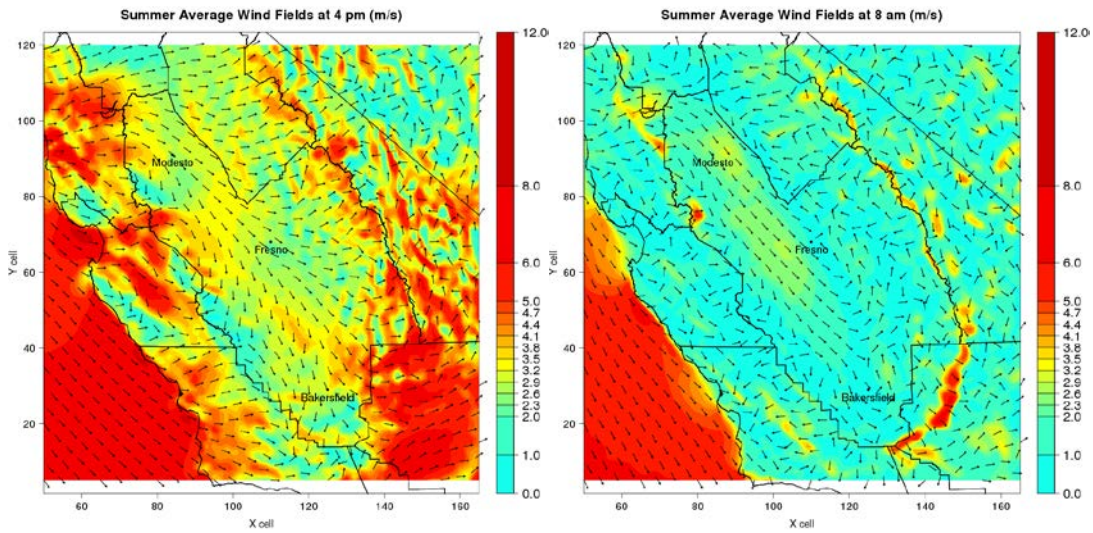

They respectively show the daytime upslope flow and the transition period in the morning in which the southernly component capturing the Fresno Eddy is visible.

In the northern SJV, the most ventilated regions are located close to Carquinez Strait, Altamont Pass, and Pacheco Pass (see Figure 10.a). In the central SJV, thermally induced flows are prevalent and deflect air flows near the valley rims perpendicular to them. Along the Sierra slopes, wind fields are strongly affected by the upslope/downslope cycle alternating easterly overnight flows and westerly daytime flows. In the evening hours, sea breeze also helps to push air up the Sierra slopes. The evening transition from upslope to downslope flow is abrupt. The Fresno Eddy, a counterclockwise horizontally oriented eddy, forms in eastern Fresno during the overnight hours due to the interaction between easterly downslope flow and marine flow channeling through the SJV. Duration of the downslope flow increases with proximity to the Sierras. In the morning, the transition from downslope to upslope flow is more gradual and takes several hours. When the downslope flow terminates, wind direction shifts southerly and opposes the marine flows. The southerly flows in the morning intercept the Fresno Eddy (see Figure 10.b) and their strength is related to the strength of the aloft eddy (Beaver, 2008) (Beaver & Palazoglu, 2009). To summarize, thermal influences in the central SJV result in Sierra drainage flows that penetrate further west during the day and the Fresno Eddy effects that extend further north at night. In the southern SJV, the predominantly northwesterly flow is deflected in a more westerly direction by the southern ranges and then it exits through the Mojave Pass to the east (see Figure 10.a). An upslope/downslope cycle very similar to the central SJV cycle occurs along the Sierra Nevada Mountains. During afternoon and evening,

flow travels upward through the Mojave Pass. It reverses during nighttime hours when the strength of the downslope flows causes the flow reversal around Bakersfield.

4.3.3 Episode Anomalies

Figure 11: Sea Surface Pressure Anomaly Averaged over [11 AM, 6 PM] for Each Episode

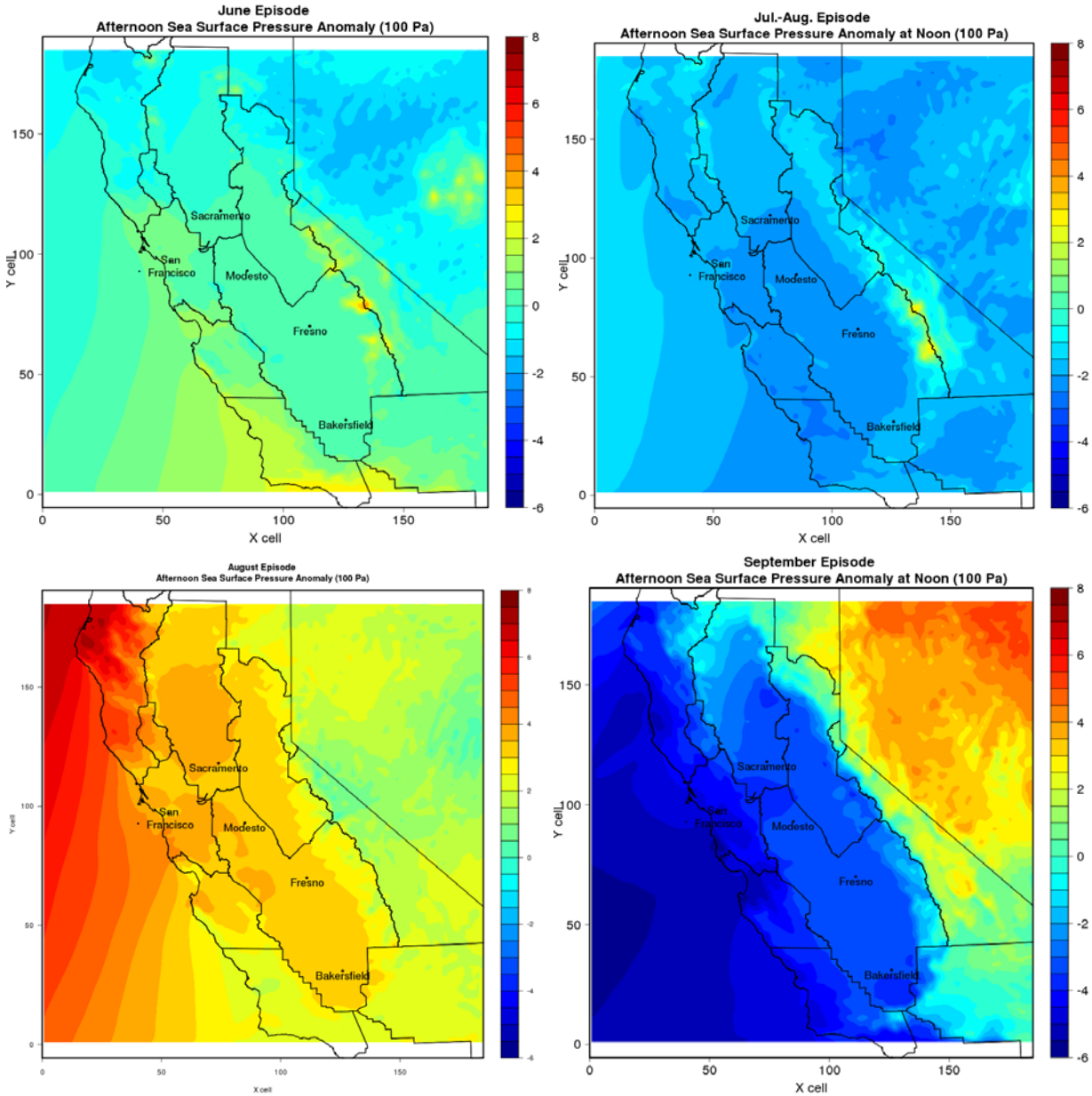

Figure 12: Surface Wind Anomaly Averaged over [11 AM, 6 PM] for Each Episode

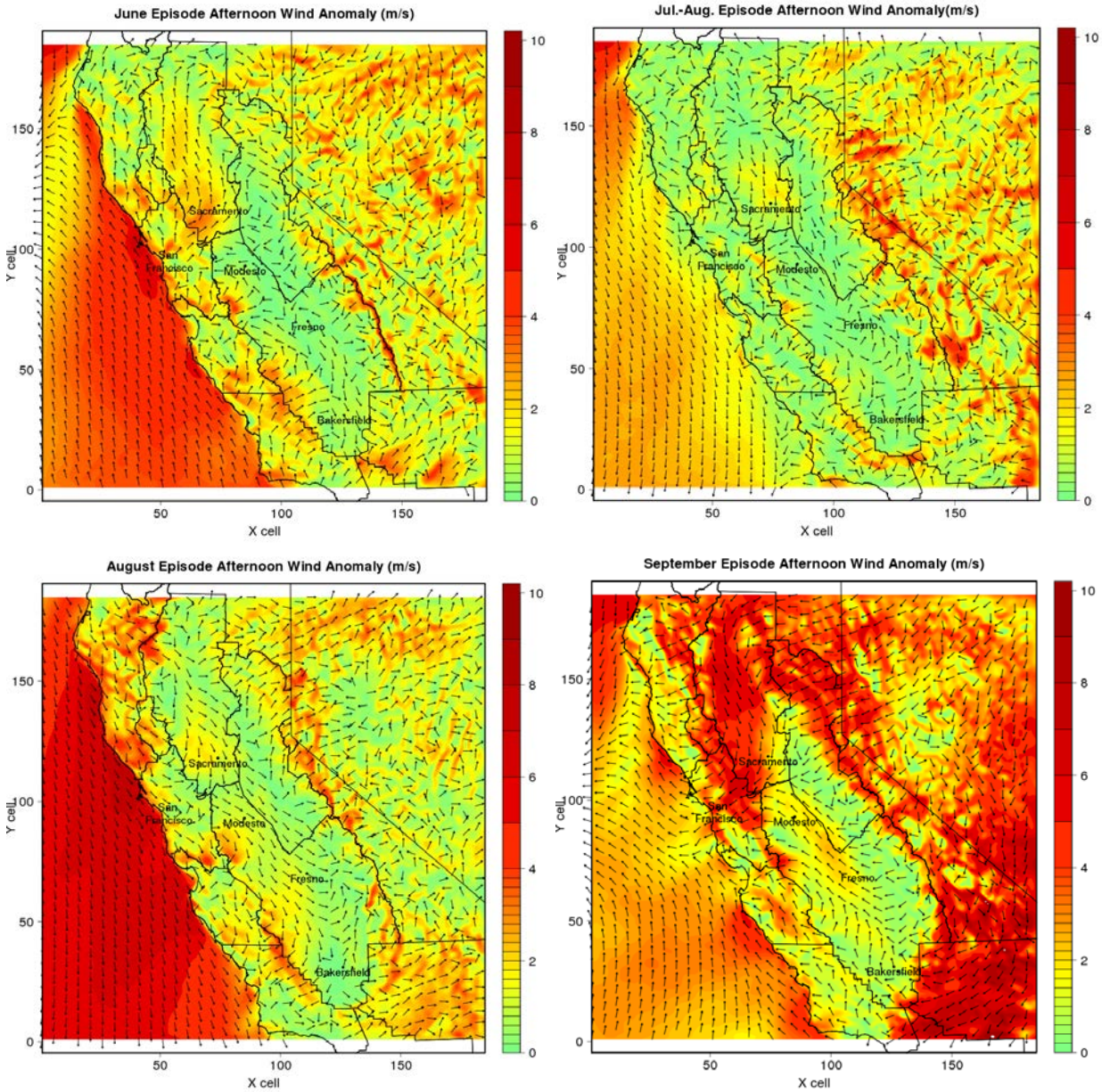

See Appendix C.1 for a zoom of the SJV wind anomaly.

Sea surface pressure maps are shown in Figure 11. An atypical sea surface pressure gradient is observed during the June episode from northern to southern Central California. A widespread depression is observed during the July-August episode but the sea surface pressure gradient is similar to the southeastern- summer average. A similar southeastern pressure gradient occurs in the August episode in the western part of the domain. The most unusual sea surface pressure pattern occurs in September: this episode shows an off-shore pressure gradient, consistent with the reversed temperature gradient.

The low anomalies occurring in the SJV during the July-August and August episodes show that the SJV winds are similar to an average summer day. The large-scale surface pressure gradient generates westerly wind, which is deflected southward by the mountains, and flows through the SJV, parallel to its axis, while thermal effects drive the flow near the valley rim and up the Sierras. The similarities in wind fields and sea surface pressure gradients between July-August and August episodes are useful in understanding the influence of temperature.

Despite similar domain-wide wind patterns, several key differences within the SJV need to be highlighted (see Appendix C.1). A key difference concerns westerly marine flows, which are more important in the August episode, especially in the northern SJV (wind speeds are around 4 m/s). This subregion is calmer in the July-August episode (wind speeds within the range of 0 – 2 m/s) and has a greater south-easterly component. Upslope flow toward the Coastal Range in the southern SJV is also stronger in the August episode. The August episode is described as "ventilated". Comparison of nighttime anomalies (see Appendix C.2) shows that July-August episode has strong downslope flow as well as the more important southerly component in the valley. Turbulent mixing in the morning is more important in the July-August episode than in August episode. The July-August episode is the most anticyclonic. These observations are consistent with the fact that anticyclonic regimes usually favor eddy development due the shallow boundary layer and limited degree of marine ventilation. The large day to night temperature swings associated with sunny hot days also contribute to the marked upslope/downslope cycle that is intimately connected to Fresno Eddy formation (Beaver, 2008).

The June episode wind fields also show typical marine flows from the SFB; however, one of their key differences is concerned with the flow in the SV. The June episode has a stronger northward component in wind fields due to its southward surface pressure gradient. Westerly wind in the SJV is weaker during the August episode, which has stronger flow between the SFB and the SJV through the gaps, notably the Pacheco Pass, in the northern SJV. In the southern SJV, an important anomaly occurs along the Coastal Range where a daytime upslope flow toward the valley develops and an even more pronounced upslope flow develops at night.

The September episode is abnormal almost everywhere in the modeling domain, as illustrated by the September anomaly map. To understand this episode the wind fields and their anomalies are plotted (see Appendix C). A very important extensive anomaly occurs in the eastern part of the domain, behind the Sierra Nevada Mountains, where there is a strong north-westerly flow. Nevada does not affect directly the SJV in our study because the model does not capture the influence of Nevada since no emissions were included for Nevada. The key feature of the September episode is the absence of marine flow. The SFB as well as the SJV are stagnant while a strong southerly wind blows through the SV. Referring to this stagnant regime occurring in the SJV, this episode will be referred to as the "stagnant" episode. This behavior is consistent with the abnormal temperature and sea surface pressure fields observed in September. Another characteristic of September episode is the strong downslope flow from the Sierras at night (exhibited in Appendix C.2) and the important and extended southeasterly flow anomaly near Fresno.

4.4 8-h Ozone

4.4.1 Summer average

Figure 13: Summer Average 8-h Ozone Concentrations over [11 AM, 6 PM] (PDT)

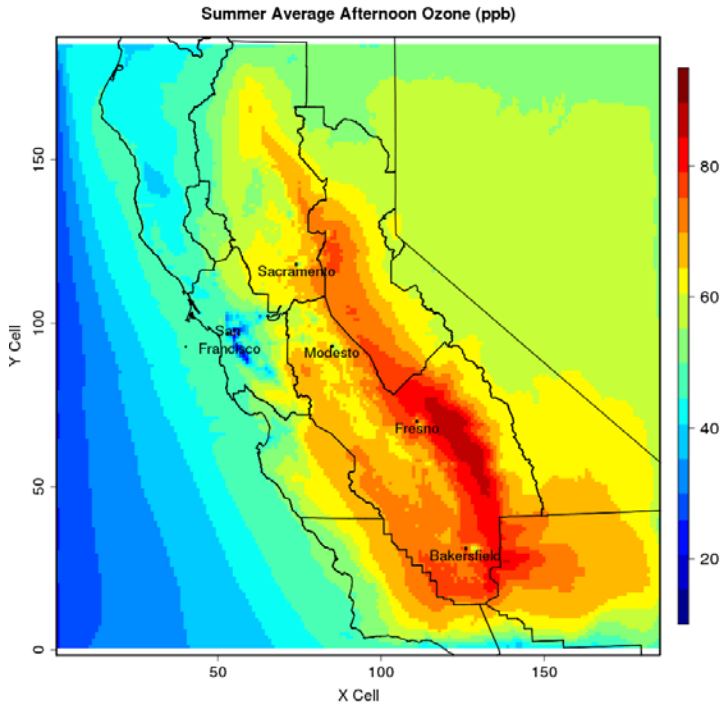

Afternoon ozone levels averaged over the entire summer are shown in Figure 13. Despite SFB being a major ozone precursors source, ozone levels in this air basin are relatively low since the pollutants are transported by the westerly marine flows toward the valley, where they accumulate, and are confined by the mountains. Consequently high ozone concentrations are observed in the valley (frequently higher than 60 ppb averaged over 8 hours) especially in the mid-southern parts of the valley where air is trapped by the surrounding mountains. The highest ozone levels (> 75 ppb) occur in the SJV especially downwind of Fresno and Bakersfield, extending from there to the foothills of Sierras. High ozone levels also occur south of the SFB along the coastal ranges. These high concentrations are directly related to the downslope flows occurring overnight and are a consequence of mixing these with morning rush hour emissions (Beaver, 2008). Ozone levels in the northern SJV and along SJV axis are relatively lower because of the marine ventilated flow entering SJV through gaps in the Coastal Range that channel through the valley.

4.4.2 Episode Anomalies

Figure 14: 8-hr Average Ozone Concentrations Anomalies over [11 AM, 6 PM] (PDT) for Each Episode

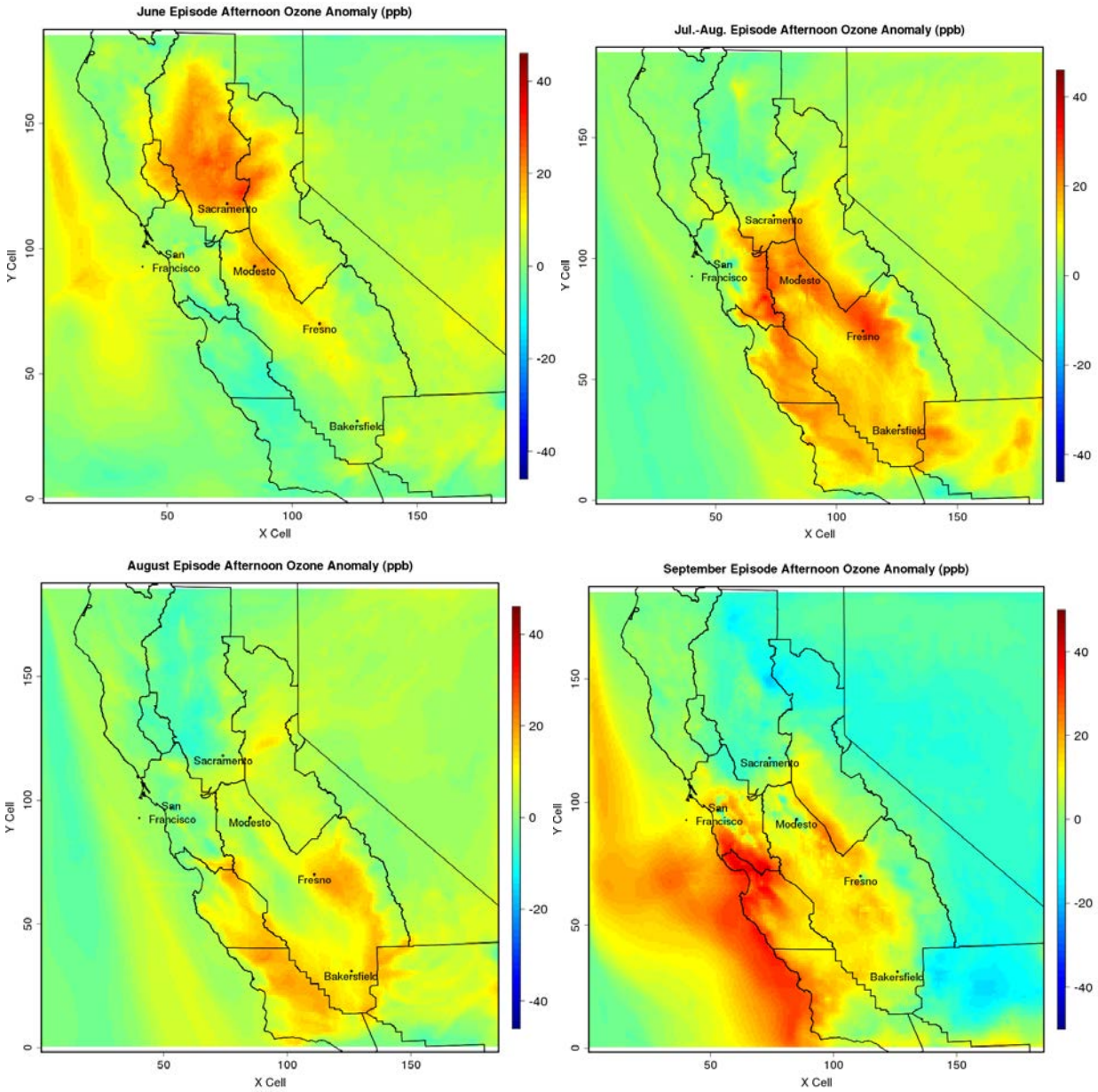

The four episodes all show higher than average ozone levels. These levels are directly related to their anticyclonic regimes. Low surface wind speeds, subsidence and increased stability inhibit pollutants dispersion. Hot, sunny anticyclonic settings also favor increased photochemical activity (Beaver & Palazoglu, 2009). The anomaly magnitudes and spatial patterns (Figure 14) associated with the four episodes are different from one another.

The July-August episode has greater anomalies than the August episode due to its higher temperatures. Higher temperatures are conducive to higher ozone concentrations, as shown in previous studies (Bloomer, Stehr, Piety, Salawitch, & Dickerson, 2009) (Sillman & Samson, 1995). The August episode shows lower ozone anomalies in the northern SJV and in the middle of the valley because of the marine ventilation. In contrast, the more stagnant regime occurring in these areas during the July-August episode is prone to higher ozone levels. The presence of a stronger Fresno Eddy in the latter episode moves pollutants more to the North and explains the high ozone anomalies north of Fresno in July-August, whereas anomalies along the Sierra Nevada are located in the area south of Fresno to Bakersfield in the August episode.

All episodes, except the June episode, have a negative ozone anomaly in the SV. We can easily link this anomaly to the slow wind speed or the wind blowing southwards (important anomaly in September) in this air basin that prevents transport of pollutants from the urban area around Sacramento and from the SFB to the northern SV. Important and extended anomalies in the SV, such as those in the June episode, are due to the presence of southerly winds in this valley, transporting pollutants from the SFB and from the urban area around Sacramento farther north. In the SJV, ozone anomalies are located along the highway 99 (passing through Modesto, Fresno and Bakersfield urban centers), which implies that pollutants remain close to their sources when marine westerly flows are weaker.

In September, the major wind anomaly occurring in the eastern part of the CCOS domain is the reason that the relatively low ozone concentrations are found in this region. Ozone in Nevada is only present because of transport from other air basins (no Nevada emissions are included in the model). Without westerly marine ventilation, ozone is not transported far from sources. The large excess of ozone along the coast is due to pollutants transport from the other air basins. The high temperatures found in the same area are also another reason why ozone levels can increase in this coastal region. The September episode-specific flow pattern is related to an unusual ozone gradient from the east to the west. The SJV exhibits moderate widespread anomalies, which are located more to the west, in the September episode.

CHAPTER 5:
First Order Sensitivity Analysis

5.1 Ozone Peak Time Statistical Analysis

Ozone concentrations are averaged over an 8-hour period because this is the averaging time required by the Federal NAAQS.

Sensitivity coefficients are based on ozone concentrations at a given time and location. A choice has to be made concerning which ozone concentrations should be used when discussing sensitivities. A possible option is to focus on the daily maximum ozone concentration, i.e., to use the daily ozone peak. The peak occurs at different times, and depends on both the date and location. This introduces a complication when one is trying to establish a link between meteorology, ozone concentrations, and ozone sensitivities. Another choice is to use the 8-h ozone average peak time. Histograms of the frequency of the 8-h ozone average peak time for the four episodes are shown in Figure 15 for 8h ozone levels > 75 ppb. Note here the peak time H is defined when the 8h ozone average maxima occur for the 8 h interval [H-3, H+4]. From the histograms we can see most of the 8-h ozone maxima occurred in the [11, 18] or [11AM, 6PM] interval, i.e. H=14. Therefore, it is reasonable to choose this interval to discuss our findings.

Figure 15: Frequencies (Shown as Probability Density) of the Peak Time of 8-h Ozone Average Maximum (for 8h Ozone Average Levels > 75 ppb) for Each Episode

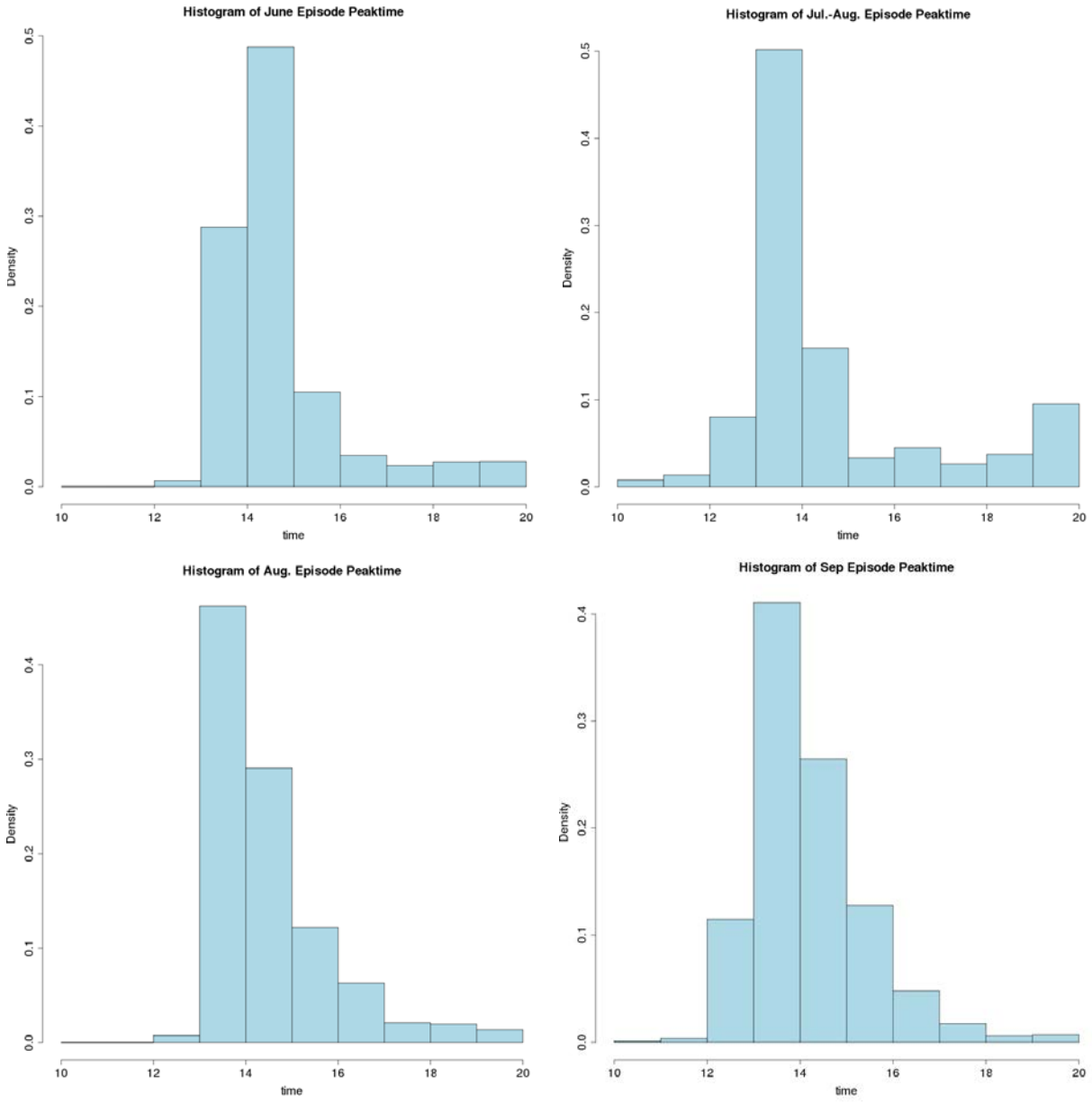

NB: The histogram cells are intervals of the form '(a, b]', i.e., they include the right-hand endpoint, but not the left one, with the exception of the first cell which includes both the right-hand and left-hand endpoints.

5.2 Ozone Sensitivities and Control Options

Ozone sensitivity describes how ozone concentration varies as a function of variations in one of its precursors. Ozone sensitivities to domain-wide anthropogenic NOx emissions ($\frac{\partial[O_3]}{\partial \varepsilon_{E_{NO_x}}}$) and to anthropogenic VOC (AVOC) emissions ($\frac{\partial[O_3]}{\partial \varepsilon_{E_{AVOC}}}$) are used to determine ozone-limiting reagents. Three ozone control options are defined, based on the relationship between the two sensitivity coefficients.

Figure 16 describes the definition of each control option. The "VOC control" option is preferred when reducing AVOC reduces ozone concentration and reducing NOx emissions would increase ozone concentrations (NOx disbenefit). The "NOx control" option is preferred when a percentage reduction in NOx emissions results in larger decreases in ozone concentrations than the same percentage reduction in AVOC emissions. Between these two options, the third option is in a transition regime, where reducing NOx emissions can reduce ozone concentrations but it is not as effective as reducing AVOC by the same percentage. In the transition regime, both sensitivities are small and positive. A decrease of either of the precursors would lead to a decrease in ozone, but relatively less efficiently than in limited regimes.

Figure 16: Definition of Ozone Control Options in Terms of Ozone Sensitivity Coefficients, i.e., Ozone Concentration Sensitivity with Respect to NOx and/or VOCs Concentrations

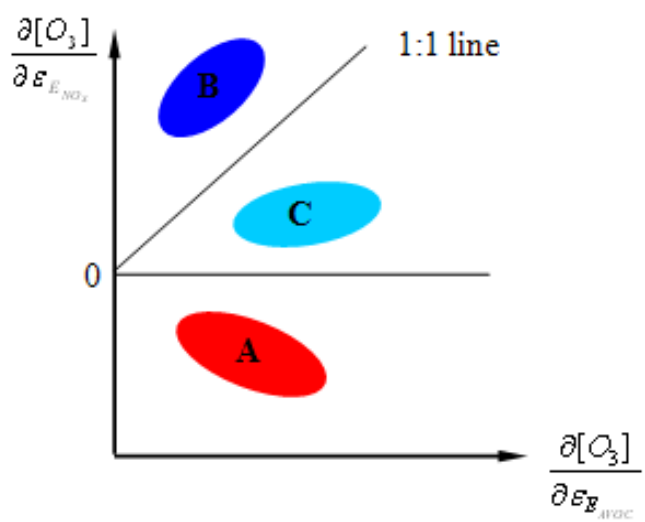

Definition of Ozone control options:

A: $\frac{\partial[O_3]}{\partial \varepsilon_{E_{NO_x}}} < 0$, VOC control,

B: $0 < \frac{\partial[O_3]}{\partial \varepsilon_{E_{AVOC}}} < \frac{\partial[O_3]}{\partial \varepsilon_{E_{NO_x}}}$, NOx control,

C: $0 < \frac{\partial[O_3]}{\partial \varepsilon_{E_{NO_x}}} < \frac{\partial[O_3]}{\partial \varepsilon_{E_{AVOC}}}$, Transition.

The signs of the sensitivity coefficient determine the control regime as indicated in the figure legend.

Figure 17: Ozone Sensitivities to NOx and AVOC and Ozone Control Regimes for Each Episode

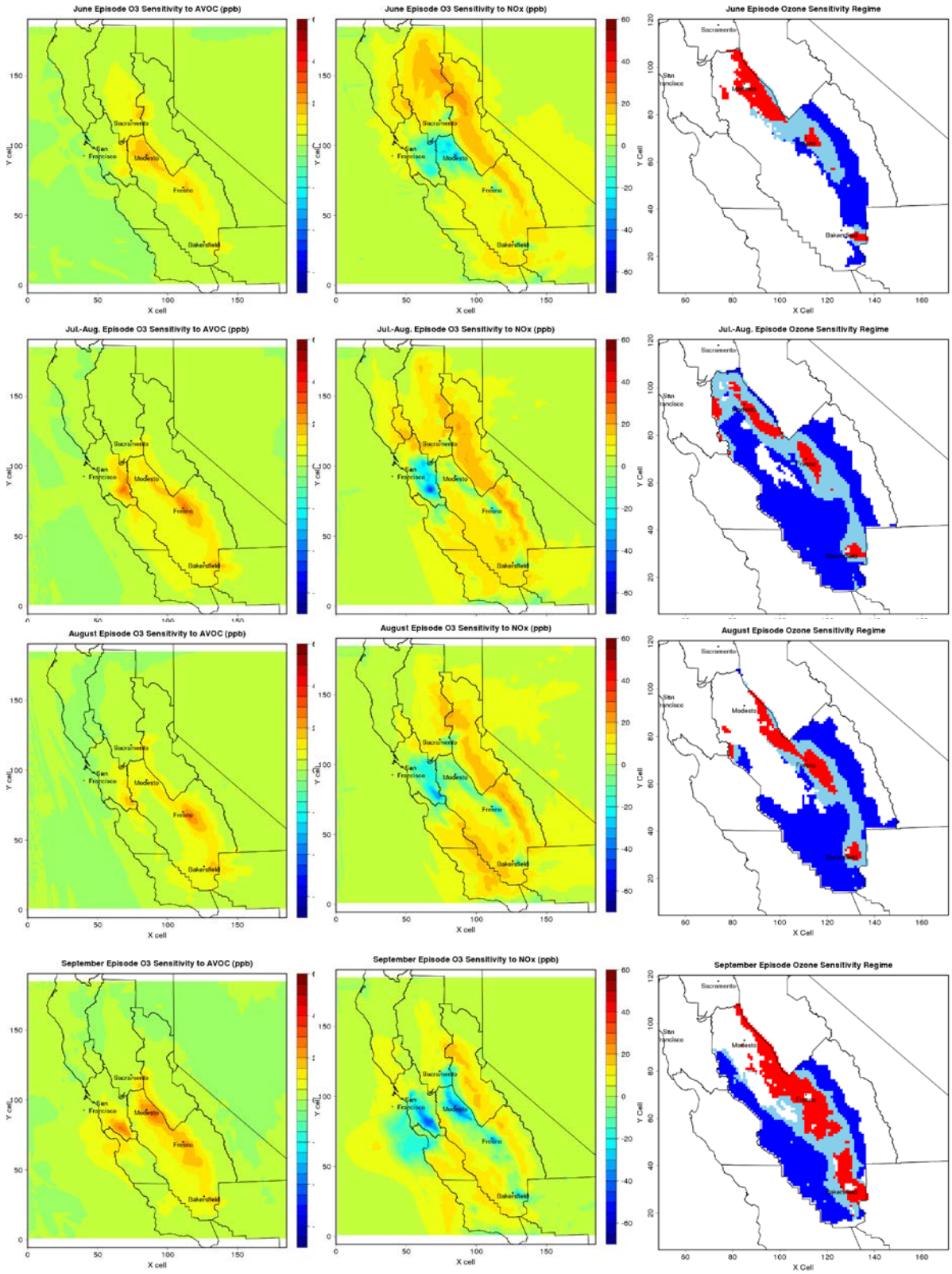

Control options are color coded: Red-VOC control; Dark-blue-NOx; Light-blue-transition regime as indicated in the third column of Figure 17. White indicates areas where the maximum 8-hour average oxone does not exceed 75 ppb.

Ozone sensitivities to AVOC (Figure 17 first column) are positive throughout the domain, which indicates reducing AVOC leads to lowered ozone levels. Greater ozone sensitivities to AVOC tend to be located in the areas where NOx emissions are also large. Ozone sensitivities to NOx change signs (Figure 17 second column). The negative sensitivities indicate a NOx-disbenefit. In general, the urban areas: Bay area, Sacramento, urban areas in the SJV, such as Fresno and Bakersfield, all exhibit a NOx disbenefit across the various meteorological conditions associated with the different episodes. The spatial extent of the NOx-disbenefits changes from episode to episode, especially for the northern part of the SJV.

Ozone control option maps (Figure 17 third column) are plotted for the cells where the 8-h ozone average concentrations are over 75 ppb. This ozone level is the current national ambient air quality standard for ground-level ozone, and is commonly referred as the 2008-standard. The white areas are those where the 8-hour average ozone concentrations do not exceed the 2008 standard and the colored areas indicate the extent of ozone exceedances. All the episodes except the June episode exhibit extensive ozone exceedances. At the high ozone (>75 ppb) locations, the extent of the NOx-disbenefit (colored in red) varies across the meteorological conditions associated with the various episodes. Focusing on a single ozone episode (July-August), in a previous study Jin et al. (2008) found that NOx-control was overall more beneficial for reducing 8-h ozone in the July-August episode. By considering different meteorological conditions, these later results indicate that AVOC control (colored in red) becomes important especially for the most stagnant (September) episode.

Meteorology variations lead to differences in ozone sensitivities and resulting control options among episodes. Anthropogenic emissions have been held constant for the various episodes. In the following, we focus on ozone control options in the SJV by comparing episodes, which differ mainly by only one variable, i.e., wind patterns or temperature levels.

5.2.1 Wind Patterns Effects

June, August and September episodes exemplify three very different flow patterns with similar moderate temperature levels. In the stagnant flow regime (September episode), NOx- disbenefit areas located around urban centers along highway 99 tend to be more extensive. Winds do not carry precursors (especially NOx) as far as in the other episodes and emissions from sources tend to remain more localized. Moreover, stagnation prevents dilution of pollutants, and this results in higher concentrations of anthropogenic emissions notably NOx. This explains why sensitivities to NOx are the lowest (negative values) in these areas. Under such conditions AVOC control is preferred near urban centers, while NOx control appears to be the best option for the remainder of the region. More areas are in the transition regime and ozone control in these conditions is particularly challenging because reducing both precursors is not particularly efficient for reducing ozone.

In more ventilated conditions (August episode), VOC-limited areas are smaller but more numerous. Whereas NOx control is more efficient for the largest part of the SJV, urban centers along the federal highway, where population is highest and exposure is greatest, would still benefit from AVOC control. This case is even more complicated because pollutants are transported from one air basin to another, i.e., from the SFB to the SJV. A NOx-disbenefit area

exists along the SFB-SJV border as a result of NOx transport from the Bay Area to the northern SJV. Consequently precursors emissions reductions may have to be performed upwind as well as locally to be really effective. This requires studying local vs. interbasin contributions, which was accomplished in this study and will be discussed in greater detail subsequently.

The June episode is particularly interesting because it has an important southerly wind anomaly in the SV that results in the highest ozone anomalies in the SJV air basin. In this specific case, the northern SJV is mostly VOC-limited whereas the remainder of the air basin would benefit from NOx-control. Indeed pronounced winds from the SFB through Pacheco Pass transport pollutants to the northern SJV, which is relatively stagnant, leading to the extensive NOx-disbenefit area in the northern SJV. Effective contributions of each air basin are discussed in the various subsections of Section 5.3.

5.2.2 Temperature Effects

We will use the detailed episodic characterization provided in the previous chapter to assess the influence of temperature on control options by making a comparison of the July-August and August episodes. Ozone regime patterns during the two episodes look very similar but have fewer VOC-limited areas in the hotter (July-August) episode, especially in the northern SJV. Sensitivity to AVOC does not significantly vary between the two episodes, while sensitivity to NOx increases with temperature. A previous study (Jin et. al., 2010) showed that increasing the temperature without changing any other parameters generally leads to an increase in ozone concentrations, increases sensitivity to VOC, and decreases sensitivity to NOx. These results appear to contradict the current results, but they merely illustrate that other factors are in play. Temperature alone cannot explain the difference in ozone limiting reagent patterns. In addition to affecting chemical reaction rates, temperature also affects other physical parameters like the height of the planetary boundary layer (PBL). On the western side of the SJV the hotter July-August episode has a lower PBL height (see Appendix D.1, Figure D-1), on the northern SJV and a higher PBL on the central and southern SJV. PBL height defines the upper limit of the shallow layer of the atmosphere. In this layer, physical quantities such as flow velocity, temperature, moisture etc., display rapid fluctuations attributable to turbulence and vertical mixing is strong. Pollutant mixing, dilution, reactions, etc. occur within this layer. A lower PBL height generally leads to less dilution and higher concentrations of pollutants. Since VOC lifetimes are longer than NOx lifetime, lower PBL heights mainly affect NOx chemistry and tend to accelerate it locally causing a local decrease in NOx sensitivity.

There is also an increase of biogenic emissions with temperature (see Figure 5 indicated by green bars) that could contribute to the increase in area of the NOx-limited regime dominance in the July-August episode (see Appendix D, Figure D.4) shows similar BVOC concentrations at 4:00 p.m. in the SJV and the Sierras in the July-August and August episodes. Since BVOC emissions are greater in the July-August episode, we assume that more BVOC have reacted in the hot episode. The high concentrations of OH found in the hot episode (see Appendix D, Figure D.5) support this idea.

As noted previously, wind fields in the northern SJV are different in the two episodes. The August episode shows a strong northwesterly flow, which allows the transport of pollutants

from the Modesto urban center toward the south along the Highway 99, which is also a pollutant source, leading to pollution accumulation. In contrast, the July-August episode shows a southerly wind anomaly component in the northern SJV, transporting pollutants to remote areas where there are no emissions, and consequently diluting the pollutants more effectively. To assess the influence of wind direction on dilution, a flow balance analysis is performed on a subregion to the east of Modesto (where the major changes in the limiting reagent regime occur, see Appendix D, Figure D-6) for NO (which accounts for 90 percent of NOx emissions). Figure D-6 reveals that NO accumulates more in the August episode within the subregion since more dispersion occurs in the July-August episode. In the hot episode, the negative sensitivity to NOx tends to become less negative, which implies that the titration of ozone by NO (Reaction 1.3) is less efficient (see Section 2.1.2). To support this hypothesis, NO, NO_2 and ozone concentrations have been plotted for the same subregion (see Appendix D, Figure D-6). In the July-August episode, ozone concentrations are higher, but NO concentrations are lower than in the August episode, while NO_2 concentrations are similar, and this implies that titration is actually less effective in the July-August episode. Emissions of NO are the same in the two episodes, but NO concentration differ due to the greater dispersion of NO in the July-August episode, and this difference is responsible for the decrease in magnitude of the ozone sensitivity to NOx.

5.2.3 Alternative Emission Cases

In order to isolate the meteorological effects on the ozone response to precursor emissions, Monday anthropogenic emissions (thereafter called "ORIG" emissions) are used for each day of the four episodes. In reality, anthropogenic emissions can have short-term variations, such as a weekly cycle of emissions. In such a cycle, NOx emissions decrease on weekends due to decreases in diesel truck traffic (e.g. Tonse et al. 2008). Emission controls and population growth may also contribute to longer-term variations in emissions. In addition, the model emission inputs may have uncertainties and thus deviate from real world values. Emission changes can affect both ozone and ozone sensitivities by altering the availability of precursor species. Hence, the spatial distribution of ozone exceedances and the associated ozone control options derived under the "ORIG" case emissions for a given episode may be different from the ones derived under alternative anthropogenic emissions.

Figure 18 Control Options as Determined from the Sensitivity Analysis under Three Alternative Emission Cases: mAVOC, mNOx, mAVOCmNOx Where the m Indicates That the Emissions Are Reduced by 20% of the Nominal Value

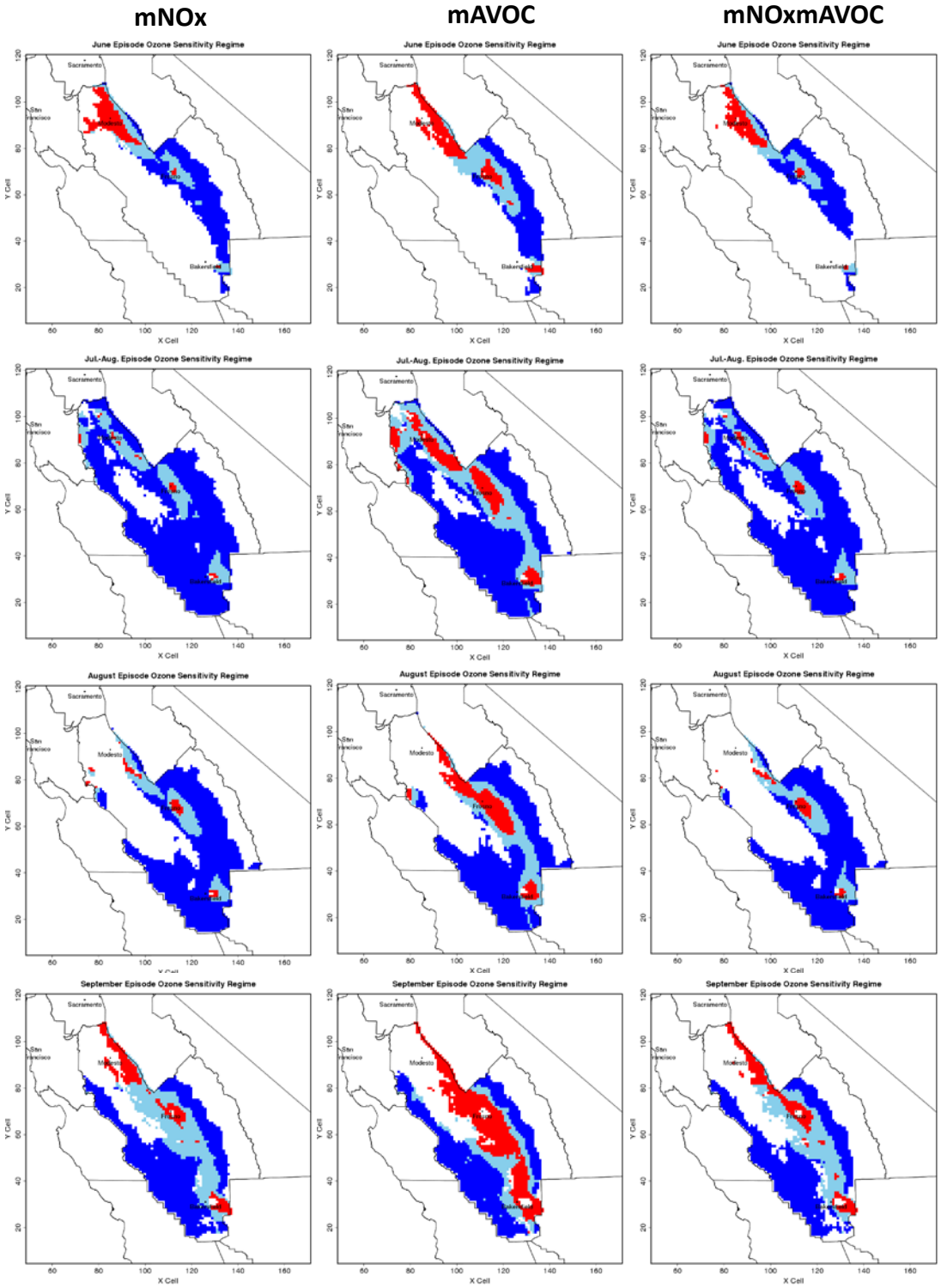

Control options are color coded: Red-VOC control; Dark-blue-NOx; Light-blue-transition regime. White indicates areas where the maximum 8-hour average oxone does not exceed 75 ppb.

We have conducted first order ozone sensitivity analysis for three alternative emissions defined in Appendix E:

Case '**mAVOC'**: AVOC emissions are reduced by 20 percent;
Case '**mNOx'**: NOx emissions are reduced by 20 percent;
Case '**mAVOCmNOx**': Both AVOC and NOx emissions are reduced by 20 percent.

The control option maps are plotted in Figure 18. In general, reducing AVOC emissions (i.e. mAVOC) has a smaller impact on the ozone sensitivities than reducing NOx or reducing both NOx and AVOC (i.e. mNOx or mAVOCmNOx), which can be seen in the difference maps shown in Appendix D.7. This is also reflected in the control option maps (Figure 18): mAVOC case (first column) has similar spatial distributions as the ORIG case shown in Figure 17. Reducing NOx has the greatest impact on both ozone levels and ozone sensitivities. Under mNOx or mAVOCmNOx cases, ozone sensitivities to NOx generally increase while ozone sensitivities to AVOC decrease, and changes are greater near larger emission sources (Appendix D.7). The net effect usually causes the ozone chemistry to shift towards NOx limitation, which leads to larger areas requiring NOx control. Examination of Figures 17 and 18 reveals that the red and light blue areas in Figure 17 are replaced by the light blue and dark blue, respectively in Figure 18. Changes in control options are limited to regions close to large emission sources (Fresno, Bakersfield, or the northern SJV).

The control options are only plotted for the locations in the SJV where ozone concentrations are greater than 75 ppb, and the colored areas indicate the extent of ozone exceedances. Comparison of the spatial extent of colored regions in Figures 17 and 18 (third column) can be used to examine the effects of various precursor emission reductions on the elimination of ozone exceedances.

Table 2: Changes in Ozone Exceedances in the SJV (% of Number of Grids with Ozone > 75 ppb) under Alternative Emission Cases

	-20% NOx	-20% AVOC	-20% AVOC & -20% NOx
June	-12	-14	-29
Jul-Aug	-8	-4	-13
August	-12	-7	-18
September	-7	-10	-17

Table 2 summarizes the percentage changes in the number of grids with ozone exceedances (>75 ppb) when the base emissions are reduced by various amounts. The effectiveness of VOC vs. NOx controls varies with episode. The July-August and August episodes benefit more from NOx control, while the June and September episodes benefit more with AVOC control. Among all the emission reduction cases considered, the July-August and September episodes showed smaller decreases in the spatial extent of ozone exceedances, which indicate the challenges of ozone control under these two sets of meteorological conditions. The July-August episode

exemplifies the highest temperature conditions and the September episode represents the most stagnant conditions.

Zhao et al. (2011) investigated air quality related meteorological conditions under future climate and found that the SJV will likely experience increases in the intensity of stagnation as well as increases in temperature levels. Consequently, frequencies of occurrence of the meteorology regimes exemplified by the July-August and September episodes may increase under future climate, which could results in even larger challenges in ozone control.

5.3 Local Versus Interbasin Contributions

Typically, emissions are perturbed across the whole modeling domain for calculating ozone sensitivities, so that all possible anthropogenic emissions that may influence air quality are included. The ozone control options derived from these sensitivities are a "regional decision". However, air quality is managed at the scale of air basins rather than regionally. The first-order sensitivity to domain-wide emission changes for any location is equal to the sum of ozone sensitivities to emissions changes associated with each air basin. These various sensitivities may vary greatly in magnitude and sign. Understanding contributions from each air basin is particularly important for the SJV because it is downwind of large emissions sources like the Bay Area, and its role in SJV air pollution is not well understood. It is not clear whether the "regional decision" should be applied to SJV or whether specific upwind air basins should be included to achieve effective ozone control. In this chapter, we evaluate the source-receptor relationships between the SJV, the SFB and the SV air basins as a function of meteorological conditions and focus on the local versus upwind contributions to ozone sensitivity in the SJV.

5.3.1 Ozone Sensitivity to NOx and AVOC Emissions from the SJV, the SFB and the SV

Sensitivity maps are shown and described in Appendix E. In this chapter, the focus is on the relationships between meteorology and ozone sensitivity patterns and magnitudes.

Comparison of the July-August and August episodes confirms that the magnitude of the ozone sensitivity to NOx varies between these episodes. The sensitivity patterns are most different in the northern part of the SJV. Interbasin contributions are due to pollutant transport from different air masses; hence, they are directly related to wind speed and direction. Comparison of the June, August and September episodes is performed to evaluate qualitatively the influence of each air basin's emissions as a function of meteorology.

A stagnant flow regime, as exemplified by the September episode, has little interbasin transport associated with it. Although there is turbulent mixing in the morning, as evidenced by the presence of the Fresno Eddy, stagnation prevents dispersion of pollutants during the day and enhances their recirculation in the morning after the commute periods. Consequently this regime emphasizes a NOx-disbenefit in the SJV that is locally based.

The June episode shows the strong influence of precursors emissions from the SFB on the northern SJV. The NOx disbenefit occurring near Modesto is mainly due to NOx emitted in the Bay Area, transported through the Coastal Range gaps, that accumulates in the northern part of

the valley as a result of the weak ventilation flow occurring in this area. In this type of episode, a reduction of SFB NOx emissions would increase the ozone in the northern parts of the SJV Southwesterly marine wind also carries SFB NOx emissions to the southern SV, affecting the Sacramento urban center. This episode is less sensitive to local emissions than the September episode.

In the August episode, stronger marine ventilation leads to greater sensitivities to SFB NOx along the western side of the northern SJV. In this episode the northern part of the valley is also influenced by air masses containing SV emissions. Ventilated episodes are the only episodes that allow an upwind contribution of the SV.

We can almost classify the SFB as an emission source because this air basin is not downwind of other significant basins in most cases. When it is (September episode), the influence of the upwind region (the SV) is very small. Similarly, the SJV is a receptor of emissions and air masses from other air basins, especially the SFB. Locations of affected areas within this air basin depend on the wind patterns. The SV can be either a source or a receptor of air masses from the SFB depending on the wind direction.

5.3.2 Predominant Contribution Patterns within the SJV

Sensitivity maps are useful for understanding how emissions from a specific air basin influences ozone levels in downwind regions as a result of prevailing meteorological conditions. The maps do not capture the relative contributions of local vs. upwind air basins (of the SJV) to the ozone sensitivity at a given location. To evaluate the relative contributions of local and interbasin sources to SJV sensitivities, we use the sensitivity to AVOC as a percentage of total sensitivity. We designate this as the "contribution, " and it is the relative sensitivity to SJV AVOC emissions and defined as:

$$C_{SJV,AVOC}\ (\%) = \frac{S_{SJV,AVOC}}{S_{AVOC}}$$

where C is the contribution, $S_{SJV,AVOC}$ is the sensitivity to SJV AVOC emissions and S_{AVOC} is the ozone sensitivity to domain-wide AVOC emissions.

Sensitivities to AVOC are used to evaluate contributions instead of sensitivities to NOx for three major reasons. First, sensitivities to AVOC are always positive and always contribute to the total sensitivity. In contrast, sensitivities to NOx may be positive or negative, and consequently may have a 'negative' contribution to the total sensitivity. Second, VOCs have a longer lifetime in the air before being consumed. They are more likely to be transported farther downwind than NOx and can capture better how wind fields influence the transport of pollutants. Third, our study has shown that AVOC controls are important for urban areas where dense population reside and for half of the meteorological conditions considered here (June and September). Using AVOC sensitivities allows us to quantify local vs. upwind contributions. A "contribution map" is shown in Figure 19: contributions greater than 50 percent indicate a major local influence, while contributions less than 50 percent indicate a greater contribution from upwind air basins, i.e., the sum of all upwind air basins but the SJV. In this way we can develop the notion of a "contribution pattern", i.e., how local and upwind contributions

spatially evolve within an episode, and evaluate the variability of this pattern with meteorology.

Figure 19: Contribution Maps Associated with Each Episode That Indicates the Relative Importance of Local vs. Upwind Contributions to Ozone Sensitivity to AVOC

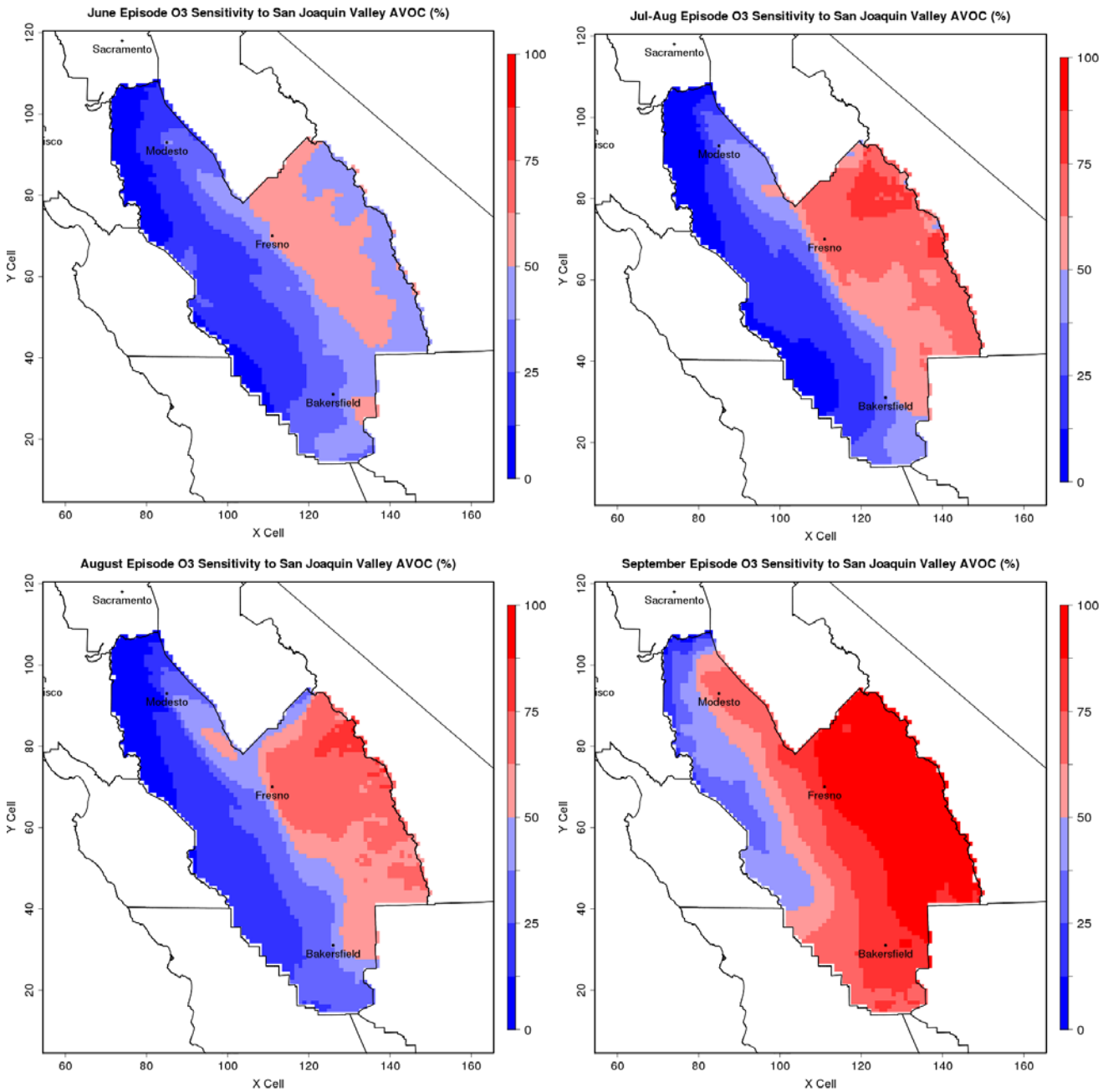

Light blue to dark blue indicates that the larger contributions come from upwind air basins (i.e. <50% from local sources). Pink to red areas indicates that the larger contributions to the sensitivity come from the local air basin (i.e. >50% from local).

Due to their similar wind fields, the July-August and August episodes have similar contribution patterns as seen in Figure 19. Temperature may influence ozone chemistry and biogenic emissions but it does not exert as strong an influence on pollutants transport as the presence of

a strong marine ventilation flow through the SJV. The contribution to the SJV ozone sensitivity to AVOC tends to be from more local sources on the eastern side of the valley. Westerly winds carry pollutants emitted along the transport corridor farther to the south, while slope flows drive pollutants toward the Sierra Nevada foothills. The western side is more sensitive to upwind emissions indicated by blue color. In the July-August episode, the south-easterly wind anomaly component in the northern SJV is associated with a local contribution from Modesto that is closer to the source. With a stronger north-westerly wind component (August episode), precursor pollutants are transported farther to the south and their influence is extended over a longer distance. The smallest local contribution occurs in the June episode, and is limited to the western side of the SJV. We observe the same East/West separation as in the August episode, except in the northern SJV where the major contribution comes from upwind areas. The strong flow through the Pacheco Pass (northern SJV) transports SFB emissions to the northern SJV, which influence this region more than the local emissions from Modesto. In stagnant conditions (September episode), ozone levels can be entirely controlled by reducing local emissions as suggested by the local contribution that dominate over most of the SJV.

In summary, upwind and local contributions are highly variable with meteorology (namely wind strength and direction) and location. Within the SJV, we define four areas, which best capture the variability of the contribution pattern to the meteorology: in the northern and southern parts of the SJV, local vs. upwind contributions vary with meteorology; in the middle part of the SJV, the western side is mostly dominated by upwind sources and the eastern side is mostly dominated by local sources. The variability of SJV ozone sensitivity to NOx and VOC emissions from local versus upwind air basins is described in greater detail in the next section.

5.3.3 Contribution of the SJV, the SFB and the SV to SJV Ozone Sensitivity

Highest ozone levels in the SJV are found in the eastern and western sides of it, more precisely along and downwind of Highway 99 and Interstate 5. The northern, the eastern and the western SJV have different sensitivity patterns to local and upwind emissions of NOx and AVOCs within the different episodes. To understand this better, the meteorology influences on ozone sensitivity contributions are investigated along eastern and western transects (shown, respectively in red and green in Figure 20-22), Each transect starts in the northern part and ends in the southern part of the SJV.

Figure 20: Eastern (Red) and Western (Green) Transects in the SJV

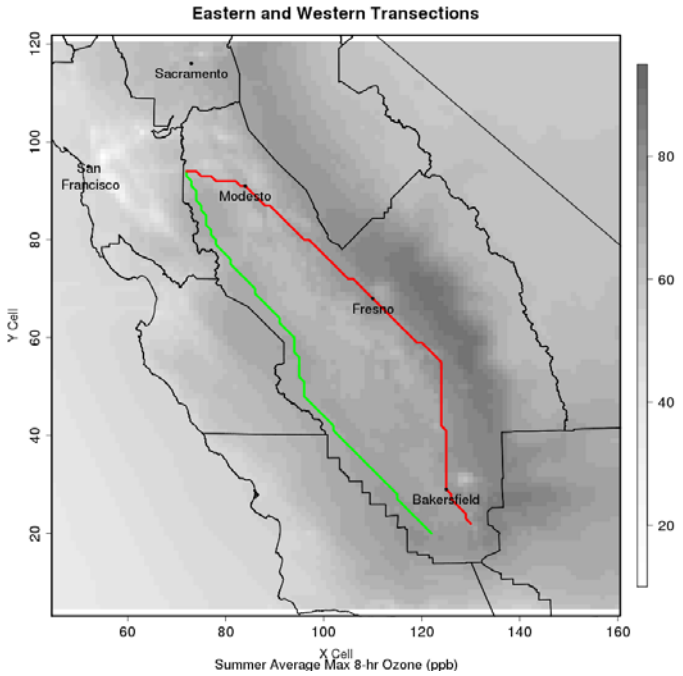

Shades of gray represent average ozone concentrations.

5.3.3.1 Along the Western Transect

Contributions to the Total Ozone Sensitivity to NOx

Figure 21: Contributions of the SJV, SFB and SV NOx Emissions to Ozone Sensitivity to NOx Emissions along Locations on the Western Transect for Each Specified Episode

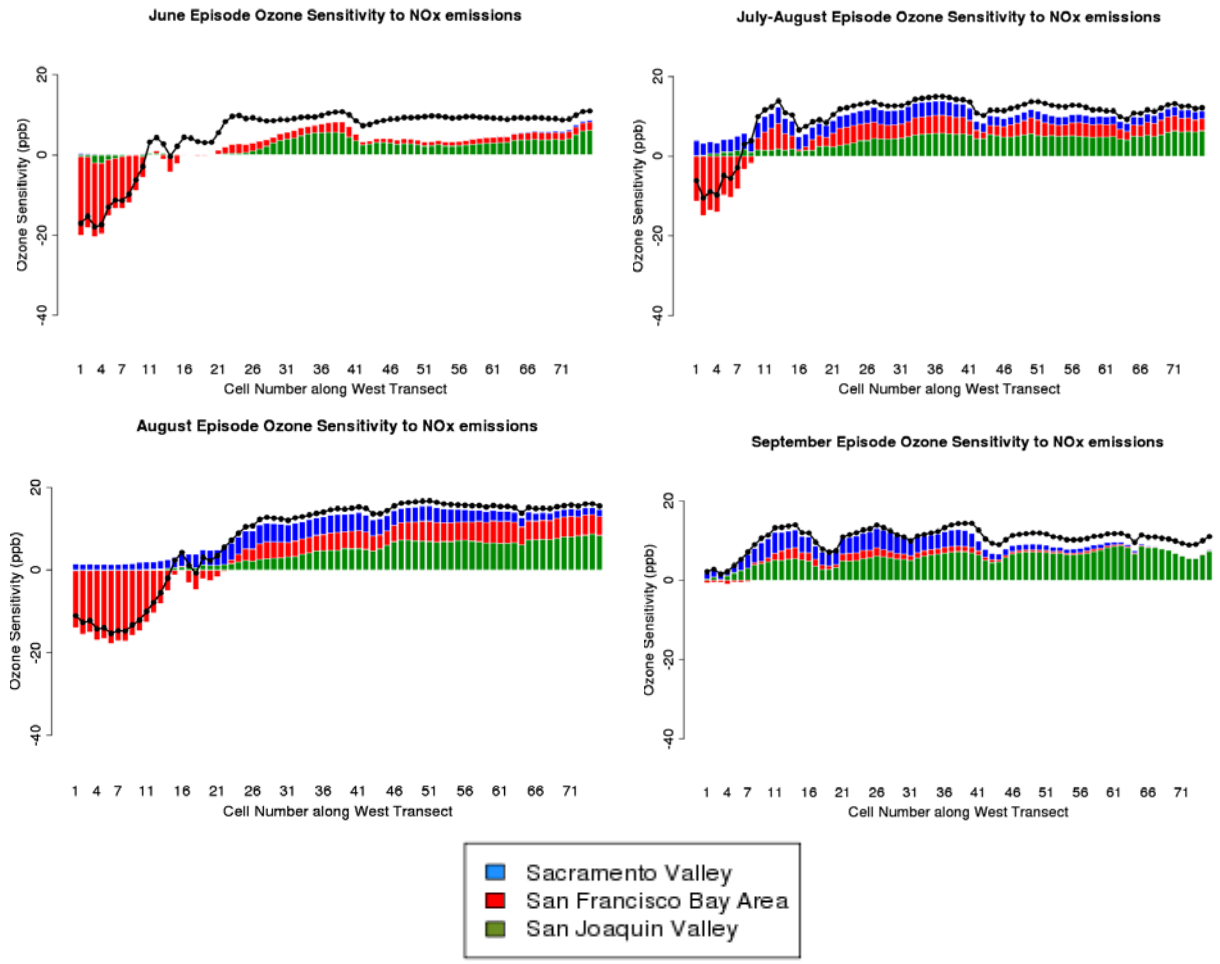

Total sensitivity is represented by black dots. Blue indicates contributions to the SJV ozone sensitivity to NOx emissions from the Sacramento Valley; Red from the San Francisco Bay Area NOx emissions; and Green from the SJV NOx emissions.

Contributions to the Total Ozone Sensitivity to AVOC

Figure 22: Contributions of the SJV, SFB and SV NOx Emissions to Ozone Sensitivity to AVOC Emissions along Locations on the Western Transect for Each Specified Episode

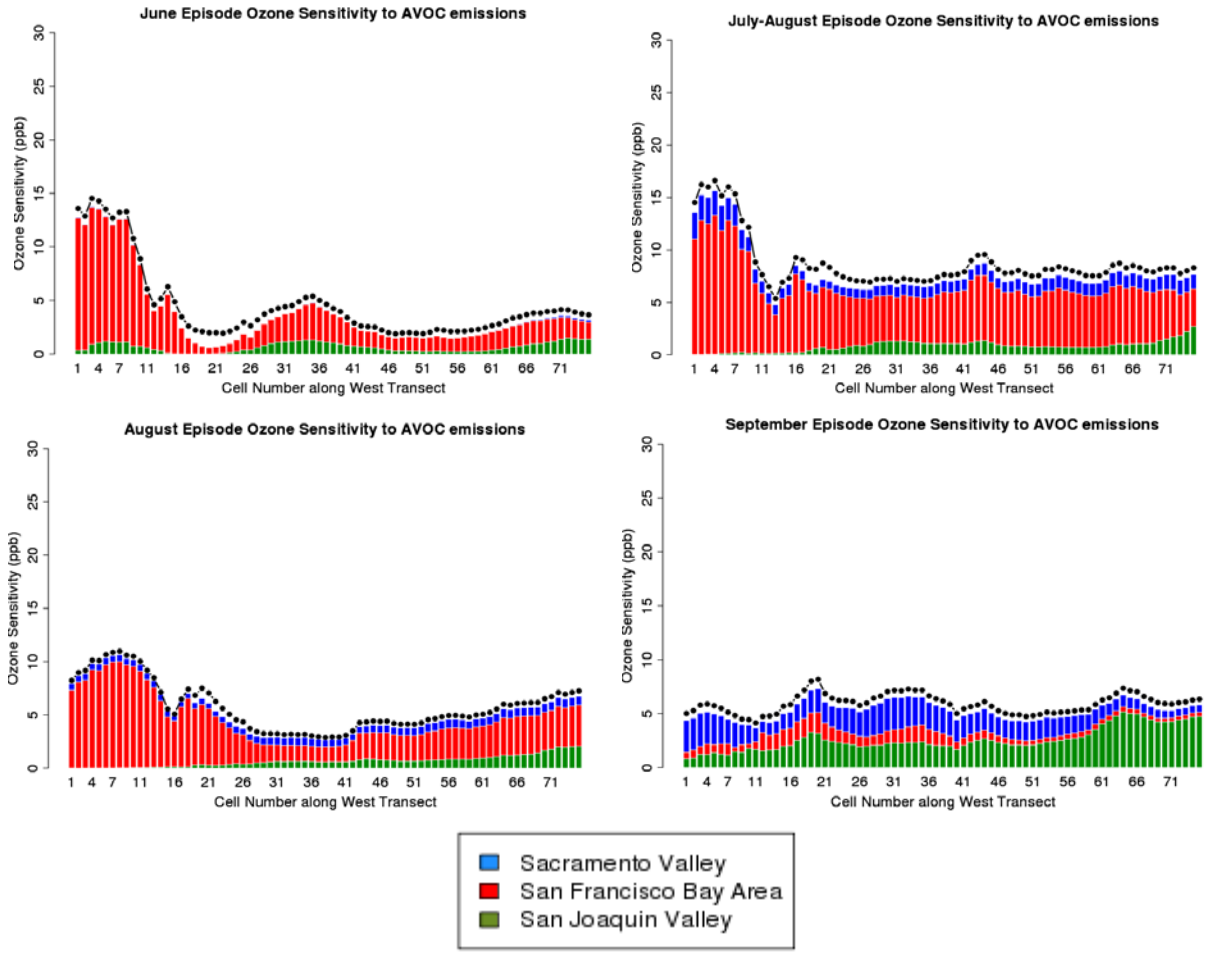

Total sensitivity is represented by black dots. Blue indicates contributions to the SJV ozone sensitivity to AVOC emissions from the Sacramento Valley; Red from the San Francisco Bay Area AVOC emissions; and Green from the SJV AVOC emissions.

From the magnitude of ozone sensitivities plotted in Figure 21-22, we can see a NOx-limited regime is predominant on the western side of the SJV except in the northern portion, where the chemistry is VOC limited except for the September (stagnant) episode.

When VOC-limited (Figure 21, negative sensitivity to total NOx), the northern SJV ozone levels are very sensitive to upwind AVOC emissions from the SFB. Hence, SFB NOx emissions are responsible for the NOx-disbenefit occurring in the North. Reducing SFB NOx emissions would increase ozone in the northern SJV. Pollutants are transported further south as sea breezes become stronger. Under very stagnant flow conditions like those in the September episode, ozone levels are affected by both local and SV emissions.

Central and southern SJV ozone sensitivities to NOx, which is the limiting reagent in the four episodes, vary with meteorology. Central and southern SJV are sensitive to emissions from all

three air basins (SJV, SFB and SV) except in the June episode. In June, the SV does not contribute to the sensitivity in the central and southern parts of the valley. The southerly marine flow prevents transport of pollutants from the SV while the strong flow in the Coastal Range carries emissions from the North Central Coast and the South Central Coast towards the SJV. In contrast, in September, the ozone sensitivity is dominated by local sources. In spite of the stagnation, the SV contributions to the ozone sensitivity to NOx are important for approximately half the western transect.

5.3.3.2Along the Eastern Transect

Contributions to the Total Ozone Sensitivity to NOx along the Eastern Transect

Figure 23: Contributions of the SJV, SFB and SV NOx Emissions to Ozone Sensitivity to NOx Emissions along Locations on the Eastern Transect for Each Specified Episode

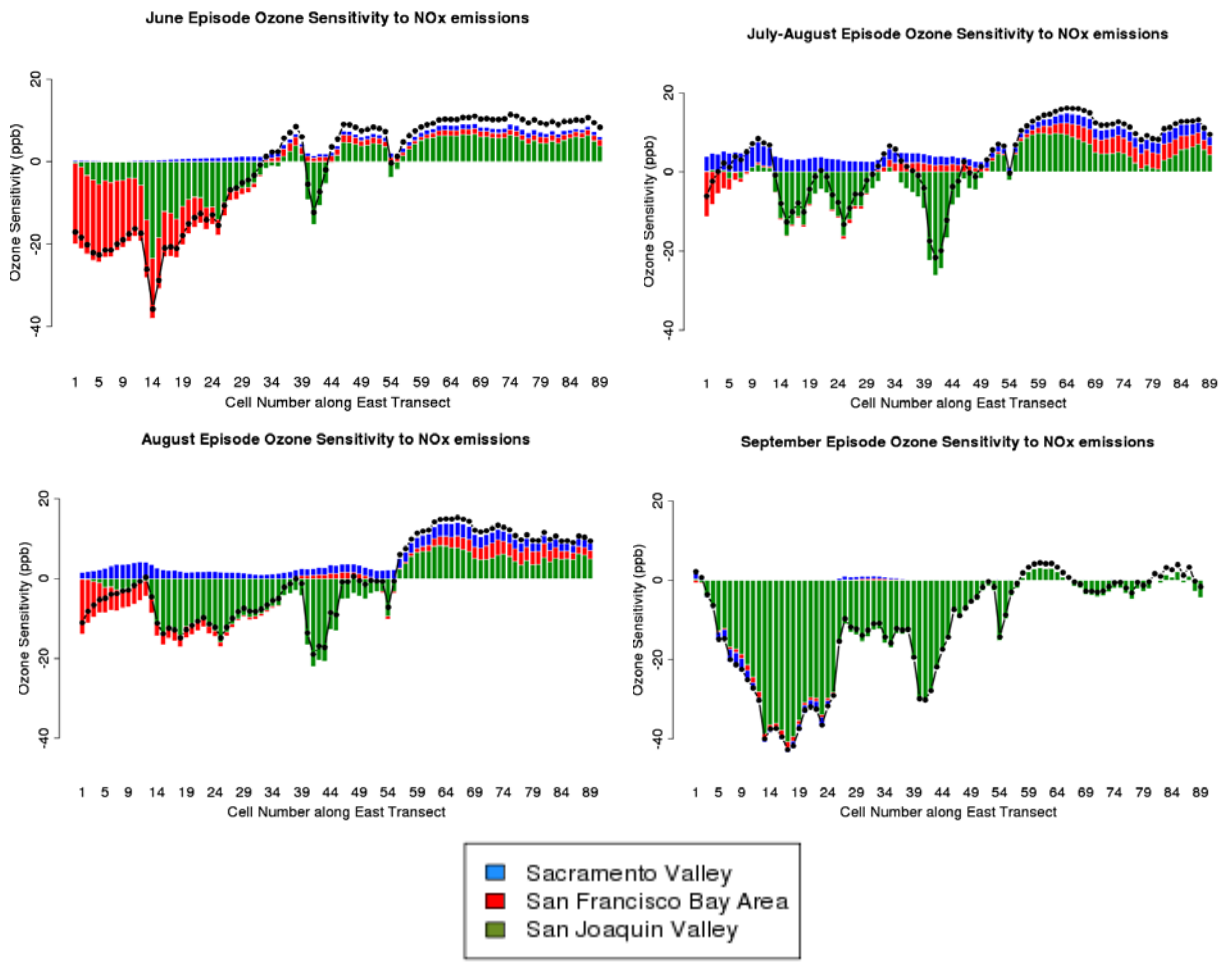

Total sensitivity is represented by black dots. Blue indicates contributions to the SJV ozone sensitivity to NOx emissions from the Sacramento Valley; Red from the San Francisco Bay Area NOx emissions; and Green from the SJV NOx emissions. Modesto, Fresno and Bakersfield are respectively located on cell numbers 13, 39, and 79.

Contributions to the Total Ozone Sensitivity to AVOC on Eastern Transect

Figure 24: Contributions of the SJV, SFB and SV NOx Emissions to Ozone Sensitivity to AVOC Emissions along Locations on the Eastern Transect for Each Specified Episode

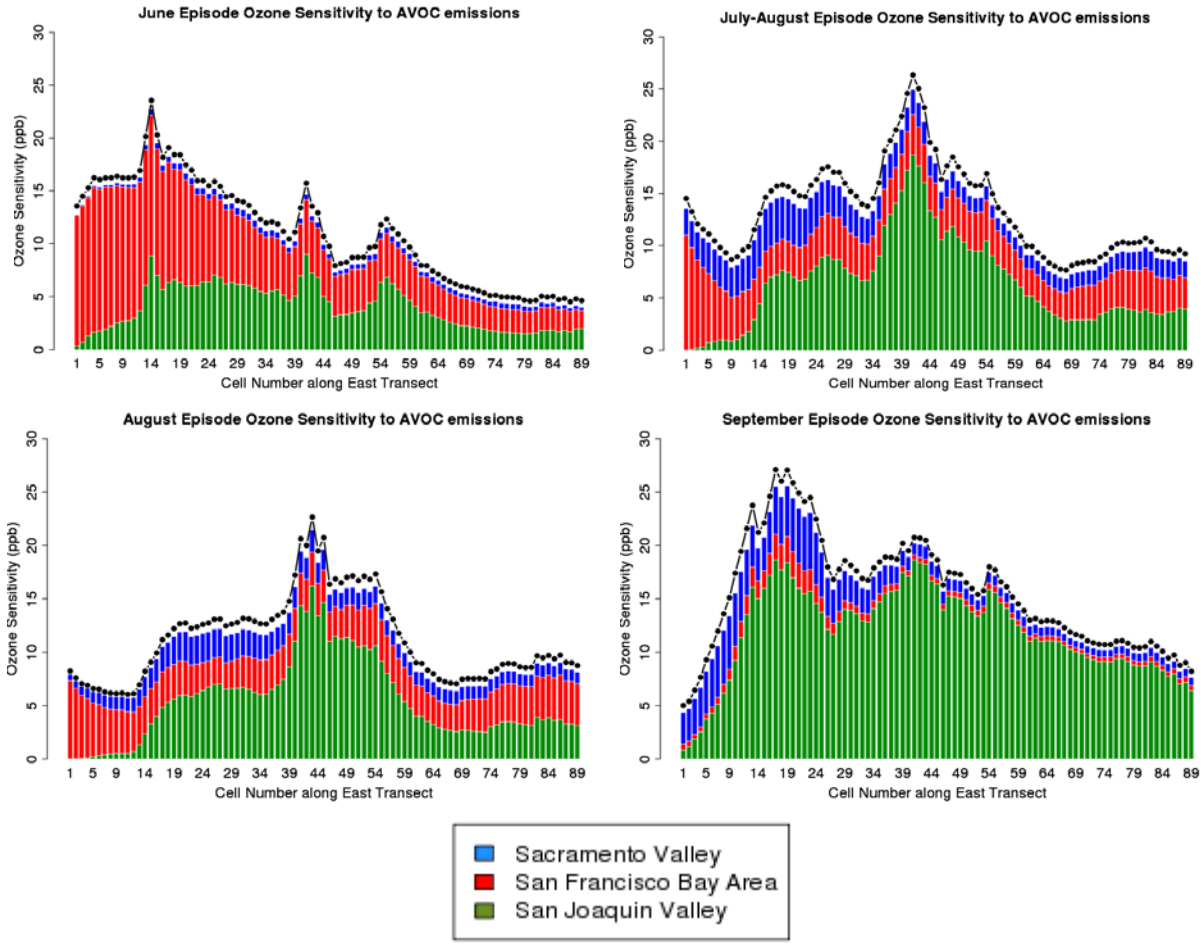

Total sensitivity is represented by black dots. Blue indicates contributions to the SJV ozone sensitivity to AVOC emissions from the Sacramento Valley; Red from the San Francisco Bay Area AVOC emissions; and Green from the SJV AVOC emissions. Modesto, Fresno and Bakersfield are respectively located on cell numbers 13, 39, and 79.

Figure 23-24 indicate that along Highway 99 on the eastern side of the valley, ozone regimes vary with location and meteorology. We have noted that there is a general trend for urban centers to be VOC-limited; however the sensitivity magnitude and the extent of the NOx-disbenefit areas depend on meteorology. Near Modesto (northern SJV), SFB NOx emissions are responsible for the NOx-disbenefit along the SFB-SJV border for all episodes except the September one). Important amounts of NOx are transported by westerly winds from the Bay Area to the northern part of the valley through the gaps in Coastal Range. The stronger the flow, the stronger and more extensive the NOx disbenefit is (to the East). The large NOx-disbenefit area in the September episode looks similar to the one in June on the control regime maps (see Figure 17); however, local emissions of NOx and AVOC account for almost 100 percent of the total sensitivity observed in September and the upwind contribution, namely from the SV, is not very significant except in the northern portion of the SJV. Emissions from the

Modesto urban center react in the vicinity of the city instead of being transported farther southeast toward the Sierras in this stagnant episode.

CHAPTER 6: Conclusions

The San Joaquin Valley (SJV) air basin of California is designated as an extreme nonattainment area for ozone due to its unique trough-like topography and diverse emissions from both local and upwind sources. The rate of ozone production can be limited by reducing emissions of either NOx or VOCs. Reducing ozone concentrations is especially challenging because ozone control regimes of NOx- and VOC-limitation change in both time and space as a function of meteorology. Four high-ozone episodes during summer 2000, exemplifying different meteorological conditions, have been selected to conduct a sensitivity analysis. Ozone sensitivities to NOx and AVOCs have been used to define limiting reagents and possible control strategies.

Ozone sensitivity patterns and source contributions lead us to divide the SJV into four subregions: the northern, the southern parts of the SJV, and the western and eastern sides of the middle SJV.

The northern part of the valley is mainly influenced by San Francisco Bay Area (SFB) emissions. Reducing AVOC emissions in the SFB would be very beneficial for this part of the SJV. Moreover, it would also decrease ozone levels downwind of urban centers in the eastern SJV. The efficiency of such a control increases with the strength of the marine flow from the Bay Area.

Remote areas on the western side of the middle SJV show a strong trend to be NOx-limited and both local and upwind sources are important for lowering ozone concentration here. Along the eastern side of the middle SJV, the limiting reagent is highly dependent on meteorological conditions and location; however, the most important sources are local despite the different wind flow patterns. Under stagnant flow conditions, reduction of local VOC emissions would be the most efficient control option, while for other meteorological conditions, local NOx reductions would be a better option.

In the southern part of the SJV, both ozone control options and source contributions vary with meteorology. Ozone formation in this area is generally dominated by both local and upwind sources and mostly limited by NOx except the urban areas. Under very stagnant conditions (September), local contributions become more important and ozone chemistry shifts toward more VOC limitation.

Reducing AVOC emissions generally has smaller effects on ozone sensitivities than reducing NOx. Overall, reducing NOx emissions causes a shift towards NOx-limitation, and the effects on control options are limited to areas close to emission centers. Hotter or more stagnant episodes like the July-August and September episodes may present greater challenges for achieving ozone reductions than other meteorological conditions.

Sensitivity calculations have been performed by one-at-a-time perturbations of input parameters. Brute-force sensitivity analysis is a straightforward approach, but it will become

infeasible for systems with large numbers of input parameters. Adjoint sensitivity analysis is a useful complement to forward methods. Adjoint equations would allow computation of the various contributions to the sensitivity of one output variable like ozone concentration at a given location in space and time from all the NOx emissions at individual locations in the modeling domain. Actual fields of sensitivity contributions are produced by the model directly and efficiently. This alternative method is recommended to assess the effects of a wider range of meteorological parameters.

GLOSSARY

AVOC: Anthropogenic VOC

BVOC: Biogenic VOC

CARB: California Air Resources Board

CC: Central Coast

CCOS: Central California Ozone Study

CCTM/CTM: CMAQ Chemical Transport Model/Chemical Transport Model

CMAQ: Community Multiscale Air Quality

CMAS: Community Modeling and Analysis System

DOE: Department of Energy

EETD: Environmental Energy Technologies Division

EKMA: Empirical Kinetic Modeling Approach

EPA: Environmental Protection Agency

LBNL: Lawrence Berkeley National Laboratory

MC: Mountain Counties

MCIP: Meteorology to Chemistry Interface Processor

MM5: Fifth-Generation PSU/NCAR Mesoscale Model

NAAQS: National Ambient Air Quality Standards

NCAR: the National Center for Atmospheric Research

NCC: North Central Coast

NCEP: National Centers for Environmental Prediction

NMHC: Non-Methane Hydrocarbons

NOAA: National Oceanic and Atmospheric Administration

NOx: Nitrogen oxide

O_3: Ozone

OH: CMAQ hydrogen oxide radical

ORIG: Original emissions case

PBL: Planetary Boundary Layer

PDT: Pacific Daylight Time

PSU: Pennsylvania State University

SCC: South Central Coast

SFB: San Francisco Bay Area

SIP: State Implementation Plan

SJV: San Joaquin Valley

SV: Sacramento Valley

UC: University of California

UTC: Coordinated Universal Time

VOC: Volatile Organic Compound

REFERENCES

American Lung Association. (2010). *American Lung Association State of the Air 2010.* Washington, DC, USA: American Lung Association.

Atkinson, R. (2000). Atmospheric Chemistry of VOCs and NOx. *Atmospheric Environment , 34*, pp. 2063-2101.

Beaver, S. (2008 24-January). *Fresno Eddy recirculation and its impact on ozone buildup in the San Joaquin Valley of California.* Retrieved 2010 йил 22-June from American Meteorological Society: http://ams.confex.com/ams/88Annual/techprogram/paper_132276.htm

Beaver, S., & Palazoglu, A. (2009). Influence of synoptic and mesoscale meteorology on ozone pollution potential for San Joaquin Valley of California. *Atmospheric Environment , 43*, pp. 1779-1788.

Bloomer, B. J., Stehr, J. W., Piety, C. A., Salawitch, R. J., & Dickerson, R. R. (2009). Observed Relationships of Ozone Air Pollution with Temperature and Emissions. *Geophysical Research Letters , 36* (L09803), p. 14.

Buyn, D. W., & Schere, K. L. (2006). Review of the Governing Equations, Computational Algorithms, and Other Components of the Models-3 Community Multiscale Air Quality (CMAQ) Modeling System. *Applied Mechanics Reviews , 59*, pp. 51-77.

Byun, D. W. (1999). Fundamentals of One-Atmosphere Dynamics for Multiscale Air Quality Modeling. In *Science Algorithms of the EPA Models-3 Community* (D. Byun and J. K. S. Ching ed., p. 39). Research Triangle Park, NC, USA: National Exposure Research Laboratory, U.S. EPA.

Byun, D. W., & Young, J. (1999). Governing Equations and Computational Structure of the Community Multiscale Air Quality (CMAQ) Chemical Transport Model. In *Science Algorithms of the EPA Models-3 Community Multiscale Air Quality (CMAQ) Modeling System* (D. Byun and J. K. S. Ching ed., p. 37). Research Triangle Park, NC, USA: National Exposure Research Laboratory, U.S. EPA.

Byun, D. W., Young, J., Pleim, J., Odman, M. T., & Alapaty, K. (1999). Numerical Transport Algorithms for the Community Multiscale Air Quality (CMAQ) Chemical Transport Model in Generalized Coordinates. In *Science Algorithms of the EPA Models-3 Community Multiscale Air Quality (CMAQ) Modeling System* (D. Byun and J. K. S. Ching ed., p. 56). Research Triangle Park, NC, USA: National Exposure Research Laboratory, U.S. EPA.

Byun, D., Pleim, J., Tang, R., & Bourgeois, A. (1999). *Science Algorithms of the EPA Models-3 Community Multiscale Air Quality (CMAQ) Modeling System* (D. Byun and J. K. S. Ching ed.). Research Triangle Park, NC, USA: National Exposure Research Laboratory, U.S. EPA.

California Environmental Protection Agency. (2010). *California Air Basin Map*. Retrieved 2010 12-April from Air Resources Board: http://www.arb.ca.gov/ei/maps/statemap/abmap.htm

Committee on Ozone-Forming Potential of Reformulated Gasoline, National Research Council. (1999). Ozone Photochemistry. In *Ozone-Forming Potential of Reformulated Gasoline* (pp. 23-32). Washington, DC, USA: National Academy Press.

Community Modeling and Analysis System (CMAS) Center. (2010). *Community Multiscale Air Quality Modeling System*. Retrieved 2010 27-August from CMAQ-Model.org: http://www.cmaq-model.org/overview.cfm

Dabdub, D., DeHaan, L. L., & Seinfeld, J. H. (1999). Analysis of ozone in the San Joaquin Valley of California. *Atmospheric Environment , 33* (16), pp. 2501-2514.

Dudhia, J., Gill, D., Guo, Y.-R., Hansen, D., Manning, K., & Wang, W. (1999). *PSU/NCAR mesoscale modeling system tutorial class notes (MM5 modeling system version 2).* Boulder, CO, USA: National Center for Atmospheric Research.

Environmental Energy Technologies Division. (2010). *Organization: Division: Environmental Energy Technologies Division.* Retrieved 2010 йил 18-August from Environmental Energy Technologies Division: http://eetd.lbl.gov/eetd-org.html

Feather River Air Quality Management District. (2010). *Ozone Chemistry.* Retrieved 2010 йил 2-June from FRAQMD: http://www.fraqmd.org/OzoneChemistry.htm

Finlayson-Pitts, B. J., & Pitts, J. N. (1997). Tropospheric Air Pollution: Ozone, Airborne Toxics, Polycyclic Aromatic Hydrocarbons and Particles. *Science , 276*, pp. 1045-1052.

Fujita, E. M., Watson, J. G., Chow, J. C., & Magliano, K. L. (1995). Receptor model and emissions inventory source apportionments of nonmethane organic gases in California's San Joaquin valley and San Francisco bay area. *Atmospheric Environment , 29* (21), pp. 3019-2035.

Grell, G. A., Dudhia, J., & Stauffer, D. R. (1994). *A description of the fifth-generation Penn State/NCAR mesoscale model (MM5).* Boulder, CO, USA: National Center for Atmospheric Research.

Hakami, A., Henze, D. K., Seinfeld, J. H., Singh, K., Sandu, A., Kim, S., et al. (2007). The Adjoint of CMAQ. *Environmental Science and Technology , 41* (22), pp. 7807–7817.

Hakami, A., Seinfeld, J. H., Sandu, A., Singh, K., Byun, D., Percell, P. P., et al. (2006). *Development Of Adjoint Sensitivity Analysis Capabilities for CMAQ.* 5th Annual CMAS Conference, 10/16/2006.

Hall, J. V., Brajer, V., & Lurmann, F. W. (2008). *The Benefits of Meeting Federal Clean Air Standards in the South Coast and San Joaquin Valley Air Basins.* Petaluma, CA, USA: Sonoma Technology, Inc.

Hanson, D. T., & Sharkey, T. D. (2001). Rate of Acclimation of the Capacity for Isoprene Emission in Response to Light and Temperature. *Plant, Cell & Environment , 24* (9), pp. 937-946.

Jin, L., Nancy Brown, Robert A. Harley, Jian-Wen Bao, Sarah Michelson, James M. Wilzak. (2010). Seasonal versus Episodic Performance Evaluation for an Eulerian Photochemical Model, *Journal Geophysical Research Atmospheres* 115 DO9302, doi:10.1029/2009JDO12680.

Jin, L.; Harley, R.A.; Brown, N.J. (2011). Ozone Pollution Regimes Modeled for a Summer Season in California's San Joaquin Valley: A Cluster Analysis. *Atmospheric Environment* 45, 4707-4718.

Jin, L., Tonse, S.R., Cohan, D.S., Mao, X., Harley, R.A., Brown, N.J. (2008). Sensitivity analysis of ozone formation and transport for a Central California air pollution episode, *Environmental Science & Technology* 42, 3683-3689.

APPENDIX A:
Ozone Regulation in the United States

A-1: California Air Basins Map

Figure A-1: California Air Basins

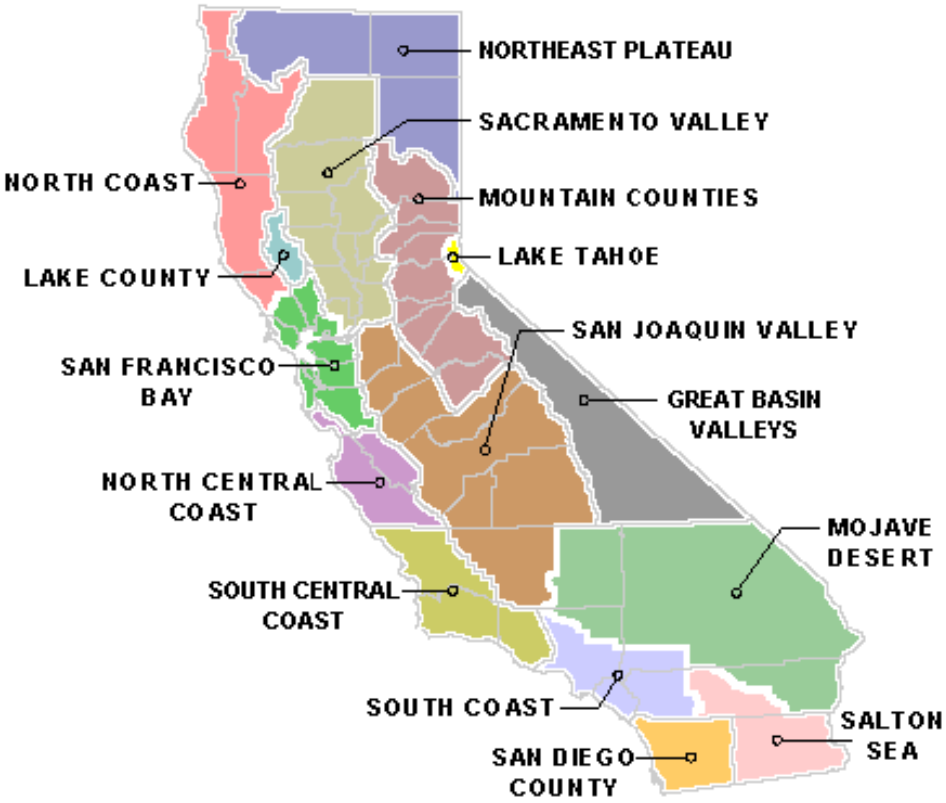

(California Environmental Protection Agency, 2010)

Figure A-2: California Relief Maps

From http://www.california-map.org

From http://www.worldatlas.com and http://www.graphicmaps.com/

Table A-3: Ozone Standards

	Level	Averaging time	
2008 standard	0.075 ppm	8-hour	To attain this standard, the 3-year average of the fourth-highest daily maximum 8-hour average ozone concentrations measured at each monitor within an area over each year must not exceed 0.075 ppm.
1997 standard	0.08 ppm	8-hour	To attain this standard, the 3-year average of the fourth-highest daily maximum 8-hour average ozone concentrations measured at each monitor within an area over each year must not exceed 0.08 ppm.

NB: Primary and secondary Standard are identical for ozone

On January 6, 2010, EPA proposed to strengthen the national ambient air quality standards (NAAQS) for ground-level ozone, the main component of smog. EPA is proposing to strengthen the 8-hour "primary" ozone standard, designed to protect public health, to a level within the range of 0.060-0.070 parts per million (ppm). EPA is also proposing to establish a distinct cumulative, seasonal "secondary" standard, designed to protect sensitive vegetation and ecosystems, including forests, parks, wildlife refuges and wilderness areas. EPA is proposing to set the level of the secondary standard within the range of 7-15 ppm-hours.

For the primary standard, ozone concentrations are averaged over 8-hour periods. The fourth-highest 8-hour value at a particular monitor in the most recent year is averaged with the fourth-highest 8-hour values from the previous two years. This produces a three-year average. To meet the standard, the three-year average must be less than or equal to the level of the standard. EPA did not reconsider the form of the primary standard.

The proposed secondary standard is designed to protect sensitive vegetation from adverse effects associated with cumulative ozone exposures during the three months when daytime ozone concentrations are the highest. Specifically, the form of this new proposed secondary standard is a "cumulative peak-weighted index," called W126. The W126 index is calculated by:

- "Weighting" each hourly ozone measurement occurring during the 12 daylight hours (8:00 am to 8:00 pm) each day, with more weight given to higher concentrations. This "peak weighting" emphasizes higher concentrations more than lower concentrations, because higher concentrations are disproportionately more damaging to sensitive trees and plants;
- Adding these 12 weighted hourly ozone measurements for each day, to get a cumulative daily value;

- Summing the daily values for each month, to get a cumulative monthly value;
- Identifying the three consecutive months during the ozone season with the highest index value, to get the cumulative seasonal index value, and;
- Averaging these maximum seasonal index values over three years.

An area would meet the proposed secondary standard if the three-year average of the cumulative seasonal index values is less than or equal to the level of the standard (i.e., 7-15 ppm-hours).

(United States Environmental Protection Agency, 2010)

Figure A-3: National Map of 8 h Ozone Nonattainment Areas

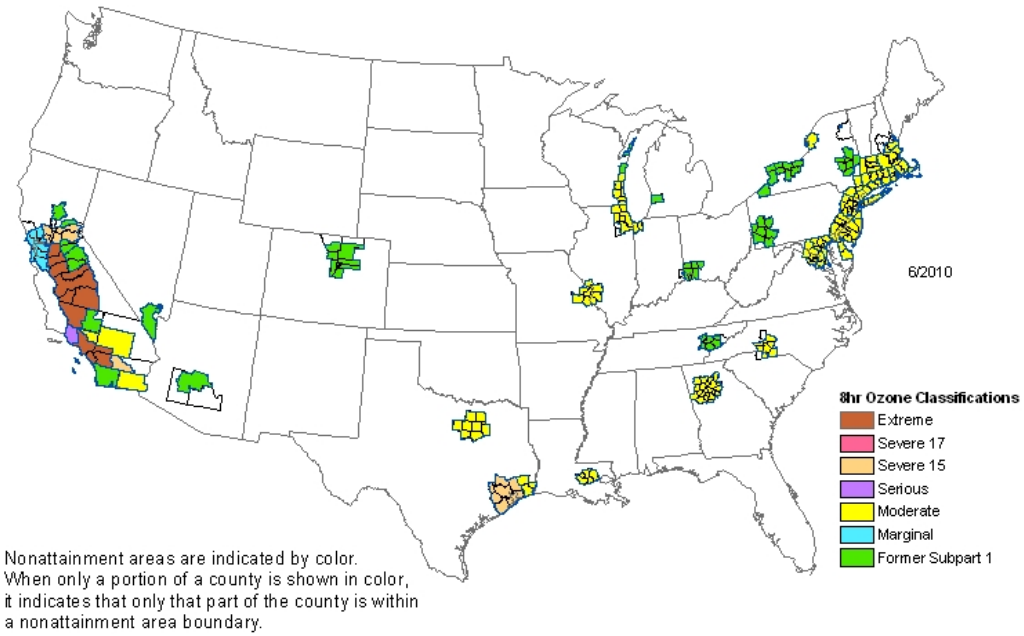

(1997 standard, June 2010)

A nonattainment area is any area that does not meet the national primary or secondary ambient air quality standard for the pollutant.

8-Hour Ozone Classifications:	Extreme: Area has a design value of 0.187 ppm and above. Severe 17: Area has a design value of 0.127 up to but not including 0.187 ppm Severe 15: Area has a design value of 0.120 up to but not including 0.127 ppm Serious: Area has a design value of 0.107 up to but not including 0.120 ppm. Moderate: Area has a design value of 0.092 up to but not including 0.107 ppm. Marginal: Area has a design value of 0.085 up to but not including 0.092 ppm.

NB: The designations process for the 2008 ground-level ozone standards is still in progress.

(United States Environmental Protection Agency, 2010)

APPENDIX B:
Science Process Modules in Models-3 CMAQ

Figure B-1: Modules in Models

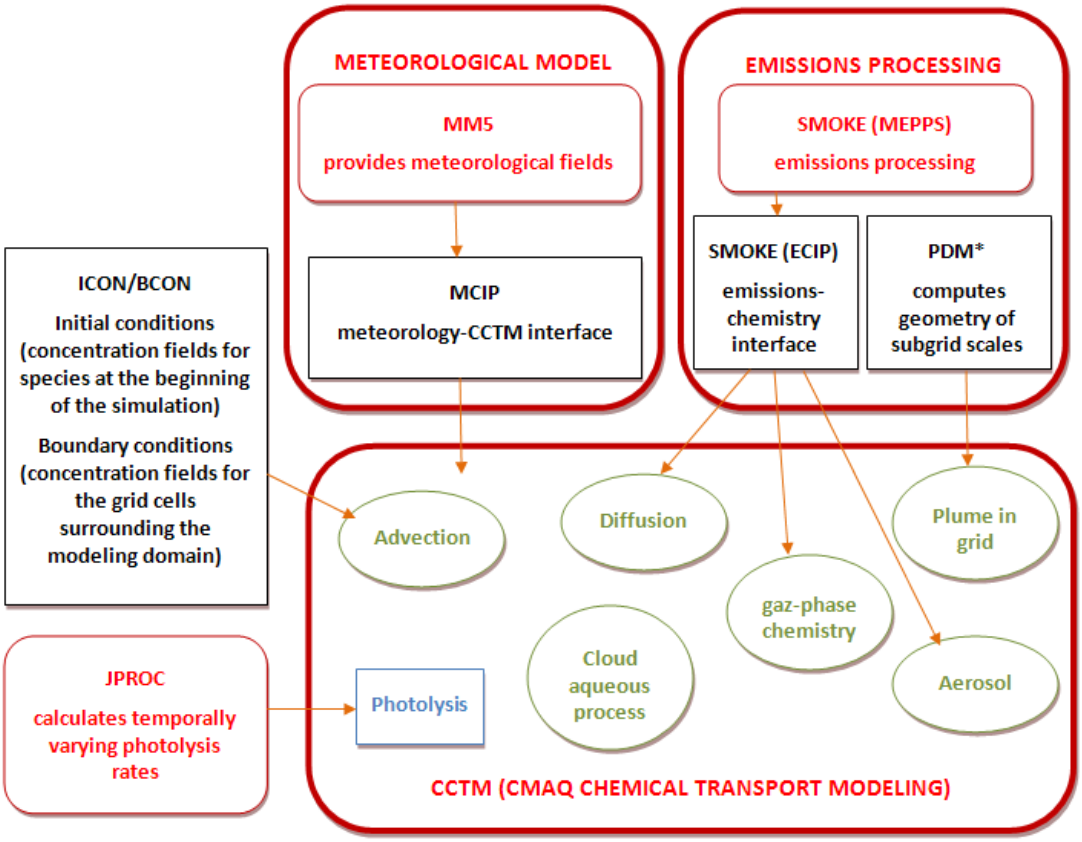

Red round rectangles: independent processors (Models-3)

Black rectangular boxes: interface processes between chemistry, emissions and meteorology (translates data from a model to another)

Green circular boxes: science process modules (update the hourly concentration field of outputs, e.g., ozone)

Blue rectangular boxes: data-provider modules (routines to feed appropriate environmental input data to science process modules)

Orange arrows: Flow of data through the modeling system

Modified from Buyn & Schere, 2006.

APPENDIX C:
Wind Fields and Anomalies

Figure C-1: Wind Anomaly at 4:00 p.m. (PDT) for Each Episode (zoom on the SJV)

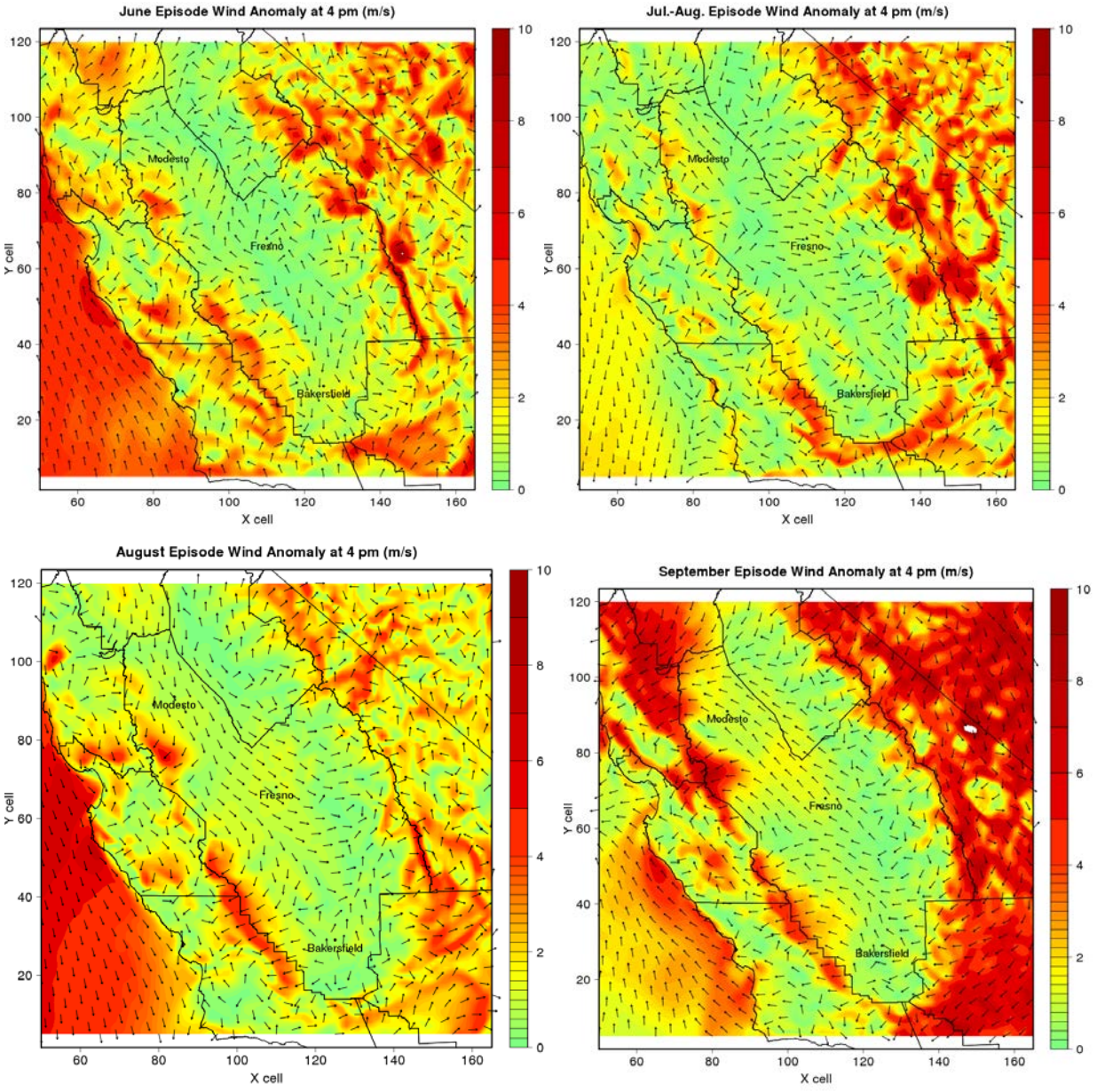

Figure C-2: Wind Anomaly at 4:00 a.m. (PDT) for Each Episode (zoom on the SJV)

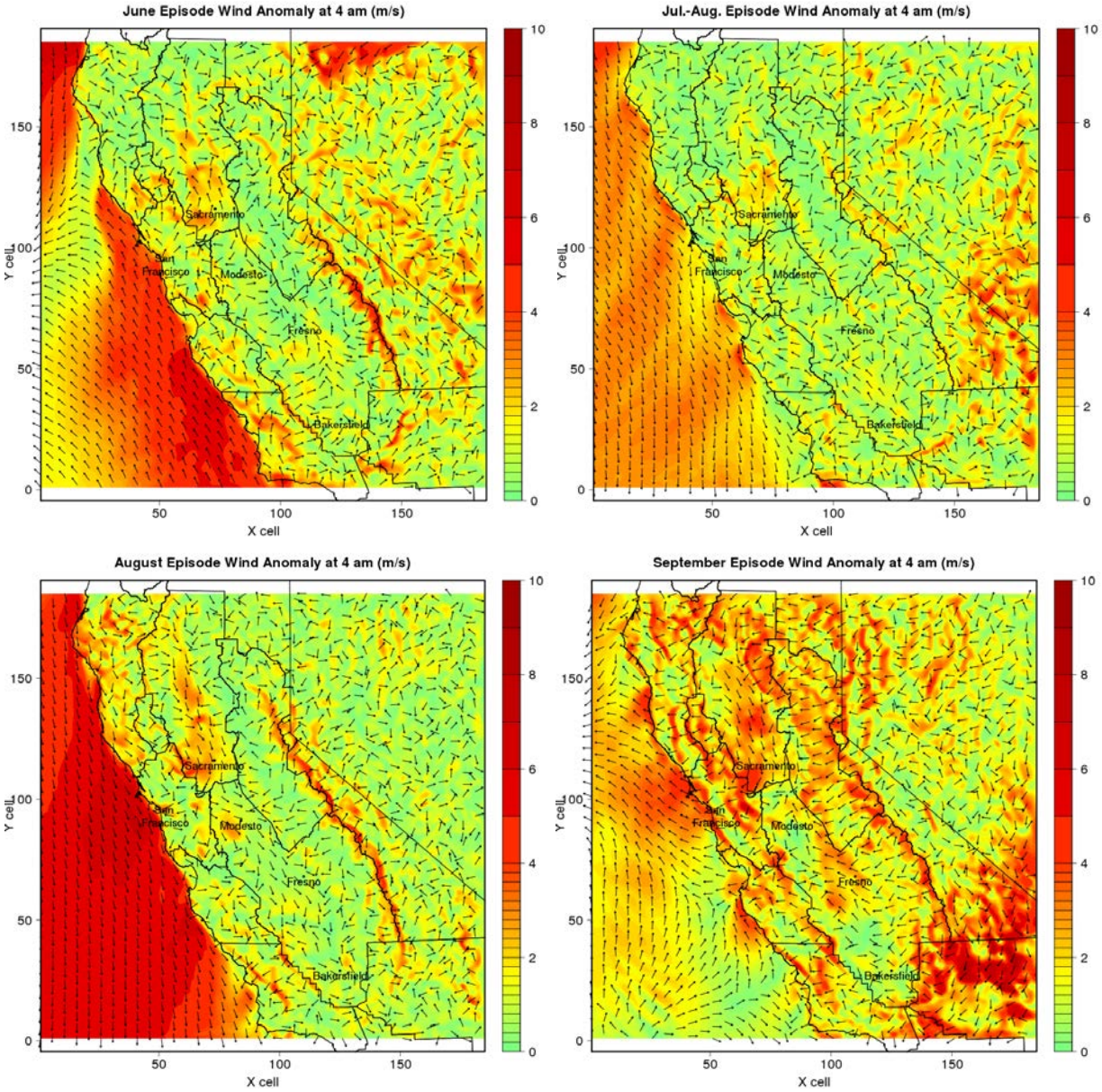

Figure C-3: Wind Fields at 4:00 p.m. (PDT) for Each Episode

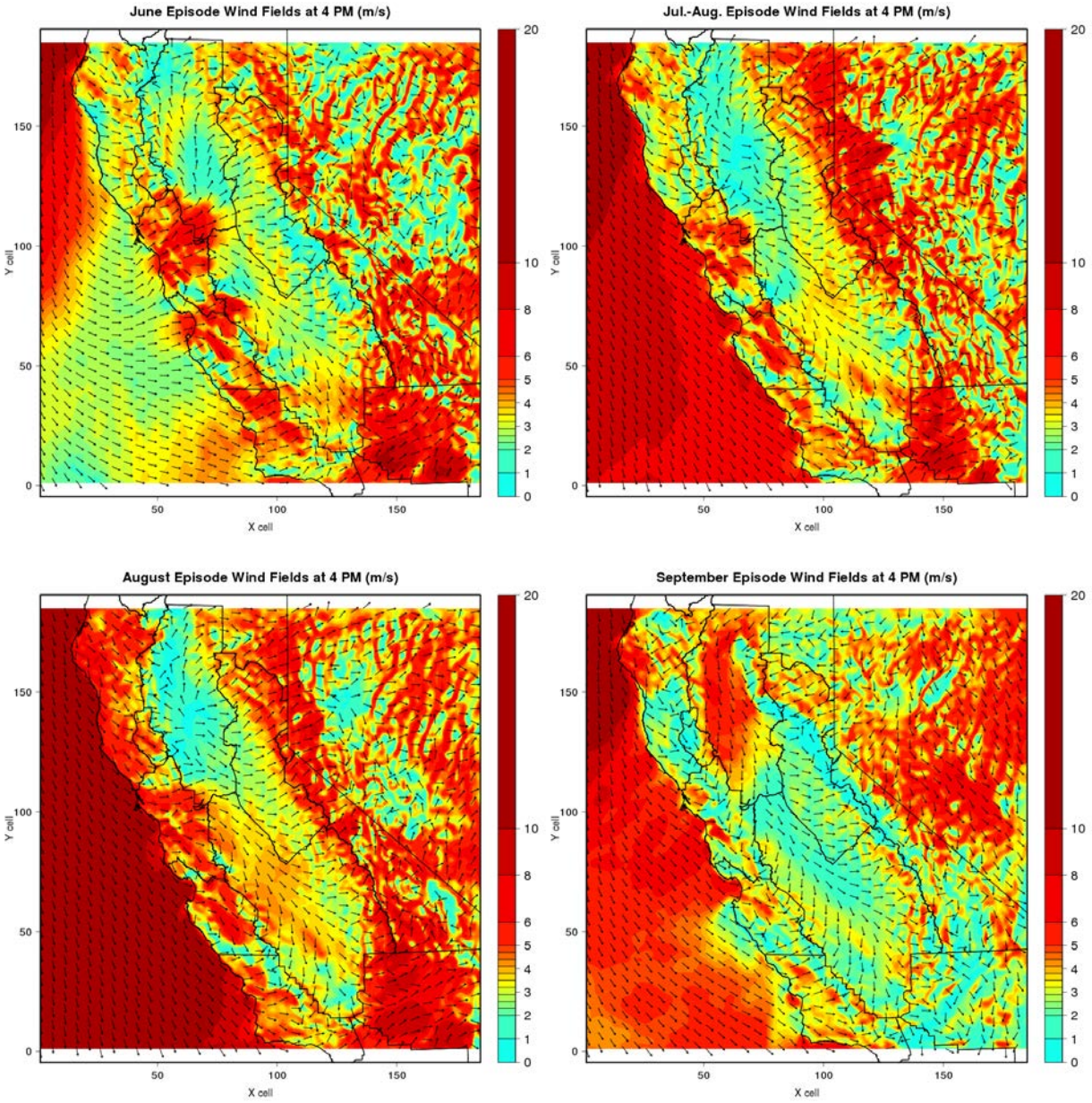

APPENDIX D:
Influences of Meteorology and Emissions

Figure D-1: PBL Height Summer Average and Episode Anomalies at 4:00 p.m. (PDT)

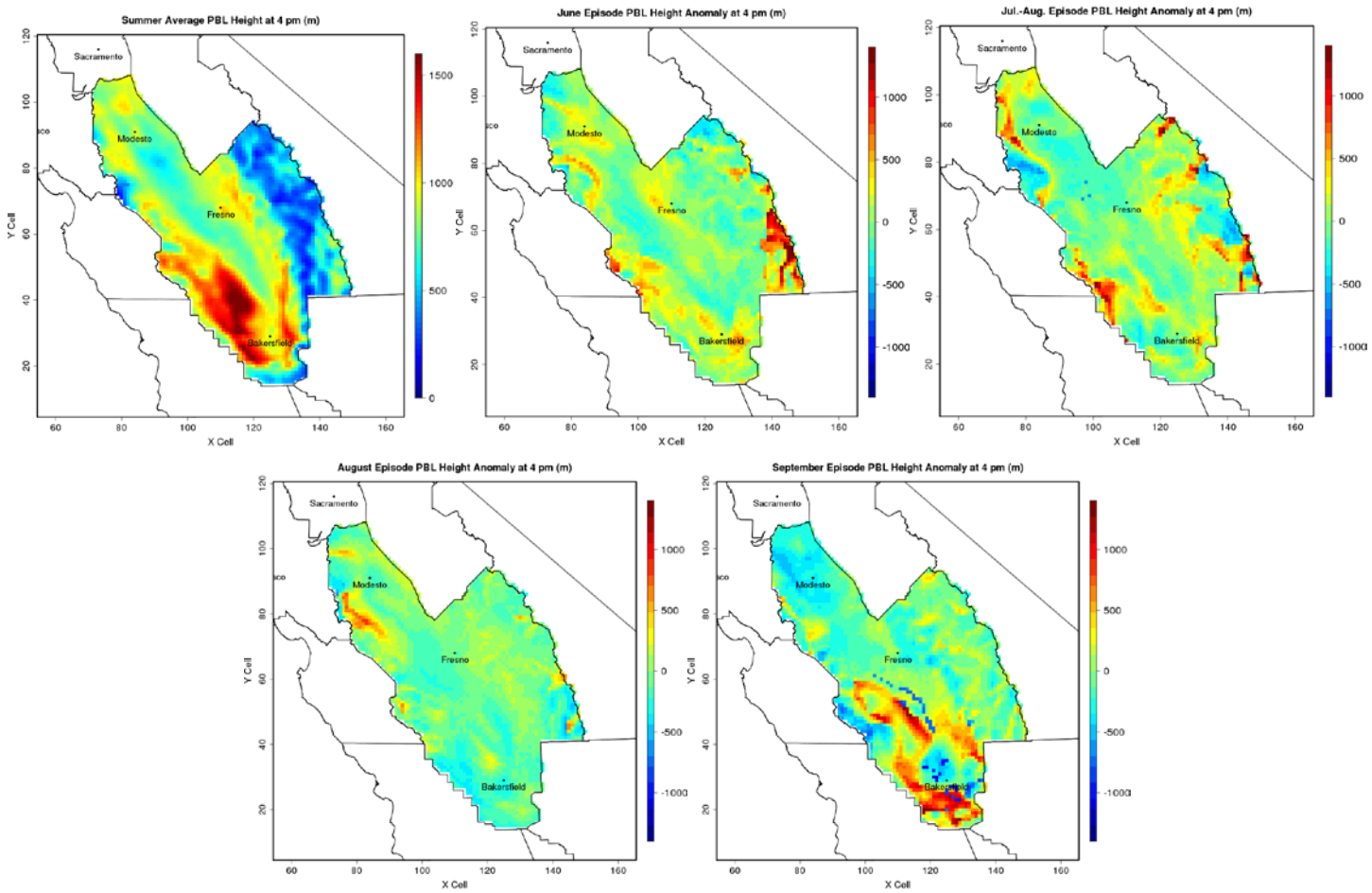

Figure D-2: Solar Radiation at the Surface Summer Average and Episode Anomalies at 4:00 p.m. (PDT)

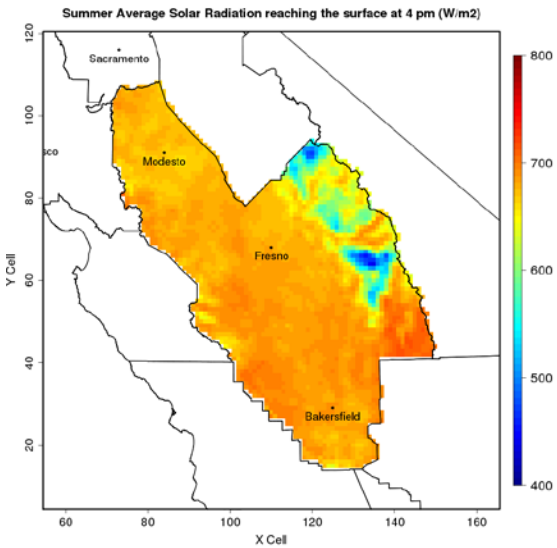

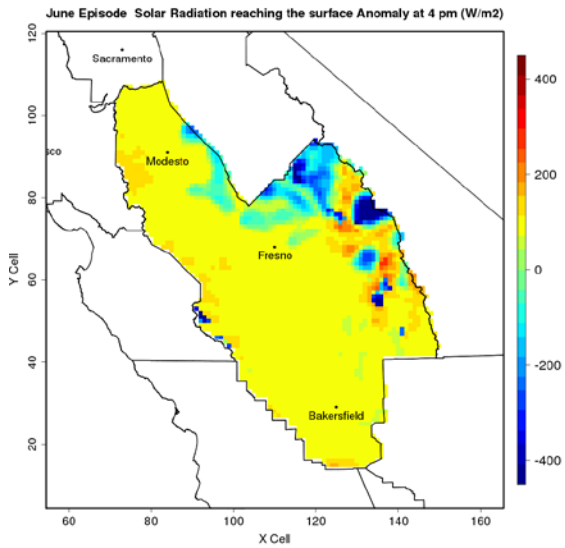

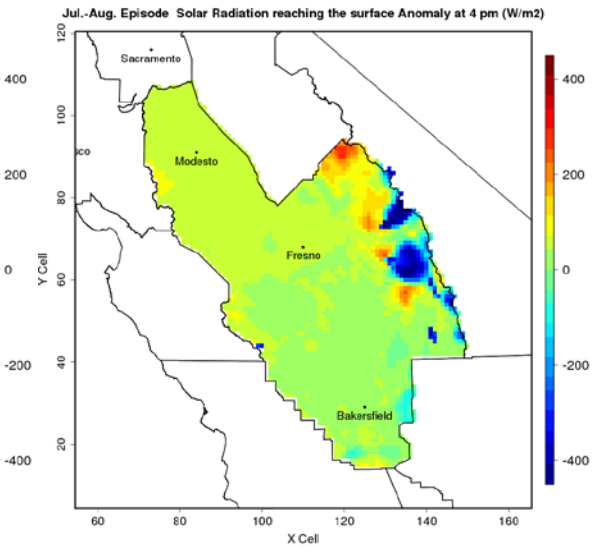

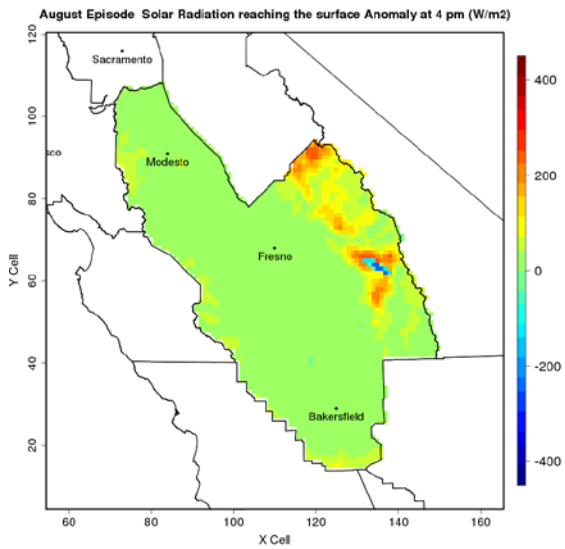

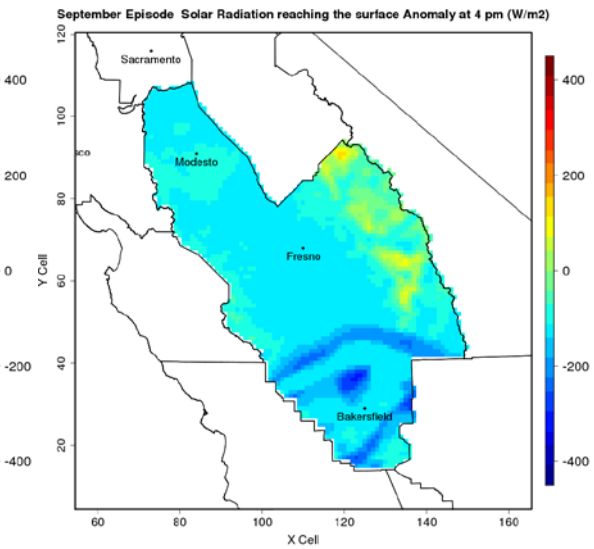

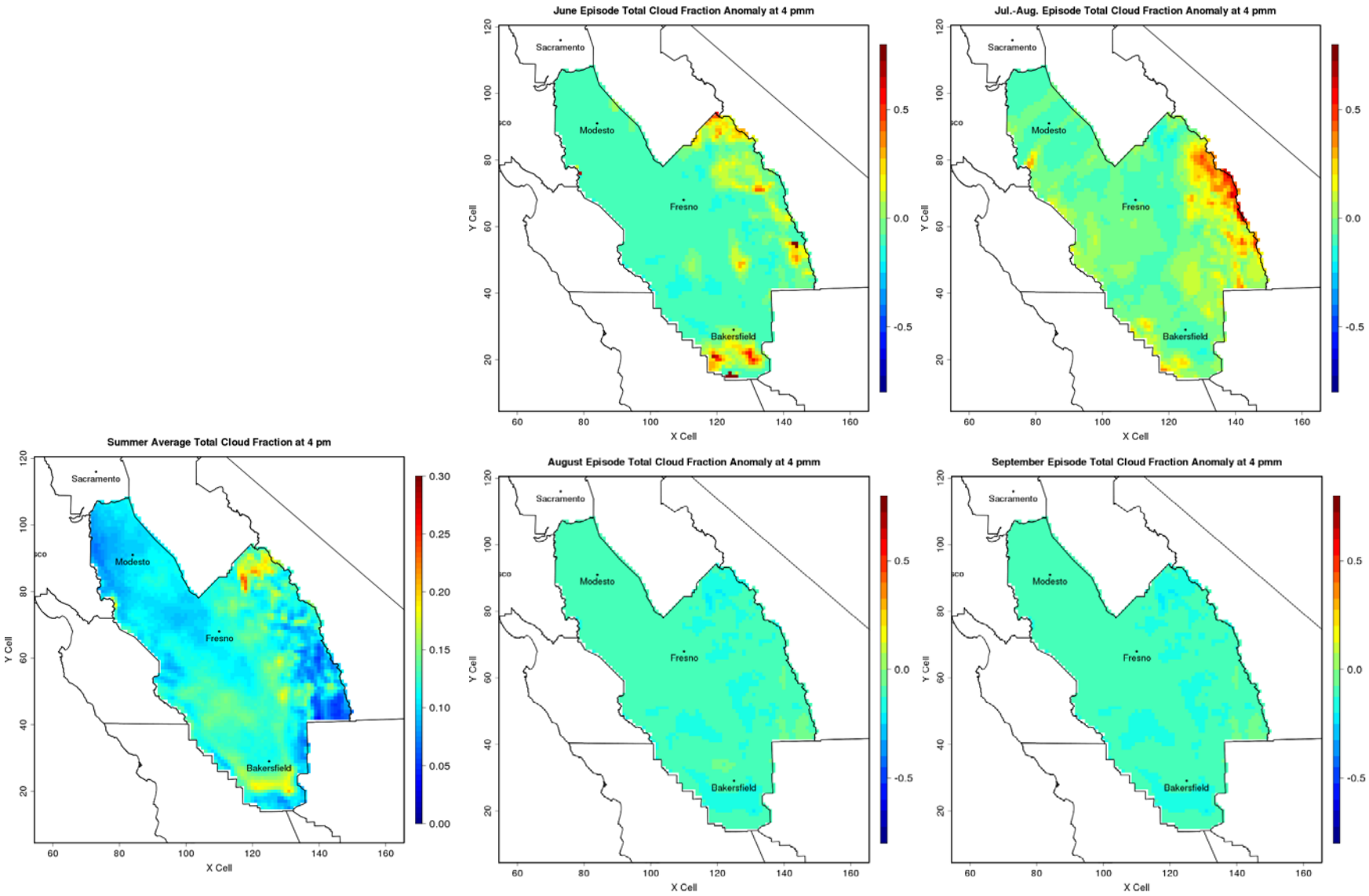
June Episode Total Cloud Fraction Anomaly at 4 pmm
Jul.-Aug. Episode Total Cloud Fraction Anomaly at 4 pmm
Summer Average Total Cloud Fraction at 4 pm
August Episode Total Cloud Fraction Anomaly at 4 pmm
September Episode Total Cloud Fraction Anomaly at 4 pmm
Sacramento
Modesto
Fresno
Bakersfield
X Cell
Y Cell
0.5
0.0
-0.5
0.30
0.25
0.20
0.15
0.10
0.05
0.00

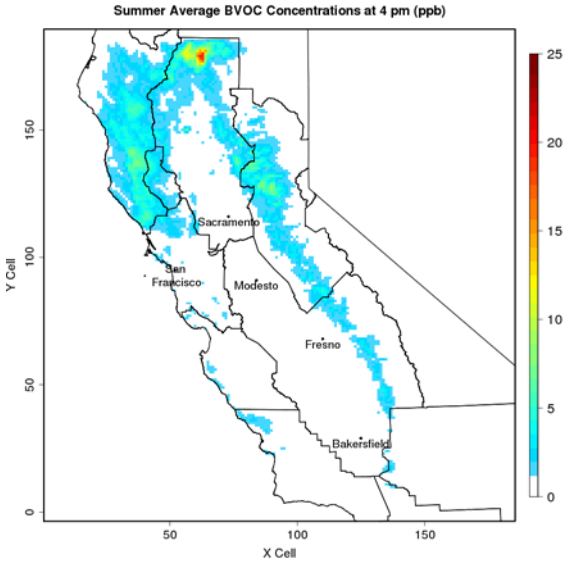
Summer Average BVOC Concentrations at 4 pm (ppb)
Sacramento
San Francisco
Modesto
Fresno
Bakersfield
Y Cell
X Cell
0
50
100
150
25
20
15
10
5
0

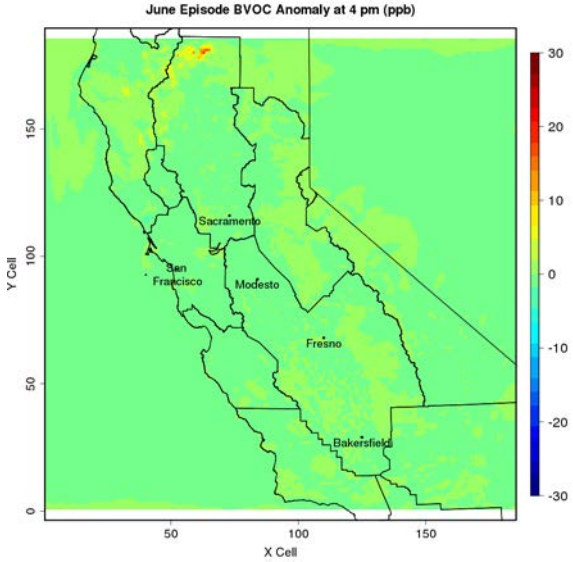
June Episode BVOC Anomaly at 4 pm (ppb)
Sacramento
San Francisco
Modesto
Fresno
Bakersfield
Y Cell
X Cell
0
50
100
150
30
20
10
0
-10
-20
-30

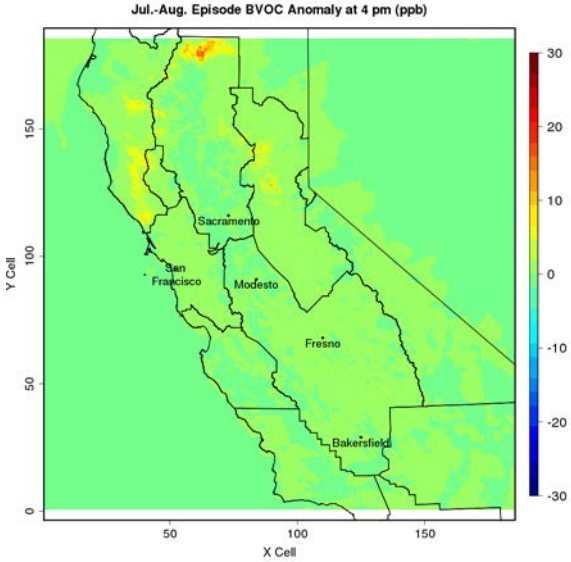
Jul.-Aug. Episode BVOC Anomaly at 4 pm (ppb)
Sacramento
San Francisco
Modesto
Fresno
Bakersfield
Y Cell
X Cell
0
50
100
150
30
20
10
0
-10
-20
-30

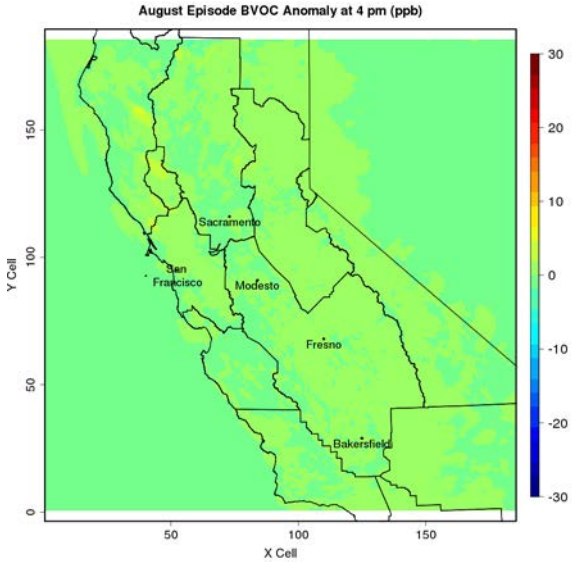
August Episode BVOC Anomaly at 4 pm (ppb)
Sacramento
San Francisco
Modesto
Fresno
Bakersfield
Y Cell
X Cell
0
50
100
150
30
20
10
0
-10
-20
-30

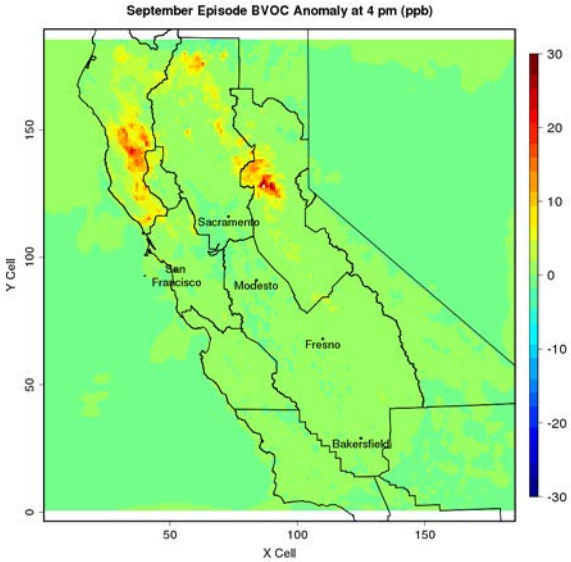
September Episode BVOC Anomaly at 4 pm (ppb)
Sacramento
San Francisco
Modesto
Fresno
Bakersfield
Y Cell
X Cell
0
50
100
150
30
20
10
0
-10
-20
-30

Figure D-5: HO Concentration at 4:00 p.m. (PDT)

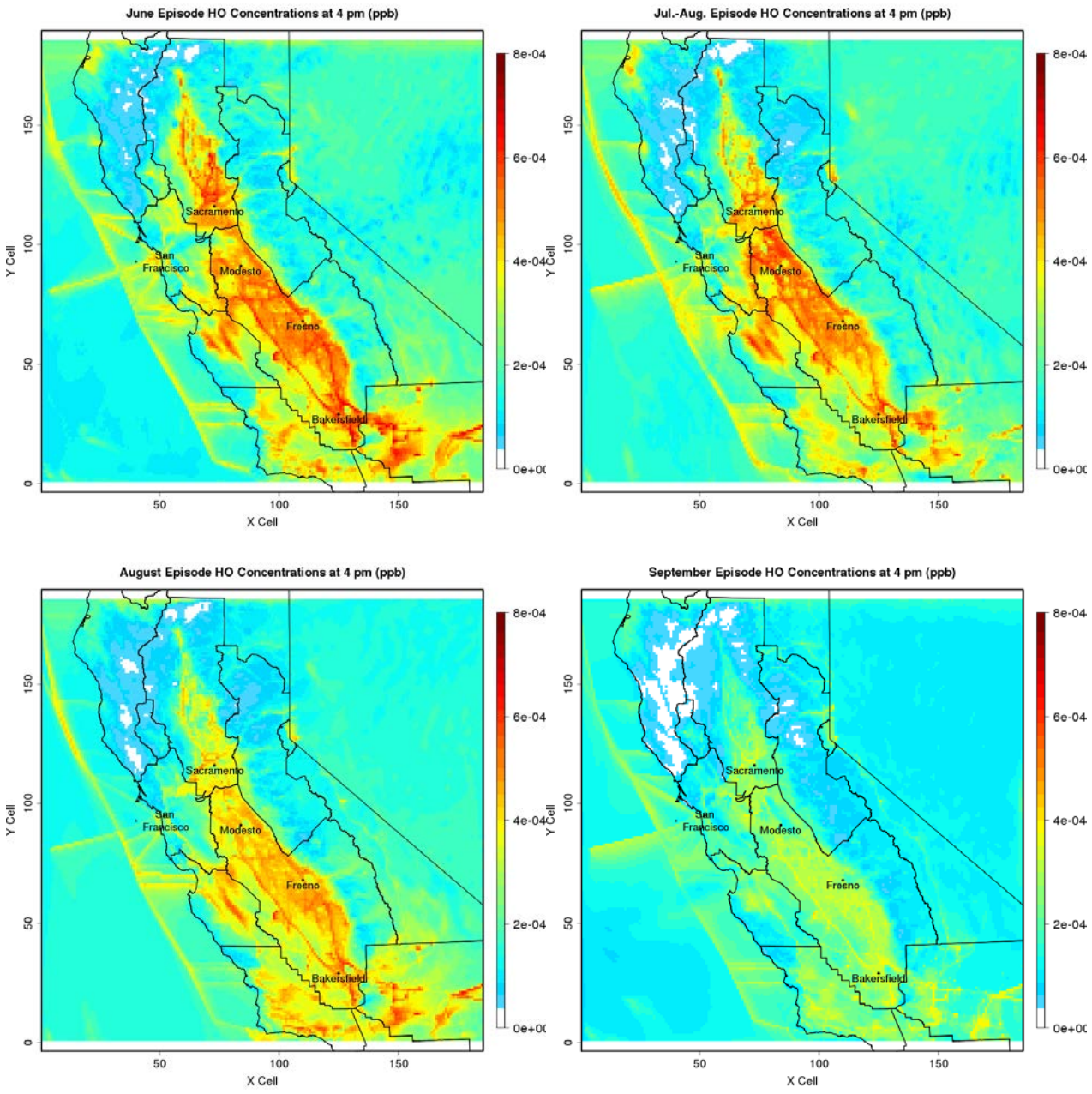

The selected subregion is 3 x 3 grid cells subdomain located in the east of Modesto (marked in red).

Figure D-6: Comparison of July-August and August episodes in Terms of NO, NO2, O3 Concentrations and Ozone Sensitivity to NOx in a Selected Subregion

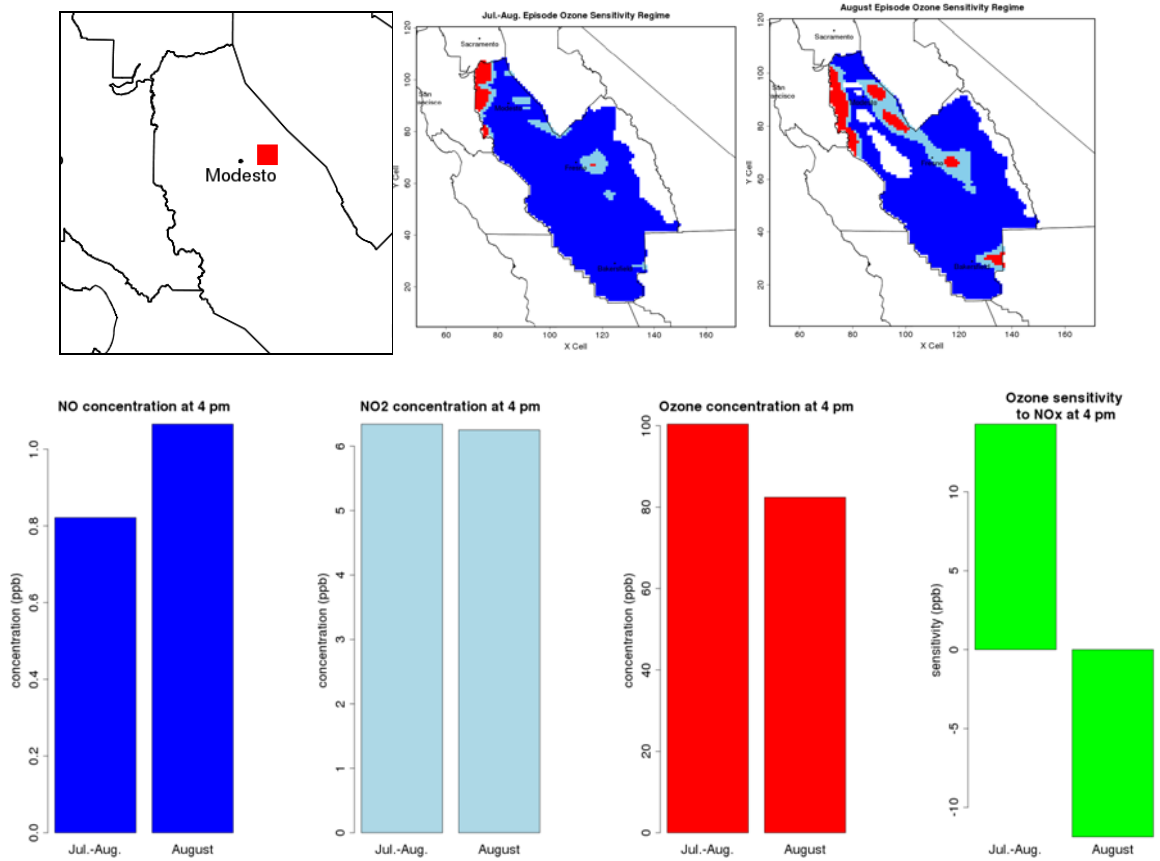

The top row figures: left - red square indicate the analysis location, middle and right figures – control option maps plotted at 4PM with red indicates VOC-control, blue-NOx-control, and lightblue-transition.

Figure D-7: Differences in the First Order Ozone Sensitivity Coefficients between the Alternative Emission Cases (AVOC emissions reduced by 20 percent) and the Original Emission (ORIG) Case

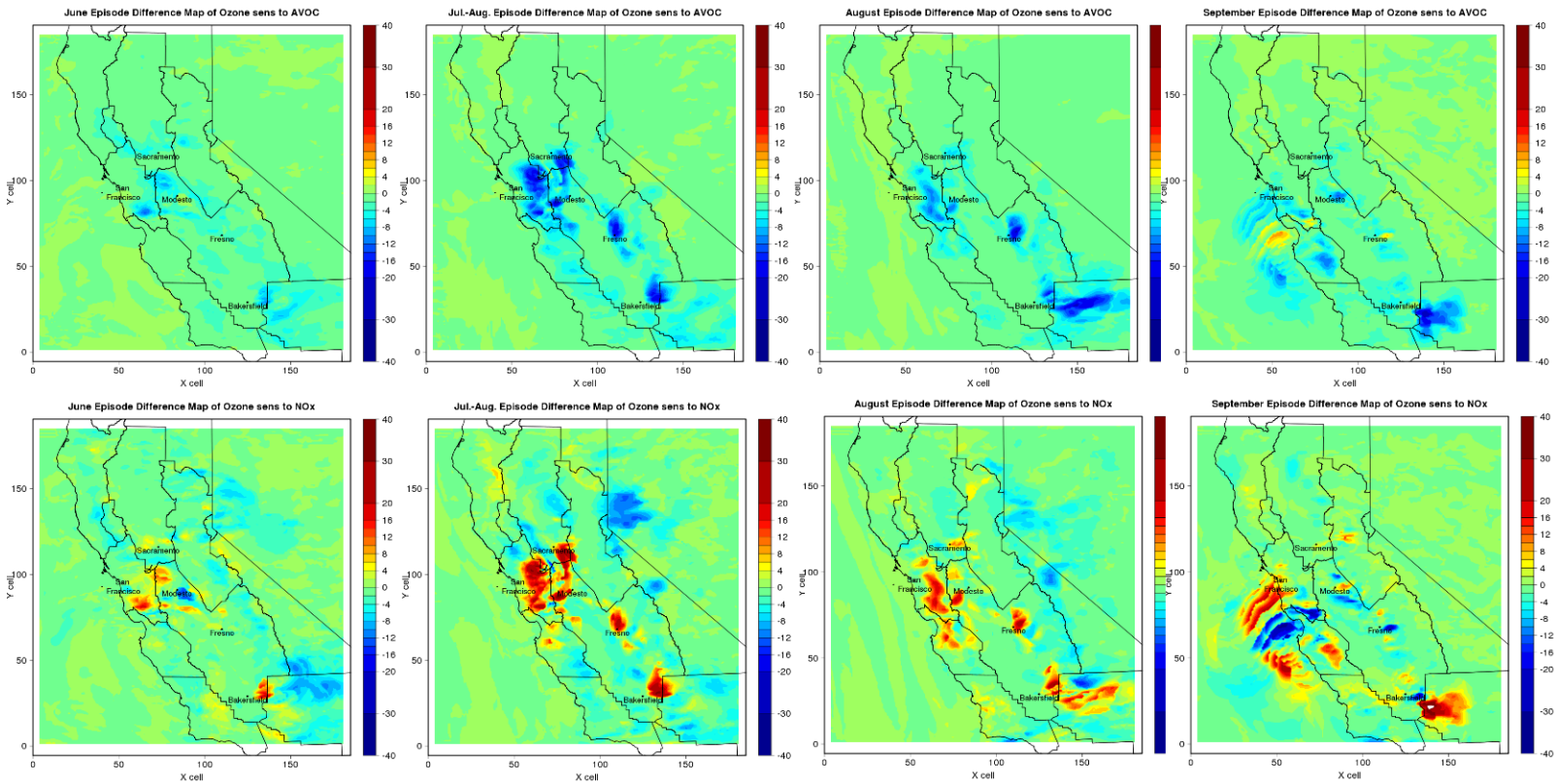

mAVOC - ORIG

Figure D-8: Differences in the First Order Ozone Sensitivity Coefficients between the Alternative Emission Cases (NOx emissions reduced by 20 percent) and the Original Emission (ORIG) Case

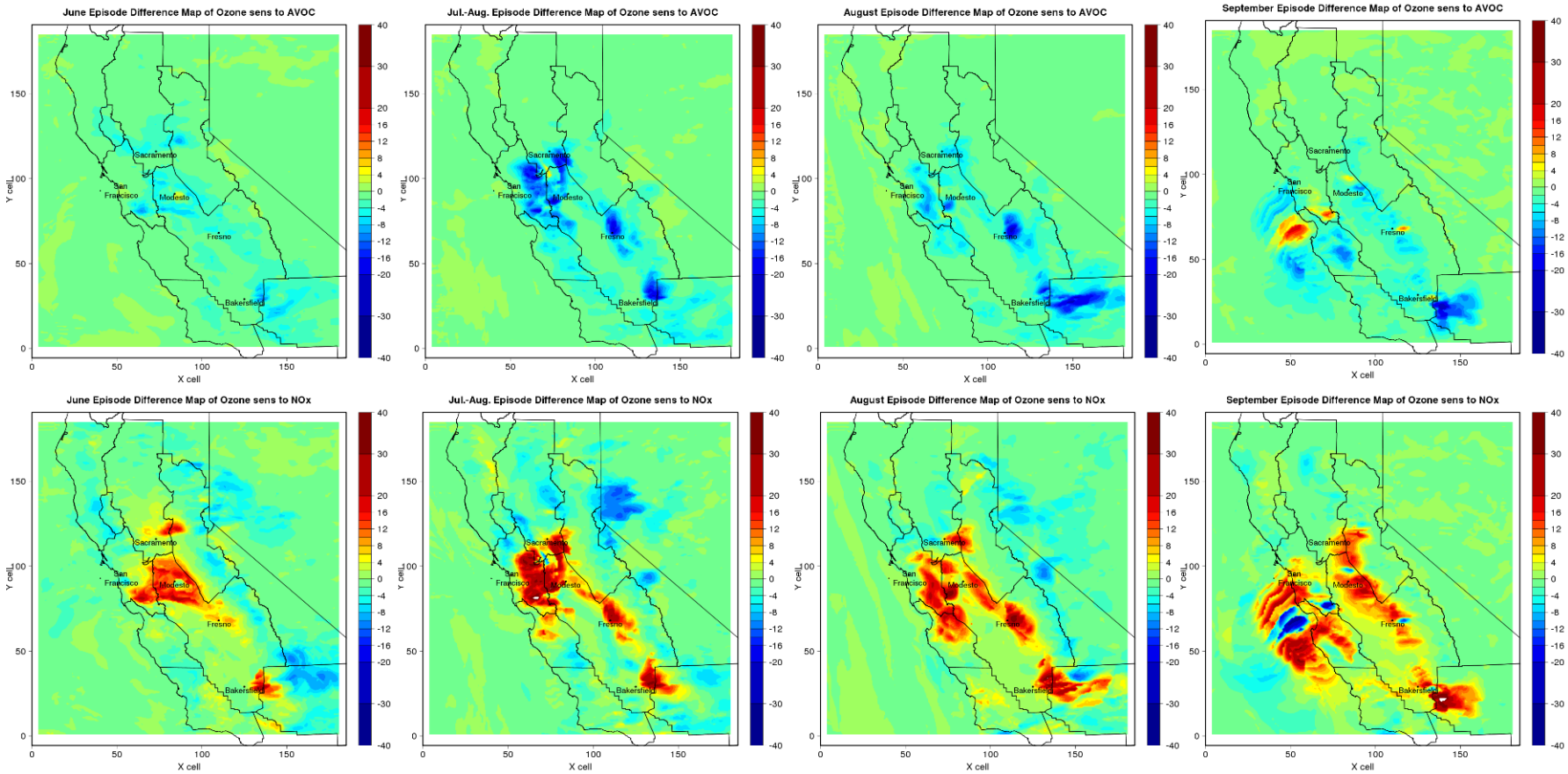

mNOx –ORIG

Figure D-9: Differences in the First Order Ozone Sensitivity Coefficients between the Alternative Emission Cases (both NOx and AVOC emissions reduced by 20 percent) and the Original Emission (ORIG) Case

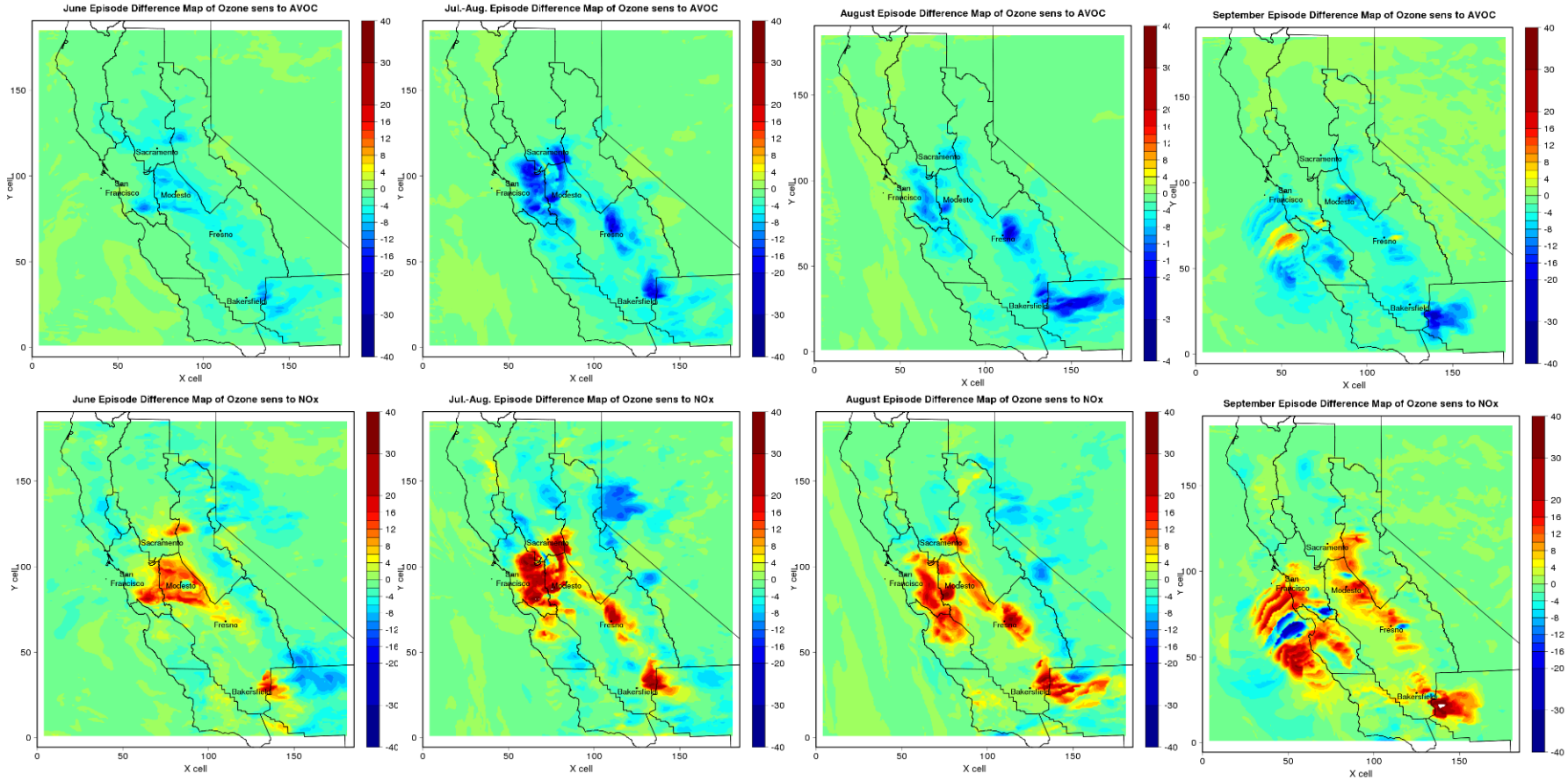

mAVOCmNOx – ORIG

APPENDIX E:
Ozone Sensitivities to SJV, SFB and SV Air Basins Emissions

E-1: San Joaquin Valley Contribution

Figure E-1: SJV Contribution to Ozone Sensitivities to NOx

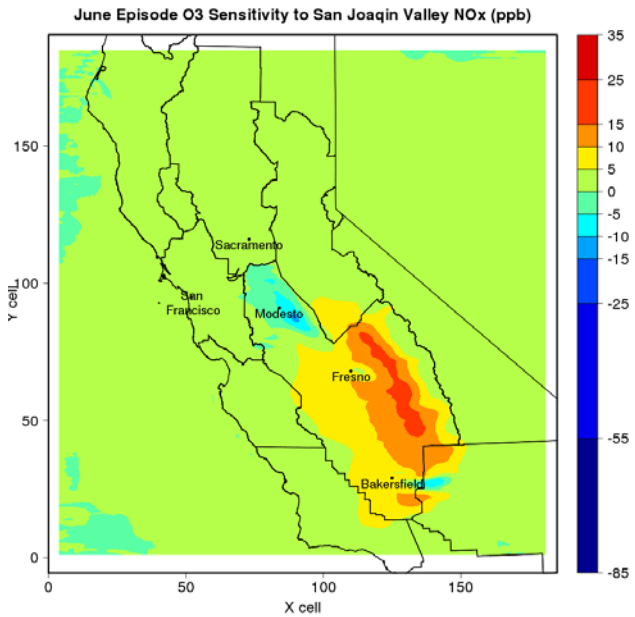

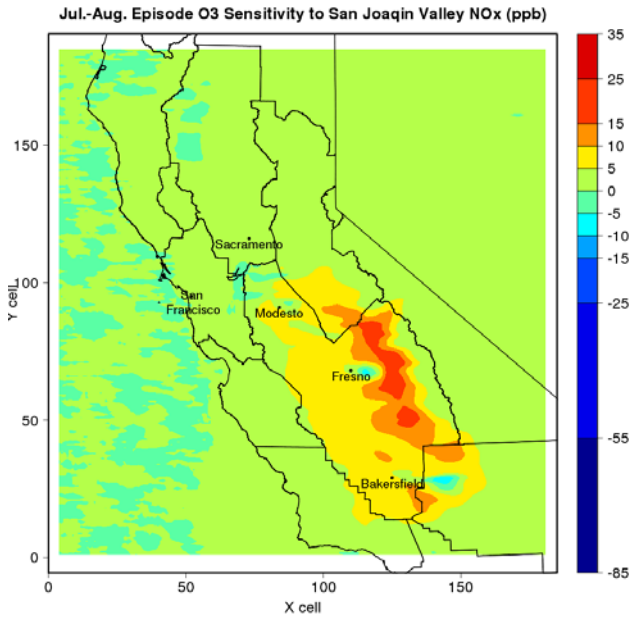

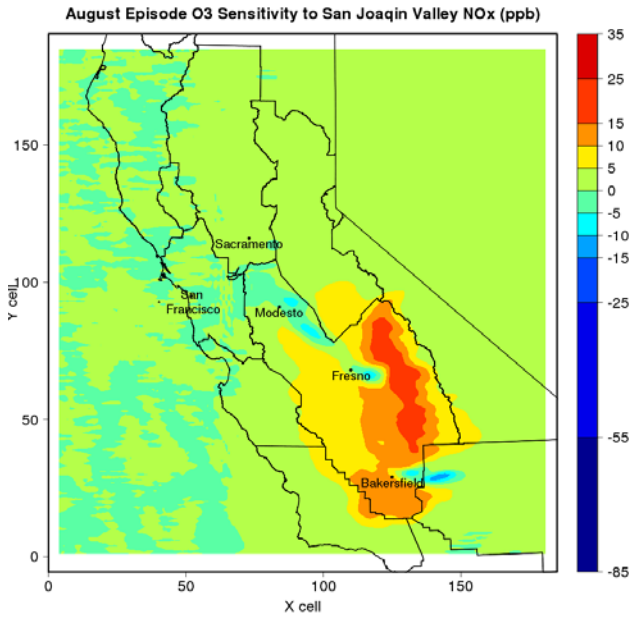

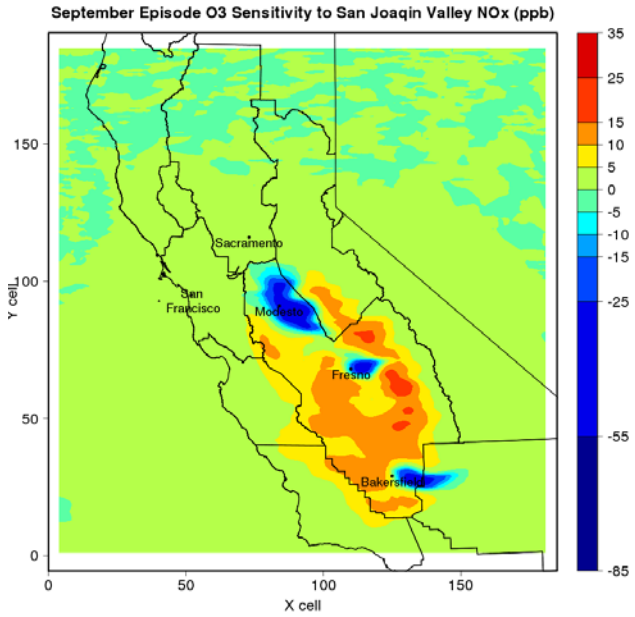

Regardless of meteorological conditions, the SJV emissions contributions are local in that NOx emitted in the SJV does not affect other air basin except the southern Mountain County. The largest sensitivities to NOx occur downwind of the eastern transect from Fresno to Bakersfield and extend to the Sierra Nevada foothills, while the NOx-disbenefit areas are located around urban centers (Modesto, Fresno and Bakersfield) because of the high NO emissions found in these areas. June, July-August and the August episodes have similar sensitivity patterns and ozone sensitivity levels. Note that in August episode, sensitivities are relatively more pronounced in the southern SJV than in July-August episode. In September, negative sensitivities are lower, notably in NOx-disbenefit areas. Hence the NOx-disbenefit area is stronger and more extensive around urban centers. Highest sensitivity areas extend more to the east, which is consistent with the lower westerly wind speeds found in this episode.

Figure E-2: SJV Contribution to Ozone Sensitivities to AVOC

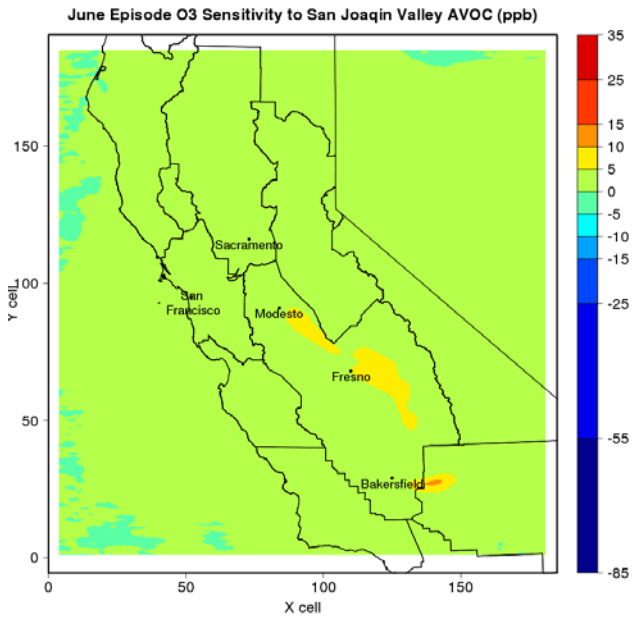

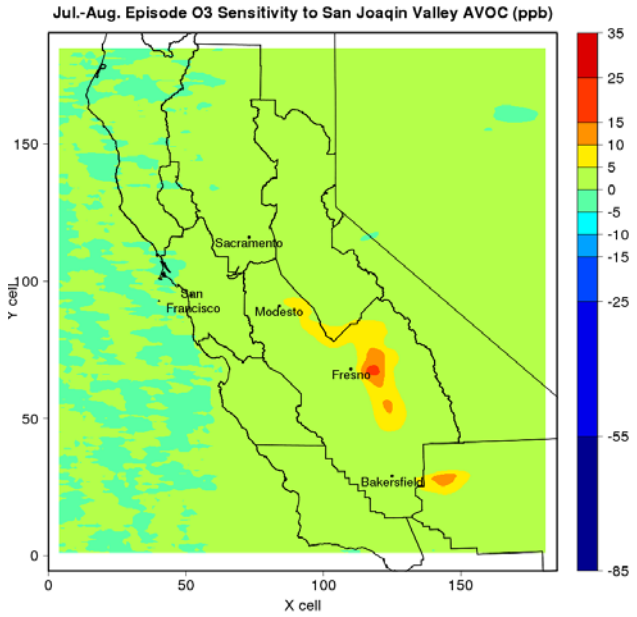

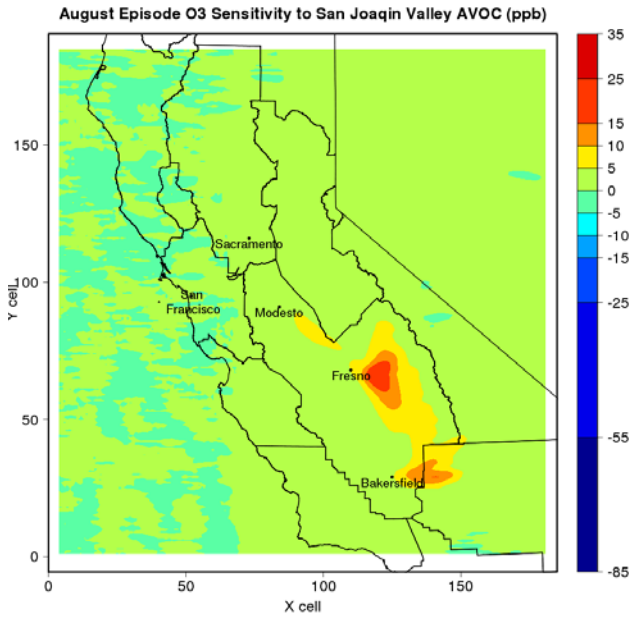

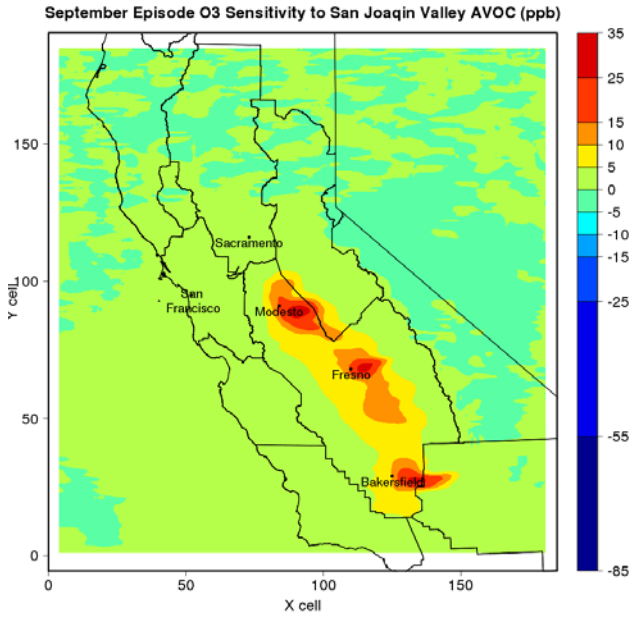

General pattern of ozone sensitivities to local AVOC emissions are similar in all episodes. Highest sensitivities (> 15 ppb) are located downwind of urban centers. Moderate sensitivities (> 5 ppb) usually extend to the east toward the Sierras owing to westerly winds (July-August and August episodes) while they extend more to the west in September. The distance between sensitive areas and emission sources increases with the strength of westerly winds. The stagnant flow regime (September episode) leads to highest sensitivities. In June, the contribution of the SJV to local sensitivity to AVOC is remarkably weak, whereas the sensitivity to NOx is comparable to August episode.

E-2: San Francisco Bay Area Contribution

Figure E-3: SFB Contributions to Ozone Sensitivities to NOx

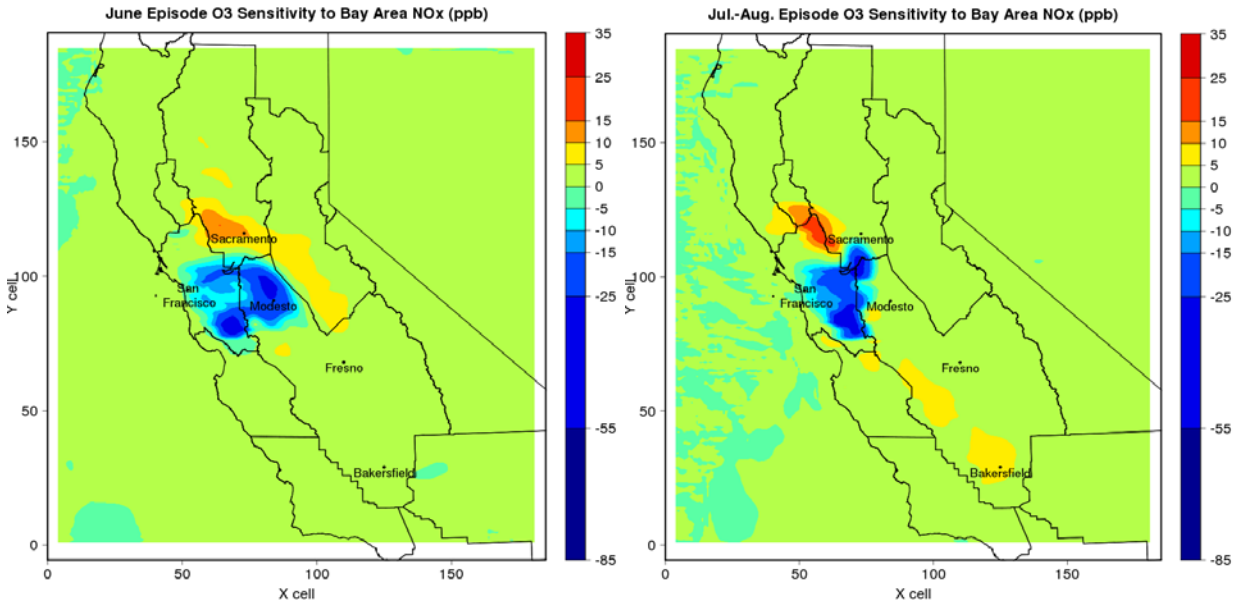
June Episode O3 Sensitivity to Bay Area NOx (ppb)
Jul.-Aug. Episode O3 Sensitivity to Bay Area NOx (ppb)
Sacramento
San Francisco
Modesto
Fresno
Bakersfield
Y cell
X cell
35
25
15
10
5
0
-5
-10
-15
-25
-55
-85

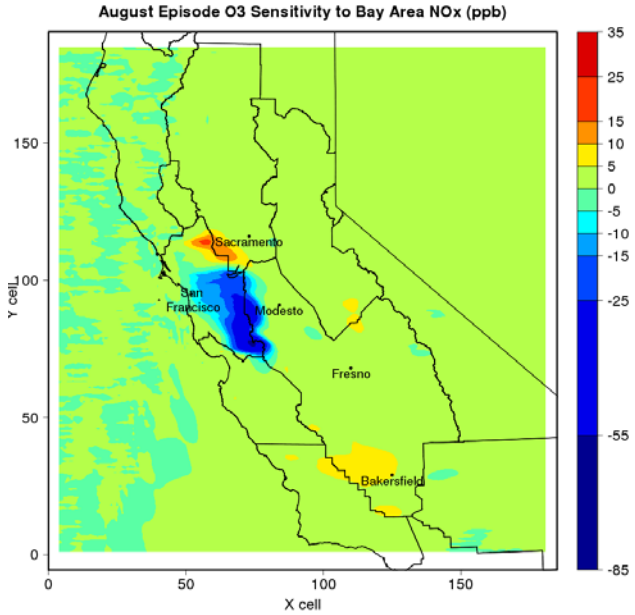
August Episode O3 Sensitivity to Bay Area NOx (ppb)
Sacramento
San Francisco
Modesto
Fresno
Bakersfield
Y cell
X cell
35
25
15
10
5
0
-5
-10
-15
-25
-55
-85

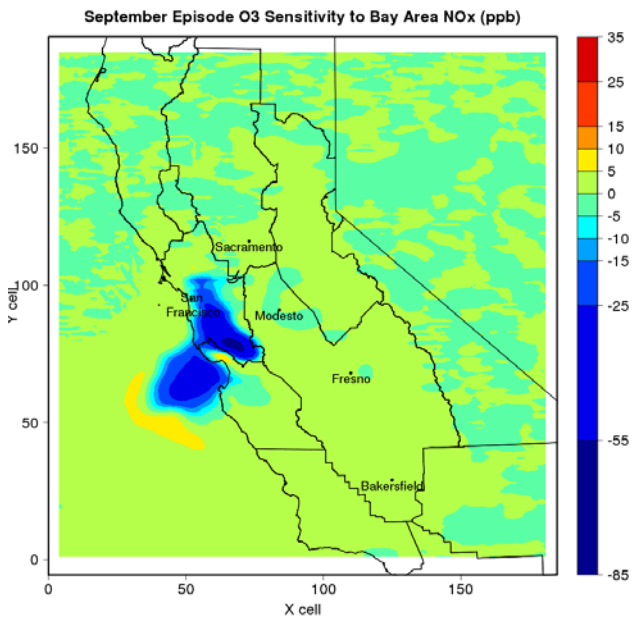

NOx emissions are responsible for the NOx-disbenefit occurring locally. In the September episode, the strong off-shore wind transport Bay Area NOx emissions to the west. Hence they do not affect other air basins. In more ventilated conditions, such as in the July-August and August episodes, the SFB NOx-disbenefit area extends to the border between the SJV and the SFB. The NOx disbenefit area tends to completely move to the northern SJV when marine flows are driven towards the SV (June episode). NOx is transported through the passes (readily visible on the map) and accumulate in the northern SJV. In this case, Bay Area NOx emissions reduce ozone levels in this latter subregion, but south-westerly winds also increase ozone sensitivity in the southern SV. In typical flow conditions (July-August and August), we note moderate sensitivities in the south-western SJV around Bakersfield. Sensitivities to NOx are more pronounced with higher temperatures. Another affected area appears in the hot episode west of Fresno along the coastal ranges. A decrease in SFB NOx emissions would generate a decrease in ozone in these parts of the SJV. This also means that the SFB emissions are responsible for part of the ozone levels in these areas.

Figure E-4: SFB Contributions to Ozone Sensitivities to AVOC

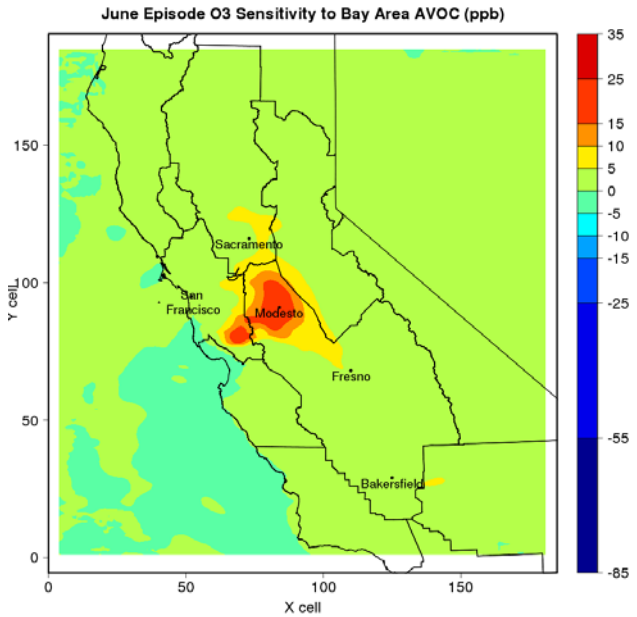

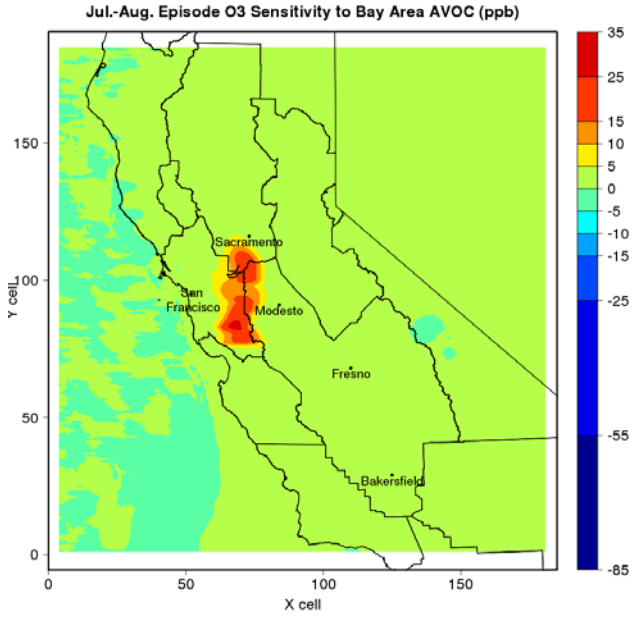

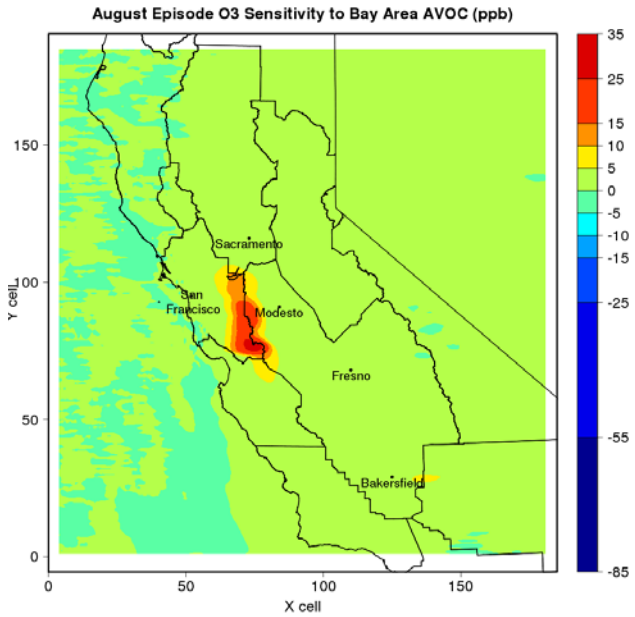

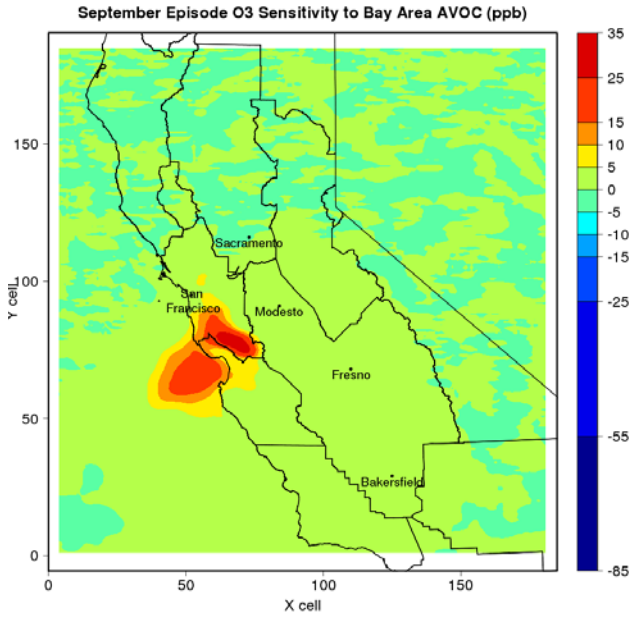

With typical marine ventilation (July-August and August episodes), SFB emissions influence is limited to the eastern part of SJV air basin and slightly extend their influence to the northern SJV and the SV. In September, easterly winds in the SFB transport local emissions to the west and prevent interbasin influence. The June episode has significant interbasin influence: the whole northern SJV is strongly affected by SFB emissions which are transported through the gaps in the Coastal Range.

E-3: Sacramento Valley Contribution

Figure E-5: SV Contributions to Ozone Sensitivities to NOx

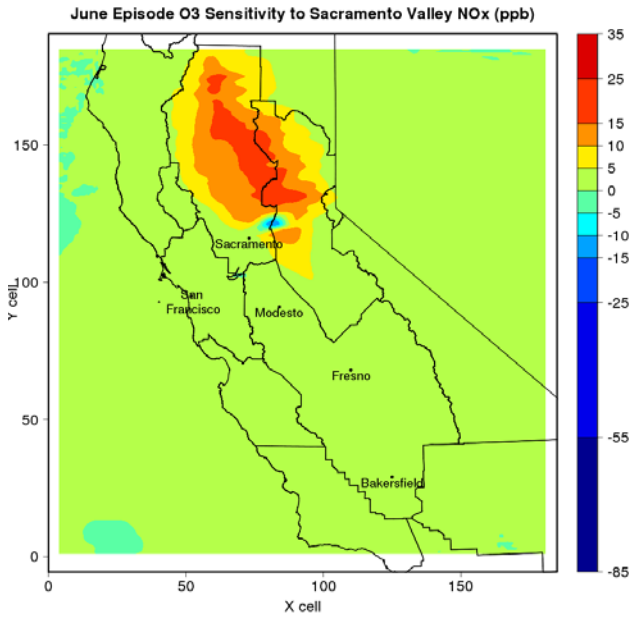
June Episode O3 Sensitivity to Sacramento Valley NOx (ppb)
Sacramento
San Francisco
Modesto
Fresno
Bakersfield
Y cell
X cell
0
50
100
150
35
25
15
10
5
0
-5
-10
-15
-25
-55
-85

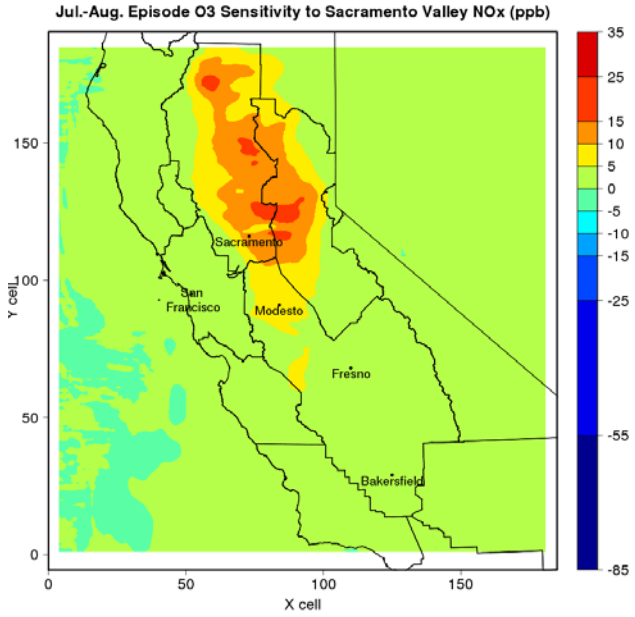
Jul.-Aug. Episode O3 Sensitivity to Sacramento Valley NOx (ppb)
Sacramento
San Francisco
Modesto
Fresno
Bakersfield
Y cell
X cell
0
50
100
150
35
25
15
10
5
0
-5
-10
-15
-25
-55
-85

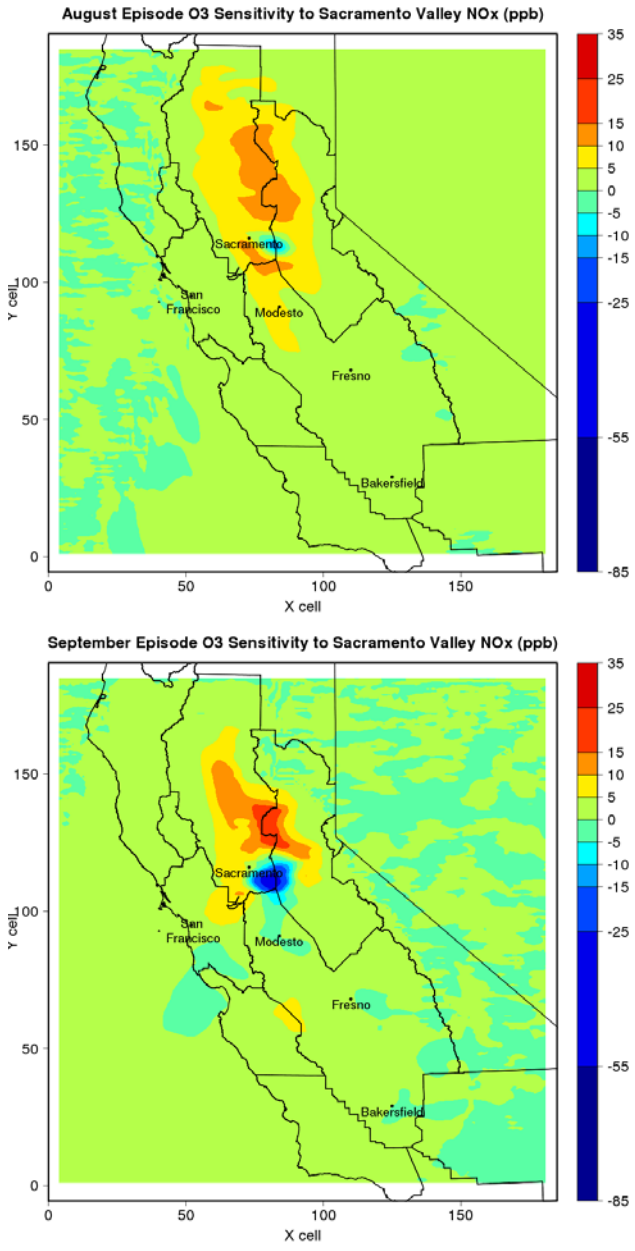

NOx emissions from the Sacramento urban center are transported east-northward to Sierras foothills. Ozone levels are more sensitive to emissions with southerly wind (in June). Note that in such conditions Sacramento is not affected by its local emissions. In July-August and August, high sensitivities extend more to the South and affect the northern SJV around Modesto. NOx sensitivities increase with higher temperatures. In September a pronounced NOx-disbenefit appears downwind Sacramento due to the stagnation of NOx emissions. The disbenefit is influenced by local sources in this episode.

Figure E-6: SV Contributions to Ozone Sensitivities to AVOC

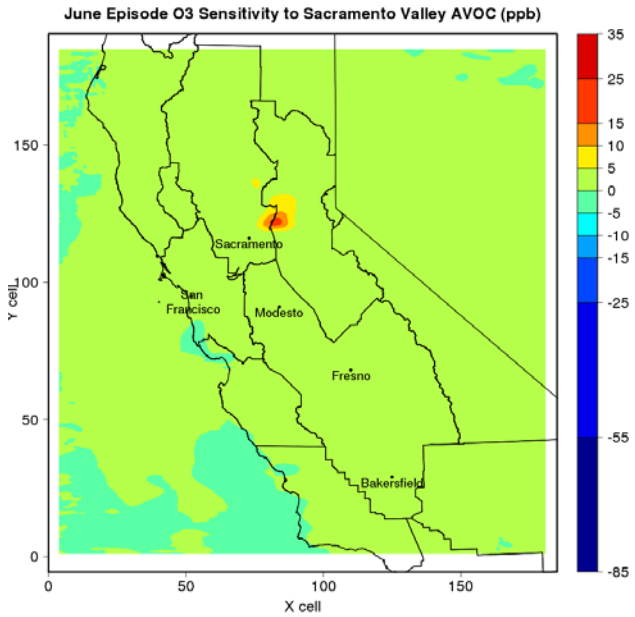
June Episode O3 Sensitivity to Sacramento Valley AVOC (ppb)
Sacramento
San Francisco
Modesto
Fresno
Bakersfield
Y cell
X cell
0
50
100
150
35
25
15
10
5
0
-5
-10
-15
-25
-55
-85

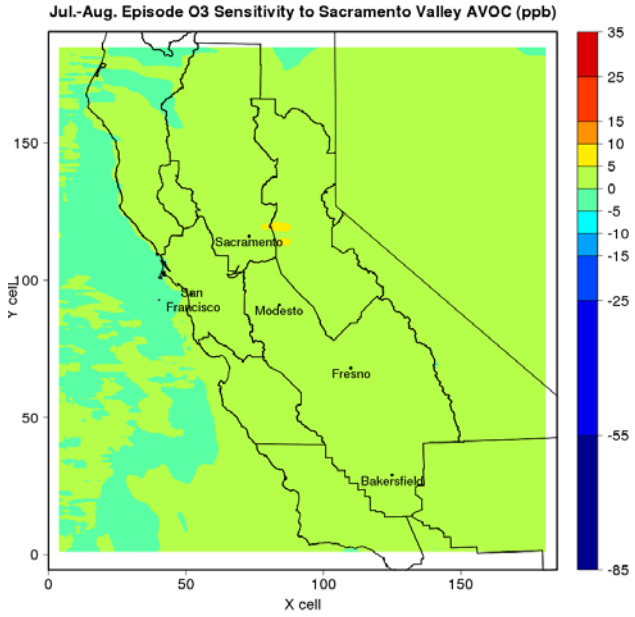
Jul.-Aug. Episode O3 Sensitivity to Sacramento Valley AVOC (ppb)
Sacramento
San Francisco
Modesto
Fresno
Bakersfield
Y cell
X cell
0
50
100
150
35
25
15
10
5
0
-5
-10
-15
-25
-55
-85

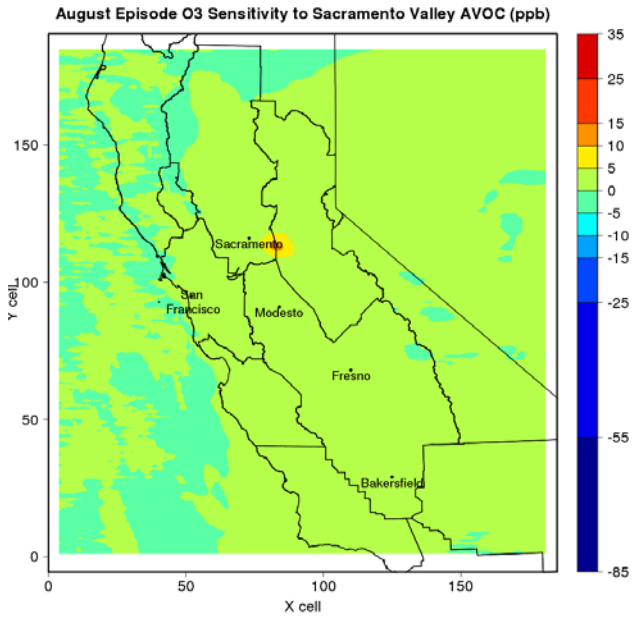

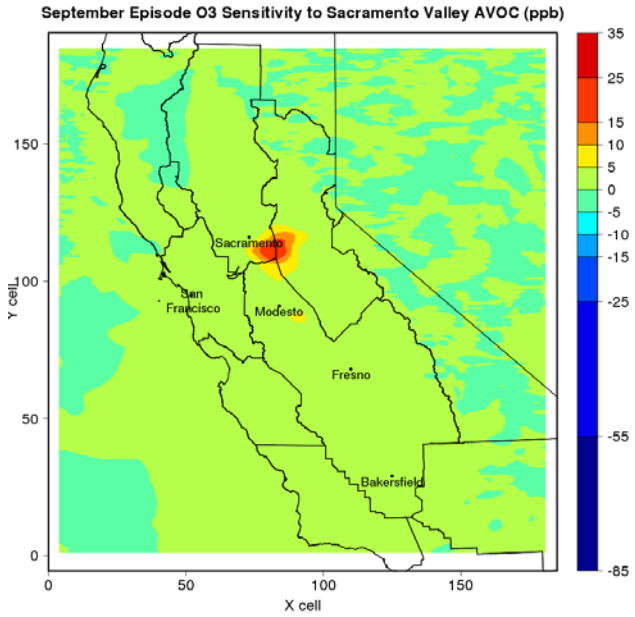

In terms of magnitude, contribution of AVOC emissions from the SV to ozone sensitivity in other air basin is insignificant. Note that the highest sensitivities to AVOC are found downwind Sacramento, with the specific location dependent on the wind direction.